ИЗМЕРИТЕЛЬНАЯ ТЕХНИКА

Number 5

May, 1959

SOVIET INSTRUMENTATION AND CONTROL TRANSLATION SERIES

Measurement Techniques

(The Soviet Journal *Izmeritel'naya Tekhnika* in English Translation)

■ This translation of a Soviet journal on instrumentation is published as a service to American science and industry. It is sponsored by the Instrument Society of America under a grant in aid from the National Science Foundation with additional assistance from the National Bureau of Standards.

SOVIET INSTRUMENTATION AND CONTROL TRANSLATION SERIES

■ This translation of the Soviet Journal *Izmeritel'naya Tekhnika* is published and distributed at nominal subscription rates under a grant in aid to the Instrument Society of America from the National Science Foundation. This translated journal, and others in the Series (see back cover), will enable American scientists and engineers to be informed of work in the fields of instrumentation, measurement techniques, and automatic control reported in the Soviet Union.

The original Russian articles are translated by competent technical personnel. The translations are on a cover-to-cover basis, permitting readers to appraise for themselves the scope, status, and importance of the Soviet work.

Publication of *Izmeritel'naya Tekhnika* in English translation started under the present auspices in August, 1959, with Russian issue No. 1 of Jan.-Feb. 1958. The six issues of the 1958 volume year were published in English translation by February, 1960. Russian issue No. 1 of January, 1959 was published in March, 1960, and the twelve issues of 1959 will be published in English translation by December, 1960.

Transliteration of the names of Russian authors follows the system known as the British Standard. This system has recently achieved wide adoption in the United Kingdom, and is being adopted in 1959 by a large number of scientific journals in the United States.

All views expressed in the translated material are intended to be those of the original authors, and not those of the translators, nor the Instrument Society of America.

Readers are invited to submit communications on the quality of the translations and the content of the articles to ISA headquarters. Pertinent correspondence will be published in the "Letters" section of the ISA Journal. Space will also be made available in the ISA Journal for such replies as may be received from Russian authors to comments or questions by American readers.

1959 Issue Subscription Prices:

Per year (12 issues), starting with 1959, No. 1

General: United States and Canada	$25.00
Elsewhere	28.00
Libraries of nonprofit academic institutions:	
United States and Canada	$12.50
Elsewhere	15.50
Single issues to everyone, each	$ 6.00

1958 issues also available. Prices upon request.

See back cover for combined subscription to entire Series.

Subscriptions and requests for information on back issues should be addressed to the:

Instrument Society of America
313 Sixth Avenue, Pittsburgh 22, Penna.

Translated and printed by Consultants Bureau Enterprises, Inc.

Number 5–May, 1959

English Translation Published June, 1960

Measurement Techniques

The Soviet Journal Izmeritel'naya Tekhnika in English Translation

Reported circulation of the Russian original 8,000.

Izmeritel'naya Tekhnika is an organ of the Academy of Sciences, USSR

See following page for Table of Contents.

MEASUREMENT TECHNIQUES

1959, Number 5 May

CONTENTS

	RUSS. PAGE	PAGE
Radio Electronics – The Most Important Tool of Technical Progress	1	301
Linear Measurements – Control of Drill Grinding by Means of an Instrument Microscope. A. D. Martynov	3	304
Attachments for the Optical Divider Head. M. M. Mergol'd	4	306
Multi-Measurement Adapter for the Control of Atomizer Needles. S. L. Gondik	6	307
Measurement of Inside Cones by Universal Instruments. A. S. Chicherova	7	308
A Device for Checking Micrometers for Dimensions Over 100 mm. Yu. F. Aksyuk and Ya. P. Volosin	9	311
A Pneumatic Detector for the Control of Coaxiality of Two Surfaces. A. V. Vysotskii	9	311
On the Theory of Errors of Self-Compensating Pressure Gage. V. I. Bakhtin	11	314
Equipment for High Precision Investigation of Aneroid Systems. K. P. Bychkovskii	15	320
Piezoelectric Acceleration Transducers. V. P. Nenyukov, A. S. Zhmur and G. L. Lyapin	17	323
Determining the Natural Frequency of Vibrators. Yu. P. Dobrolenskii	19	326
Measuring Equipment for Investigating the Process of Rock Compression Filling. G. F. Lyubenko	20	327
An Aspect of the Effect of Temperature on the Resistance of a Conductor Covering a Surface. B. I. Puchkin	22	329
Thermotechnical Measurements		
Reproducibility of the Boiling Temperature of Oxygen. M. P. Orlova	23	330
Selection and Calibration of Tungsten and Molybdenum Wire for Thermocouples. S. K. Danishevskii	25	333
Electrical Measurements		
Calculation of a Photoelectric Fluxmeter. S. G. Rabinovich and A. N. Tkachenko	30	339
Photoelectric Amplifiers F_{17}. A. M. Kasperovich	35	348
Zero Indicator for High Resistance Measuring Circuits. T. B. Rozhdestvenskaya and G. F. Pankratov	39	354
A Null Indicator for DC Measuring Devices. M. Kh. Shliomovich and M. Sh. Kapnik	41	356

CONTENTS (continued)

	RUSS. PAGE	PAGE
Measurements at High and Ultrahigh Frequencies		
Frequency Errors in Measuring Capacity by Means of Q Meters. G. M. Strizhkov	45	362
Frequency Deviation Meter Errors and a Method of Checking Them. I. M. Sorkin	48	366
Measuring the Voltage Standing-Wave Ratio of a Generator by Means of a Phase Shifter. L. S. Liberman	52	372
A Transistor Amplifier for Operation with Measuring Wire Transducers. P. V. Novitskii and G. N. Novopashennyi	53	374
Equipment for Measuring Permittivity at Super-High Frequencies. A. I. Tereshchenko	54	375
Acoustical Measurements		
Calibration of Objective Noise-Meters by Meand of "Standard" Noises. D. Z. Lopashev	56	377
Radiation Measurements		
An Ionization Chamber for Absolute Measurements of the Radioactivity of Preparations. F. M. Karavaev	60	381
Radioactive Sources in Measurement Techniques. V. S. Merkulov	62	384
The Committee of Standards, Measures, and Measuring Instruments		
New Specifications for Measures and Measuring Instruments Approved by the Committee on New Standards	64	387

RADIO ELECTRONICS – THE MOST IMPORTANT TOOL OF TECHNICAL PROGRESS

March 16, 1959 marked the centenary of the birth of the eminent Russian scientist and inventor of radio, Alexander Stepanovich Popov, whose discovery was widely applied not only in the field of communications but also in the most diversified branches of science and technology. Today, it is impossible to conceive technical progress without the widest application of radioelectronics.

On May 7th, the Soviet people celebrated the traditional holiday – Radio Day. This day is connected with the date of May 7th, 1895 when A. S. Popov, for the first time in history, publicly demonstrated his radio receiver at a session of the Russian Physicochemical Society.

A. S. Popov not only created the first radio receiver, but also performed a number of other works which served as a basis for the further development of radio engineering and its practical application.

However, under conditions prevalent in Czarist Russia, the inventor of radio had difficulties in obtaining support for his work. The development of radio technology received a wide support only as a consequence of the victory of the great socialist October Revolution, during the first years of Soviet power.

On December 2, 1918, the great founder of the Soviet state V. I. Lenin confirmed the status of the Nizhegorod Radio Laboratory. The creation of this laboratory, according to direct instructions of V. I. Lenin, was to become the first stage in the organization of a state socialist radio technology institute in Russia.

In the past forty years, radio technology in our country became not only a powerful means of communication but also one of the most important factors in developing the country's productive forces and a tool for scientific research. The development of radio technology during recent years is of particular importance. For the last ten years, from 1948 to 1957, the output of state production of radioelectronic equipment increased eighteen-fold.

Soviet scientists successfully continued the work begun by A. S. Popov and performed a number of basic research works on radio-physical problems, extensively studied the properties of electromagnetic energy propagation, developed many new electronic devices, and created the most advanced radio electronic equipment of various designation.

The works of Soviet radio physicists and radio engineers who won the A. S. Popov Gold Medal – Academicians A. I. Berg, B. A. Vvedenskii, M. A. Leontovich, and A. L. Mints, Corresponding Members of the USSR Academy of Sciences V. P. Vologdin, A. A. Pistol'kors and also of other Soviet scientists and engineers obtained wide publicity.

The role of radio electronics in the development of instrumentation and measurement techniques is especially important.

While in the first stage of its development, instrumentation was based on mechanics and afterward on electrical technology; in recent times, radio electronics played a revolutionary role in instrumentation.

In all forms of measuring instruments, beginning with weights, mechanical instruments, etc., electronic components became more and more essential, improving to a great extent the sensitivity, accuracy, and reliability of instruments, securing the possibility of automatic measurements and also of automatic regulation and control.

With the development of radio-electronics, the division between control and measuring instruments and automatic regulators and computers becomes less pronounced.

In resolutions of the Twenty-first Congress of the Communist Party of the Soviet Union, it was noted that the transition to complete mechanization and automatically controlled production by means of electronic technology was the most characteristic feature of modern technological progress and represented the main direction in the construction of new machines.

In April 1959, the Lenin Award for the most outstanding work in science and technology was awarded to Soviet scientists N. G. Basov and A. M. Prokhorov for the development of a new principle of generation and application of radio waves (development of molecular generators and amplifiers).

The discovery and development of this principle is a momentous achievement contributing to the intensive development of a new branch of science – quantum radio physics and radio technology. Molecular oscillators have a high frequency stability and are, therefore, applied as frequency and time standards.

Among those who obtained the Lenin Award in 1959 for the creation of a synchrophasitron of ten billion electron volts are the Director of the Radio Technology Institute of the USSR Academy of Sciences Academician A. L. Mints, and the senior scientific collaborators of the same institute, F. A. Vodop'yanov and S. M. Rubchinskii.

On the occasion of the Radio Day in 1959, the Presidium of the USSR Academy of Sciences awarded A. S. Popov Gold Medals to the renowned Soviet radio physicist Professor S. M. Rytov for a series of works in statistical radio physics and to Dr. L. Essen (England) for work in creating an atomic frequency standard.

Radio measurement techniques assumes an ever increasing importance in the development of radio electronics. The improvement of electronic equipment imposes increasingly demanding requirements for accuracy with respect to the basic parameters of radio engineering quantities. The necessity has arisen for the creation of a stock of radio measurement instruments for servicing and controlling electronic equipment and also the means for its checking. It has become necessary to increase considerably the accuracy of the frequency standard, to create primary standard radio measurement devices, and to develop methods of control.

The branches of scientific research institutes and construction bureaus for radio electronics achieved outstanding results in development and creation of radio measurement instruments, including those working at ultrahigh frequencies. The measurement laboratories of metrological institutes of the Committee for Standards, Measures, and Measuring Instruments created primary standard instruments for the measurement of basic radio engineering quantities. Standard measuring instruments for the millimeter-wave range are being also developed.

Molecular oscillators and atomic frequency standards have been made in the All-Union Scientific Research Institute of Physicotechnical and Radio Engineering Measurements and in the Khar'kov State Institute for Measures and Measuring Instruments and they are being introduced in the time and frequency service.

A number of state-controlled laboratories for measurement techniques have been engaged in successful work in verification of radio measurement instruments.

A setback in introducing the new radio measurement technique is the fact that the radio engineering industry still does not concentrate sufficiently on the production of new accurate measuring instruments (for the measurement of attenuation, power, current, voltage, etc.), which have been developed by metrological institutes and which are required by industry and scientific research institutions.

Work on standardization of electronic measurement instruments is still considerably lagging behind, and the development of norm documentation (instructions, methodical directions) with respect to their verification requires considerable effort. This effect must command the central attention of specialized and metrological electronic measurement institutes and laboratories.

Radio electronics, pioneered by our eminent compatriot A. S. Popov, is one of the most important tools of technological progress.

Its importance is especially significant in connection with achievements of Soviet scientists, designers, engineers, and workers, which resulted in launching the first artificial earth satellites and the space rocket toward the moon – the first artificial satellite of the solar system. A considerable share of these achievements is due to Soviet radio specialists, who secured the rocket control, and their placing in the intended orbit with a high degree of accuracy, and also the reception of radio signals from cosmic bodies which are at great distances from the earth.

Magnificent possibilities in the development of radio electronics are outlined in "Control Statistics of the Development of People's Economy of the USSR for the years 1959-1956," which was accepted at the Twenty-first Congress of the Communist Party of the Soviet Union. Our country, being the home of radio, needs a many-sided development of the most important branch of science and technology and its wide application in the People's Economy.

CONTROL OF DRILL GRINDING BY MEANS OF AN INSTRUMENT MICROSCOPE

A. D. Martynov

The application of optical methods in controlling the geometric form of drill points is convenient not only in checking small drills, but also in checking such parameters as the lip clearance angle and the eccentricity of chisel edges in drills of all sizes, as the contact methods and the means of control available for this purpose do not secure a sufficiently accurate and convenient checking.

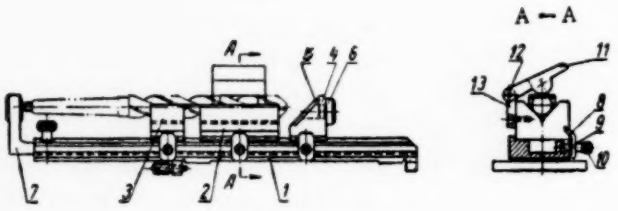

Fig. 1.

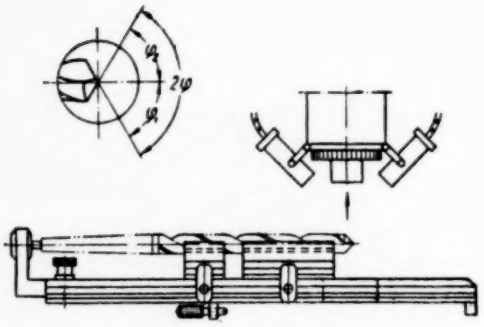

Fig. 2.

In the VNII of the tool industry, a method of measuring all parameters characterizing the correctness in grinding drill points by means of an instrument microscope has been developed. A special bench serves for clamping the drill which is to be checked (Fig. 1).

On base 1), a large and a small fastening prism 2) and 3), together with bracket 4) with a metallic mirror 5) set at an angle of 45° and a rest 6) are fixed. Mirror 5) is designated for the reflection of light beams under an angle of 90° and the rest 6), for preventing the axial movement of the drill in checking the axial wobble of cutting edges. A movable support 7), fixed by a screw, fits into the groove of base 1). Support 7) serves for preventing the movement of the drill when the point angle, the lip clearance angle, and the eccentricity of the chisel edge are checked.

Prisms 2) and 3) and bracket 4) are fixed on base 1) by means of cleats 8), screws 9), and nuts 10). Screws 9), together with cleats 8) and nuts 10), can be moved along T-shaped groove in base 1).

For the purpose of clamping the checked drill to the bedding prism 2), the latter is provided with a rotating clamp 11), whose rotation axis 12) is fixed on plate 13), fastened by screws to the bedding prism. In the right-hand side of base 1), there is an opening through which the light from under the microscope table falls on the objective.

Before the measurement, the bench is set by means of a cylindrical mandrel in such a manner that the axis of bedding prisms coincides with the horizontal sighting line in the microscope ocular.

All the drill parameters are checked in reflected light with the exception of the point angle which is checked in transmitted light.

For measurements in reflected light, an illuminator for top illumination is fixed on the microscope tube;

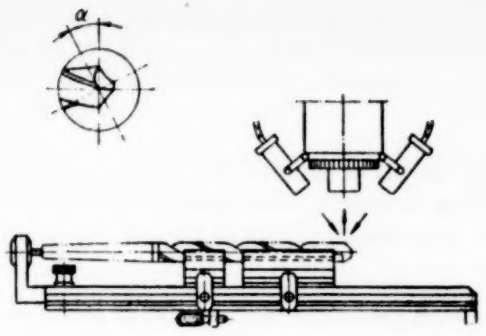

Fig. 3.

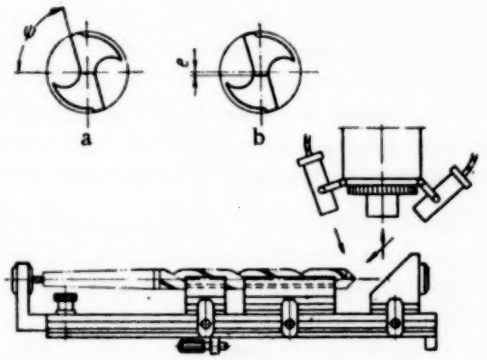

Fig. 4.

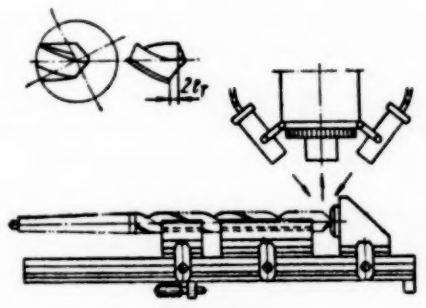

Fig. 5.

for checking the slope angle and the eccentricity of the chisel edge, a prop 4) with the reflective mirror 5) is placed on base 1).

The measurement of the point angle 2φ (Fig. 2) is performed in transmitted light. By turning the drill, its cutting edges are placed in horizontal position. By looking through the ocular, the focused image of the cutting edge is made to coincide with the sighting line, and the magnitude of angle φ_1 is read off through the angle-measuring ocular. Further, by turning the drill, the second cutting edge is focused and its angle φ_2 is determined; according to the results of these two measurements, the point angle 2φ is obtained.

The lip clearance angle α (Fig. 3) is measured in reflected light. By observation through the ocular, the image of the intersection point between the back and front surfaces, which is visible on the strip, is made to coincide with the cross-hairs. After that, the vertical sighting line is rotated until it coincides with the intersection line between the back surface and the cylindrical strip surface, and the magnitude of angle α is read off by the angle measuring ocular.

The measurement of the web angle ψ (Fig. 4a) is performed by means of the reflective prism. By rotating the drill, the image of the transverse edge is made to coincide with the horizontal sighting line. Then, the horizontal sighting line is rotated until it coincides with the cutting edge and the magnitude of angle ψ is read off by the angle measuring ocular.

The eccentricity of the chisel edge $\underline{e}$ (Fig. 4b) is checked by means of a reflective prism. By turning the drill, the image of the transverse edge is made to coincide with the sighting line and the readings are taken on the microscrew. After that, the drill is rotated through 180°, the image of the chisel edge is again made to coincide with the same sighting line and a second reading is taken on the microscrew. The eccentricity $\underline{e}$ of the edge is determined as the half-difference between these readings.

The measurement of axial wobble of outer corners $2e_T$ (Fig. 5) is performed in reflected light. By observation through the ocular, the vertical sighting line is made to coincide with the intersection line between the back surface with the cylindrical strip surface and a reading is taken on the microscrew. After that, the sighting line is rotated together with the intersection line between the back surface and the cylindrical strip surface, and a second reading on the microscrew is taken. The difference between these two readings is the magnitude of the axial wobble of outer corners $2e_T$.

ATTACHMENTS FOR THE OPTICAL DIVIDER HEAD

M. M. Mergol'd

An optical divider head can be easily adapted for checking the angles between notches marked on side or end surfaces of various parts. We developed very simple adaptors permitting wide application of the divider head for this purpose, in conjunction with the ocular head, tube, objective, and stand of a small microscope-type instrument which is widely used in machine construction.

The stand 1), taken off an instrument microscope, together with the ocular head, tube, and objective (Fig. 1) are fastened on a guide in the dove-tailed form of a massive base 2), placed on the bench of the optical divider head and able to move freely along the bench. Here, the optical axis of the microscope must coincide with the axis passing through the center line of the mandrel of the divider head and the headstock, which is achieved by determining the corresponding height of base 2).

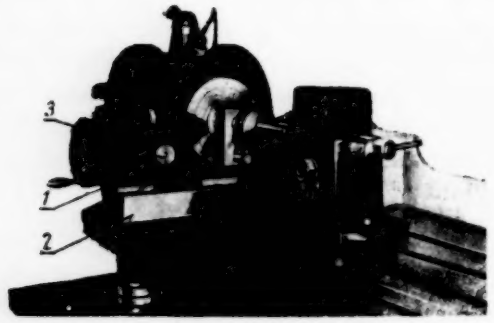

Fig. 1.

The angles in parts having notches on cylinder surfaces are measured in the following manner: the measured part is fixed in the centers of the mandrel and the headstock. The microscope is focused for a sharp image of the notch indented by means of mechanism 3), after which the angles between the notches are measured as usual.

For measuring the angles on parts having notches on end-side surfaces, an additional attachment is used (Fig. 2), which consists of a small flat mirror 1) fixed by means of holder 2) and stand 3) on a compact cylindrical base 4) which can be freely moved along the bench. A flat mirror is set at an angle of 45° with respect to the investigated end-side surface of the part, and the microscope is adjusted to obtain a sharp image of notches marked on the end-side surface of the object, which are reflected by mirror 1). The angles between the notches are, in the given case, also measured in the usual manner.

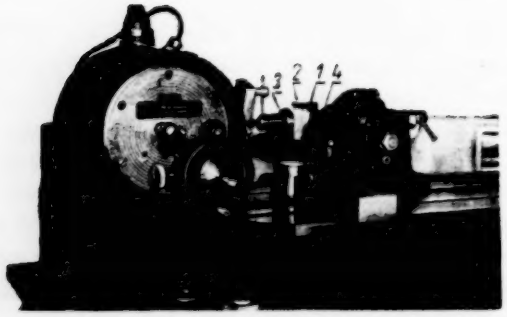

Fig. 2.

If the microscope is provided with an illuminator, the attachment can be also used for the investigation of various cutting tools, dies, gears, and other parts.

For the measurement of angles between the center lines of visible openings or grooves, located along the circumference on end-side surfaces of parts, an additional illuminator with a 6.3 v electric lamp provided with a green filter and fed from the transformer of the optical divider head is used. This illuminator is placed on the bench, at the center level and on the left side of the part investigated. The light beams, passing through openings or grooves in the part, are reflected from mirror 1), fall on the microscope objective, and the observer, viewing the clearly visible contour of the opening or the groove, performs the corresponding measurement of center line angles.

From the Editor: In a similar sighting arrangement, F. G. Kotel'nikov uses, beside this, a centering four-screw face chuck for the control of arc scales.

There are cases where in various enterprises by either dismantling (temporarily or permanently) instruments which are in service or by using microscope tubes which became unserviceable, arrangements similar to the described ones are constructed. These adaptations are of undoubted interest as there are no specialized adaptations. However, the practice of dismantling serviceable instruments cannot be approved of.

The manufacturing plant must become familiar with and produce on customer's demand, specialized optical sights for the heads, as well as a number of other adaptors (the contact zero-point instrument, shims for the head and the headstock, a device for the control of cams, and others), which are manufactured by all foreign firms producing divider heads.

The revised All-Union State Standard 9016-59 for optical divider heads provides the corresponding requirements with respect to the provision of a complete set.

MULTI-MEASUREMENT ADAPTER FOR THE CONTROL OF ATOMIZER NEEDLES

S. L. Gondik

The adapter developed at the Khar'kov Tractor Plant serves for the control of the following atomizer needle parameters (Fig. 1): trueness of the outside cylindrical surface having a diameter of 5 mm (tolerance not greater than 0.001 mm), the eccentricity of the 1.5 mm diameter and of the 60°30' shutting cone with respect to the 5 mm diameter (tolerance 0.004 mm).

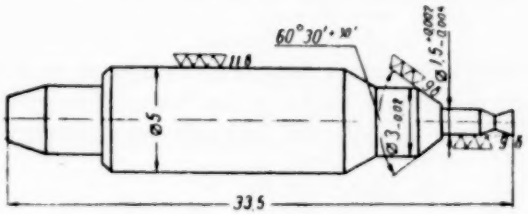

Fig. 1.

The control of the indicated parameters is performed simultaneously. The adapter construction is shown in Fig. 2.

On a wooden block 1), a plate 2) is fixed by means of wood screws, where the following parts are mounted: three stands 3) for the installation of small-size micrometers, a stand with prism 4) (at a 60° angle) for placing the needle to be checked 5), a stand with support 6), limiting the displacement of the needle and a stand 7) with a device for rotating the needle. This device consists of a roller on which another rubber roller 8) is fixed, and of a pilot wheel 9). The needle 5 which is being checked having a diameter of 5 mm, is placed on prism 4). By rotating the pilot wheel 9) clockwise, the rubber roller 8) which is set at an angle of 10° with respect to the rotation axis, pushes the needle placed in the prism until it stops at the support, thus placing it in the measuring position. When the part is placed in the measuring position, the measuring end-pieces of the micrometers are resting against the 1.5 mm and 5 mm diam surfaces and the 60°30' shutting cone of the checked needle. When the pilot wheel is

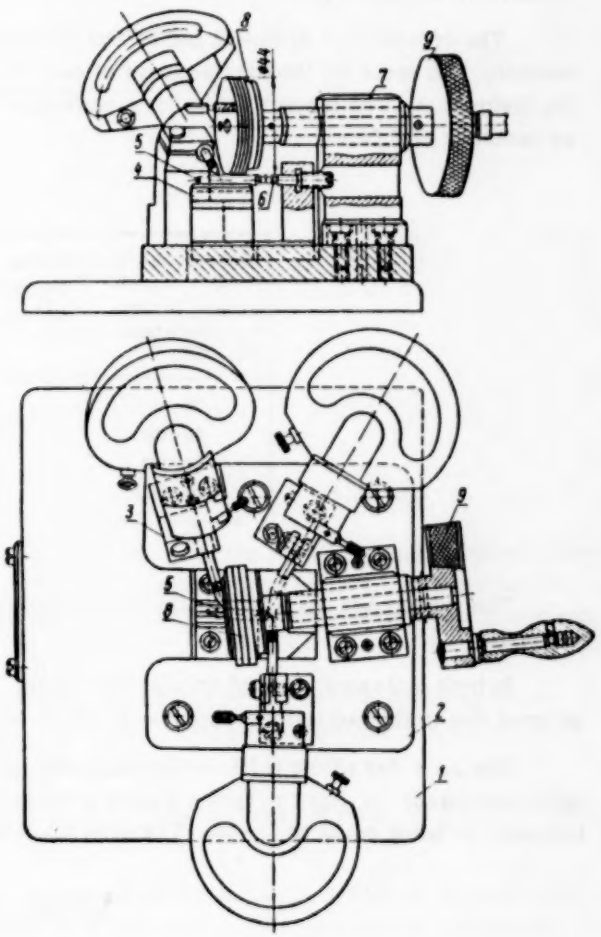

Fig. 2.

further rotated, the needle turns through an angle of 360° about its axis and the deviation of the checked dimensions from their true values is determined according to the deflection of micrometer hands from their initial positions. After the measurements are completed, the pilot wheel 9) is turned counterclockwise and the checked needle is removed from the measuring prism 4).

The introduction of the described device in industry assured new accuracy in determining the controlled dimensions and greatly improved the efficiency of control; the part can be checked in 10 sec.

MEASUREMENT OF INSIDE CONES BY UNIVERSAL INSTRUMENTS

A. S. Chicherova

Indicating inside micrometers NI, manufactured by the "Kalibr" plant in conjunction with a depth gage, are used for measuring conical openings.

Using the depth gage as a support fixing the height, the indicating device is slightly tilted back and forth in the vertical plane and the minimum dimension is read off the indicator, which is accepted as the true dimension in the plane perpendicular to the axis.

The construction of PK-32 and PK-32 instruments, produced by the plant LIZ (Fig. 1) is based on this method. The scale for the measurement of cone diameters at a determined height is mounted on stem 1) of the instrument. The support bar 2) has a vernier making it possible to establish the measurement height with an accuracy of 0.05 mm.

TABLE 1

Measurement ranges of indicating inside micrometers NI, mm	Radius of the measuring end-piece, mm	Slope of the measured cone	Error due to radii of the measuring end-pieces, mm
35–50	9	1°	3
50–100	12		3.6
100–160	24		7.2
160–250	22		6.6

The support bar has a spherical cross section in order to facilitate the tilting of the instrument in the vertical plane.

In both indicated cases of cone measurement, a double error in the determining of diameters can occur: an error due to the radii of measuring end-pieces and the error due to tilting the instrument.

The error due to the radii of measuring end-pieces (Fig. 2) is caused by the shift of point $\underline{n}$ (when a cylinder is measured) to point $\underline{m}$ (when a cone is measured). Therefore, the cone diameter will be shown by the indicator as being equal to $\overline{D}-2\Delta$. The error 2Δ is determined according to the equation

$$2\Delta=2(a-R)=2R(\sec\alpha-1),$$

where R is the radius of the measuring end-piece and α is the angle of the measured cone.

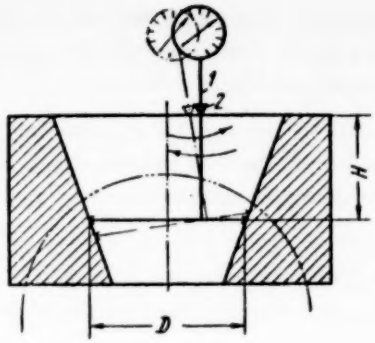

Fig. 1.

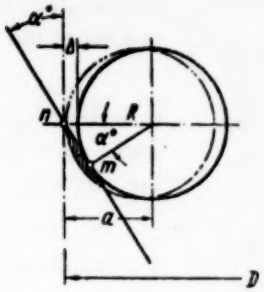

Fig. 2.

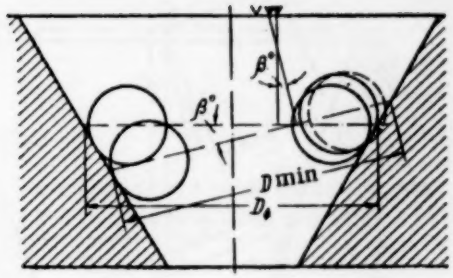

Fig. 3.

TABLE 2

Slope angle of the cone α, deg	Error in cone dia. meas. due to end-piece radius of 1.5 mm, μ	Error in cone dia. meas. due to end-piece with 0.5 mm radius
6	16	5.5
10	45	15
15	120	40
20	180	60

TABLE 3

Error in setting the height of PK-32 instr. traverse	Slope angle of the cone α, deg	Error in cone diameter measurements
0.05 mm	3	5
	6	10
	10	17
	15	20
	20	36

In determining the measurement errors due to the radii of end-pieces of the indicating inside micrometers NI, manufactured by the "Kalibr" plant, data were obtained (Table 1) from which it follows that these inside micrometers cannot be applied for the measurement of even flat cones ($\alpha_{max} = 1°$) without introducing corrections for the radii of end-pieces.

The special instruments for the measurement of inside cones PK-32 and PK-33 have end-pieces whose radii are of the order of 1-1.5 mm, but even for these reduced radii, it is necessary to introduce a correction when steep cones are measured, which is confirmed by calculation data given in Table 2.

The errors in cone measurements due to tilting are determined in the following manner for the PK-32 and PK-33 instruments.

For a decrease or increase of angle δ (Fig. 3) which corresponds to the minimum value of the cone diameter at a given height, and if the distance between the centers of end-pieces remains constant, the shaded segment will decrease, i.e., the indicator will give a larger reading.

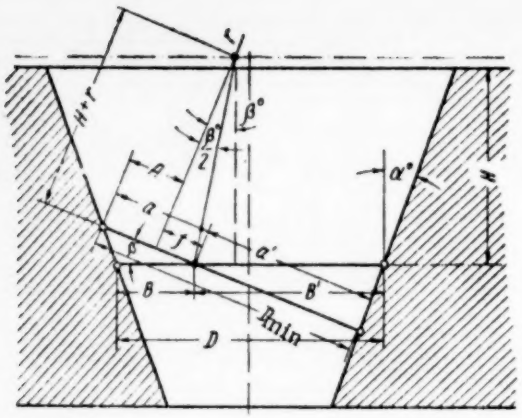

Fig. 4.

Thus, the minimum diameter is determined in a unique plane set at angle β with respect to the cone axis and not in the plane perpendicular to the axis.

Using trigonometric relations for oblique-angle triangles (Fig. 4) we obtain the following equations relating the minimum diameter and the diameter given in the diagram:

$$D = D\text{min}\cos\beta + \left[2A - 2(H + r)\operatorname{tg}\frac{\beta}{2} - D\text{min} \right] \operatorname{tg}\alpha \sin\beta,$$

where D_{min} is the minimum diameter obtained by the measurement performed with the indicating instrument with a spherical traverse; α is the slope angle of measured cone; r is the radius of the support bar; H is the height at which the cone diameter is located according to the drawing; A is the distance between the instrument axis and the tangent to the immobile end-piece; β is the angle between the instrument axis and the vertical or the angle between the planes where D_{min} and D are located.

The validity of this equation was confirmed in practice.

In the measurement of flat cones with slopes up to 1°, the difference between D and D_{min} can be neglected, but for cones with slope angles greater than 1°, this difference must be taken into account. Therefore, the use of PK-32 and PK-33 instruments is time consuming, as a recalculation of dimensions obtained by measurement, applying the given rather cumbersome equation is required.

Moreover, it is necessary to bear in mind that in measuring cones with a large slope angle, the setting of the base distance with an accuracy of 0.05 mm, which is provided by the PK-32 and PK-33 instruments is not sufficient (Table 3) and, therefore, it is necessary to set the instrument bar according standard length measures.

In order to simplify the method of controlling steep cones by the PK-32 and PK-33 instruments, it is necessary to provide these instruments with a flat support bar, so that the instrument axis is set parallel to the cone axis.

In this case, the actual dimension of the cone diameter will be equal to the instrument reading plus a correction for the measuring end-piece radii:

$$D = D_{\text{ind}} + 2R(\sec\alpha - 1).$$

We also propose that these instruments be provided with means for a greater accuracy in measuring the distance from the base.

The radius of measuring end-pieces, which will be used in determining the correction of the measurement results, should be indicated in technical characteristics of the instruments.

A DEVICE FOR CHECKING MICROMETERS FOR DIMENSIONS OVER 100 MM

Yu. F. Aksyuk and Ya. P. Volosin

The proposed device permits the checking of micrometers with a wide measurement range (over 100 mm) by means of length standards with the maximum size of the block equal to 25 mm, thanks to the presence of an auxiliary adjustable stopper.

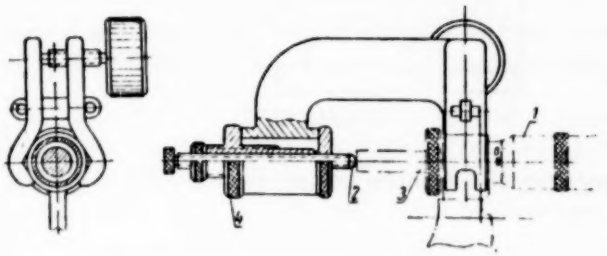

The device (see Fig.) consists of a bracket, clamp, and a unit for setting the position of the auxiliary stopper. The clamp is made in such a manner that the device can be mounted on micrometers produced by the plant "Krasnyi Instrumental'shchik" as well as on micrometers made by the plant "Kalibr" without limitations in the application of the stopper device.

The device is simple to make and is very compact (it can be easily placed in the box under the dial-type indicator).

The checking of the micrometer is done in the following manner: the zero notch of the drum of micrometer 1) is made to coincide with the zero notch on the stem, and the micrometer screw is clamped by the arrester device after which the checking device is fixed on the micrometer; after that, the position of the auxiliary stopper 2) is regulated in such a manner that its spherical surface is located at the center of the stopper measuring surface of microscrew 3) pressing it with a force corresponding to the measuring force of the micrometer; then, the position of the movable stopper is fixed by means of stop screw 4) and, after the stopper device of the micrometer is released, the zero setting is checked; afterwards, the accuracy of the micrometer is checked in the same manner as required for micrometers for small measurement ranges.

The use of the described device secures the necessary measurement accuracy.

This device was tested and it is applied in KhIGIMIP and at KhTZ. Its application increased the efficiency in checking large micrometers by 10-15%.

A PNEUMATIC DETECTOR FOR THE CONTROL OF COAXIALITY OF TWO SURFACES

A. V. Vysotskii

The existing method of controlling the coaxiality of two surfaces – the measurement of the "wobble" of one surface with respect to another surface when the object is rotated – has the following drawbacks: in the first place, the necessary rotation of the object prolongs the measurement time and, consequently, reduces the control efficiency; in the second place, the method is applicable only for the coaxiality control of two cylindrical surfaces. In the case where the coaxiality of surfaces one or both of which has a form different from the cylindrical is checked, this measurement method yields large errors.

As an example, let us consider the case where the coaxiality of cylindrical and elliptical surfaces of a part (automobile piston) is being checked.

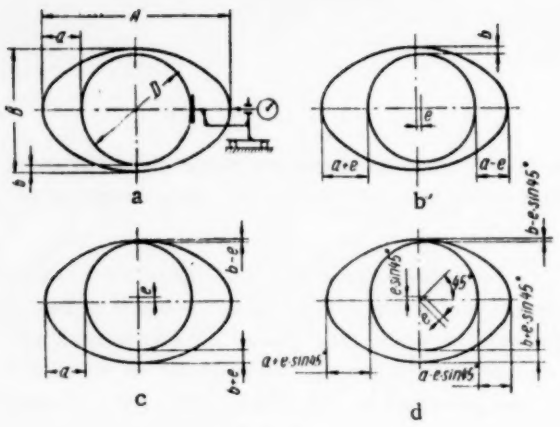

Fig. 1.

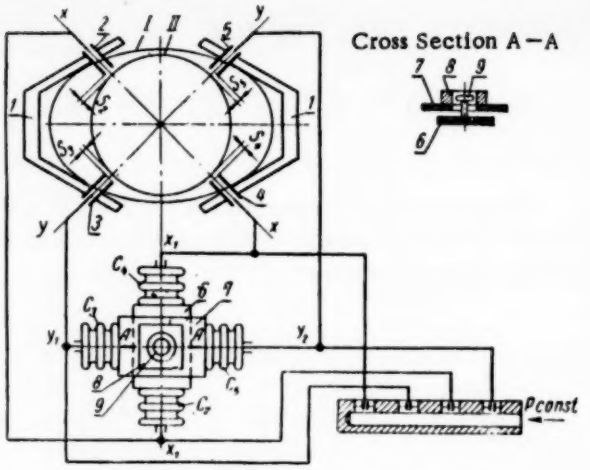

Fig. 2.

When an object with ideal coaxiality is checked (Fig. 1a), the indicator will show a variation of dimension equal to $i_1 = a - b$, where $a = \frac{A - D}{2}$ and $b = \frac{B - D}{2}$.

When the axis of the cylindrical surface is displaced by the amount i in the direction of the large or small axis of the ellipse, (Fig. 1b and 1c), the indicator will show a variation of dimension equal to $i_2 = i_3 = a - b + e$.

When the axis of the cylindrical surface is shifted by the same amount in a direction at an angle of 45° with respect to ellipse axes, the indicator will show a variation of dimension equal to $i_4 = a + e \cdot \sin 45° - (b - e \cdot \sin 45°) = a - b + 2e \sin 45°$; $i_4 = a - b + 1.41\ e$, i.e., for the same deviation from coaxiality e, the indicator readings will differ by 0.41 e.

Figure 2 shows a device for measuring coaxiality by means of a special pneumatic detector, which is free from imperfections of the "wobble" method of measuring the coaxiality.

On the elliptical surface I, two prisms 1) carrying four measuring nozzles 2), 3), 4), and 5) are installed diametrically opposite each other on two section lines X—X and Y—Y at a 90° angle against cylindrical surface II, whose coaxiality with surface I is being measured.

In the case where surfaces I and II are coaxial, the clearances between the nozzle ends and the surface II are equal among themselves ($S_2 = S_4$, $S_3 = S_5$).

If the surfaces are not coaxial, the equality among the clearances and the equality of pressure in corresponding bellows C_2 and C_4 and C_3 and C_5 of the detector are disturbed. Carriers 6) and 7) placed at an angle of 90° with respect to axes $X_1 - X_1$ and $Y_1 - Y_1$, are connected to the bellows. The disturbance of the equality of pressures in the bellows pairs causes the carriers 6) and 7) to move from their neutral position. A contact 8), made in the form of an inside cylindrical surface, is attached to carrier 7), and a contact 9) in the form of an outside spherical surface is attached to carrier 6). The radial clearance between these two surfaces is equal to the noncoaxiality tolerance, increased by the transmission ratio of the pneumatic system. In the case where the deviation from coaxiality exceeds the allowable value, contacts 8) and 9) close, and the signal "waste" is given.

The use of two carriers moving in a mutually-perpendicular direction and contacts in the form of cylindrical surfaces, permits the obtaining of correct measurement results by geometric addition, independently of the direction of the maximum eccentricity of axes.

ON THE ARRANGEMENTS OF LENGTH STANDARDS IN A SET

F. P. Volosevich

In the factory "Kalibr," plane-parallel length standards which are provided in a set of 87 pieces of various lengths up to 100 mm, are placed in a box in 8 rows (14 small plates in a row). In the factory Krasnyi Instrumental'shchik, the same plates are placed in 6 rows with 26 plates in a row.

Such a difference in the arrangement of plates in the set is not convenient, as the worker has again to remember each time the place of each plate.

Controller N. N. Belanov of the Kirov Plant Measurement Laboratory proposed a rational and uniform method of arranging the plates in a set, thereby making the work of controllers easier.

The plates should be arranged according to a determined scheme in 7 rows. The size of the box is not increased. In a way, the set is divided into two parts. On the left-hand side, in the first row, the protective plates are placed, in the second row, the millimeter plates with fractions in hundredths, in the third row those in tenths, etc. On the right-hand side, in the top row, plates from 1 mm to 10 mm are placed and further – the plates down to 0.5 mm and, finally, all the plates beginning with 20 mm.

Experience showed that the arrangement of plates proposed by N. N. Belanov makes it possible to use the set from a distance covered by the extended arm without looking at the marking plates and it proved to be very convenient in work.

The All-Union Government Standard 9038-59 for plane-parallel length standards regulates the composition of sets but does not indicate the way of their arrangement in a set.

The proposal of N. N. Belanov, permitting the standardization of arranging the plates in a set for convenience in work, should be also introduced in other plants.

From the Editor: The plant "Kalibr" already accepted this proposal.

ON THE THEORY OF ERRORS OF A SELF-COMPENSATING PRESSURE GAGE

V. I. Bakhtin

For an investigation of basic sources of error in a previously described bellows micromanometer (see [1]) based on the self-compensation measurement principle, let us consider the schematic diagram of this instrument (see figure).

The measured gas pressure Δp deforms the sensitive element consisting of two bellows. Small displacements of the sensitive element are registered by an electronic indicator. The voltage at the indicator output U_{ind} is amplified by a control unit to the magnitude U_{cu} and is fed to the terminal of the compensating mechanism which is, in the given case, a magnetoelectric device whose pulling force P acts on the sensitive element and balances the gas pressure. The reading indicator serves for measuring the compensating force, transformed into an electric quantity, which is proportional to the measured parameter Δp.

The errors of self-compensation measurements consist of self-compensation errors and errors in measuring the compensating force. In order to determine the self-compensation errors, let us write the equilibrium conditions for the parts of the measuring system of the pressure gage

$$\left.\begin{aligned} K_{se}\,\Delta W &= S\Delta p - P,\\ U_{ind} &= K_{ind}\Delta W,\\ U_{cu} &= K_{cu}\,U_{ind}\\ P &= \frac{K_{cm}}{R}\,U_{cu} \end{aligned}\right\} \qquad (1)$$

where K_{se} is the rigidity of the sensitive element, K_{ind}, K_{cu}, and K_{cm} are the coefficients of the indicator, control device, and compensating mechanism, respectively, R is the resistance of the winding of the magnetoelectric device, S is the effective surface area of the sensitive element, ΔW is the displacement of the sensitive element, U_{ind} is the voltage at the indicator output, and U_{cu} is the voltage at the output of control units.

The elimination of intermediate coordinates in the common system (1) yields:

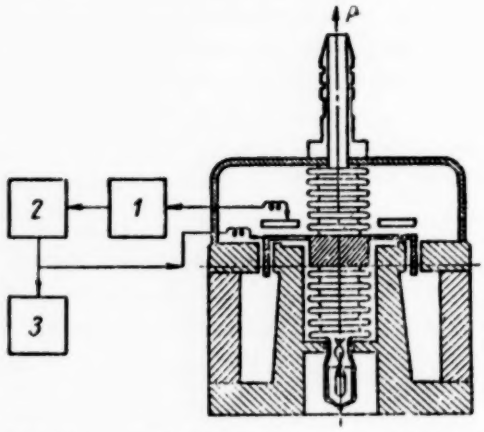

1) Indicator; 2) control unit; 3) reading unit

$$\frac{K_{se}\,R}{K_{ind}\,K_{cu}\,K_{cm}}\,P = S\Delta p - P.$$

Calculating the following magnitude from the right-hand and left-hand sides

$$\frac{K_{se}\,R}{K_{ind}\,K_{cu}\,K_{cm}}\,S\Delta p = \frac{1}{K}\,S\Delta p,$$

we have

$$\theta_{const} = S\Delta p - P = \frac{S\Delta p}{K+1}. \qquad (2)$$

where $K = \frac{K_{se}}{K_{ind} K_{cu} K_{cm}}$ is the transmission factor of automatic transmission linkages, and

where θ_{const} is the constant error of the proportional static self-compensation. The constant error decreases with an increase of K and increases when the pressure measured augments. For $K = 10^4$, we have $\theta = 10^{-2}$% of the measured quantity.

The hysteresis of the sensitive element is proportional, in the first approximation, to the displacement of the sensitive element. As

$$\Delta W_{max} = \frac{\theta_{const\ max}}{K_{se}},$$

the maximum error due to hysteresis in the working stroke of the sensitive element is equal to

$$\delta \Delta W^{wo}_{max} = \frac{a}{100} \cdot \frac{\theta_{const\ max}}{K_{se}}.$$

For the bellows, a = 8 – 15%, and for better membranes, produced in factories, a = 0.03-0.10%. For small displacements, in the most adverse case, the hysteresis error, expressed in units of force, will be equal to:

$$\theta^{wo}_{hys\ max} = \frac{a}{100} \theta_{const\ max}.$$

Immediately after unloading, this force is balanced by the pulling force of the compensating mechanism. Therefore,

$$\delta P^{wo}_{hys\ max} = \frac{a}{100} \cdot \frac{S}{K+1} \Delta p_{max} \qquad (3)$$

and, correspondingly,

$$\delta I^{max}_{hys\ max} = \frac{a}{100} \cdot \frac{S}{K_{cm}\ (1+K)} \Delta p\ max \qquad (3')$$

where I is the current passing through the winding of the magnetoelectric compensating mechanism. For a pressure gage of the bellows type with $K = 10^4$, a = 10%, and Δp = 100 mm Hg, the hysteresis error is equal to 10^{-3} mm Hg.

Obviously, beside the error due to hysteresis in the working stroke, there is the hysteresis error caused by the initial tightness of the sensitive element (the case where the electrical circuits were switched off). Let the total stroke of the sensitive element be limited to 0.3 mm for constructional reasons. Then

$$\delta P^{full}_{hys\ max} \quad \frac{a}{100} K_{se} \quad 0.3; \qquad (4)$$

and correspondingly:

$$\delta I^{full}_{hys\ max} \quad \frac{a}{100} \frac{K_{se}}{K_{cm}} \cdot 0.3. \qquad (4')$$

Therefore, the lesser the rigidity of the sensitive element, the smaller the error. For a modification with bellows of a pressure gage with K_{se} = 200 g/mm, $\delta P^{full}_{hys\ max}$ = 6g, or 0.2 mm Hg* for S = 20 cm².

Let us consider the self-compensation errors introduced by the drift of volt-ampere characteristics of electronic tubes and parameters of electronic components. The enumerated causes give rise to the following errors: δU_{ind}, δU_{cu}, δK_{ind}, and δK_{cu}. However, it is permissible to neglect the change in transmission factors: the calibration curves of two pressure gages with equal compensating mechanisms, but different K_{ind} and K_{cu} are equal to: **

$$I = \frac{S\Delta p}{\left(1+\frac{1}{K}\right)K_{cm}}.$$

The error in the control unit signal $\delta U_{cu} = K_{cu}\delta U_{ind}$ causes a change in the compensating force equal to $\delta P = K_{cm}\frac{\delta U_{cu}}{R}$ and a shift of the sensitive element by $\delta\Delta W$ until it reaches a new equilibrium position.

Eliminating the previous value $K_{se}\ \Delta W = S\Delta p - P$ from the new equilibrium condition for the sensitive element, we obtain:

$$K_{se}\ \delta\Delta W = \delta P^{x},$$

where δP^{x} is the actual change of the pulling force. It is obvious that

$$\delta P^{x} = \frac{K_{cm}}{R}\delta U_{cu}^{x} = \frac{K_{cm}\ K_{cu}}{R}\delta U_{ind}^{x}$$

Here, δU^{x}_{cu} and δU^{x}_{ind} are the actual changes of output signals as a consequence of the drift of the indicator parameters, as well as a consequence of the change in the data transmitter capacity when the sensitive element has moved by a distance $\delta\Delta W$. On the other hand, the change of the indicator signal due only to the change in the data transmitter capacity δU^{c}_{ind} is equal to: $\delta U^{c}_{ind} = K_{ind}\delta\Delta W$.

As

$$\delta U_{ind} = \delta U^{c}_{ind} + \delta U^{x}_{ind}$$
$$\delta\Delta W = \frac{\delta P^{x}}{K_{se}},$$

then

$$\delta U^{x}_{ind} = \delta U_{ind} - \frac{K_{ind}}{K_{se}}\delta P^{x}.$$

The substitution of the last relation in the expression for the force increase yields:

$$\delta P^{x} = \frac{1}{K+1}\cdot\frac{K_{cm}\ K_{cu}}{R}\delta U_{ind}$$

Correspondingly,

$$\delta I^{x} = \frac{1}{K+1}\cdot\frac{K_{cu}}{R}\delta U_{ind}.$$

* This error in bellows, as shown by experiment, can be considerably reduced by the application of alternating loading with a frequency of 1000 cps and an amplitude of 0.5 mm in 2000-3000 cycles.

** The analytical expression for the calibration curve can be easily obtained from the relation $\frac{K_{se}R}{K_{ind}K_{cu}K_{cm}}P = S\Delta p - P$ by substitution of $P = K_{cm}I$. It is equally valid for the bellows as well as the membrane pressure gages [4].

Or, as K >> 1, omitting the indices for P and I, we can write:

$$\delta P = \frac{K_{se}}{K_{ind}} \delta U_{ind} \tag{5}$$

$$\delta I = \frac{K_{se}}{K_{ind} K_{cm}} \delta U_{ind} . \tag{5'}$$

The change in the output signal of the control unit causes a change in the compensating force and a shift of the sensitive element by $\delta \Delta W$. By the same reasoning as in the previous case, it can be shown that

$$\delta P = \frac{K_{se}}{K_{cu} K_{ind}} \delta U_{cu}; \tag{6}$$

$$\delta I = \frac{K_{se}}{K_{se} K_{ind}} \delta U_{cu} . \tag{6'}$$

If errors in output signals of the indicator and the control unit are simultaneously present, it can be shown, by similar reasoning, that

$$\delta P = \frac{K_{se}}{K_{se}} \delta U_{se} + \frac{K_{se}}{K_{ind} K_{cu}} \delta U_{cu}, \tag{7}$$

$$\delta I = \frac{K_{se}}{K_{se} K_{cm}} \delta U_{ind} + \frac{K_{se}}{K_{ind} K_{cu} K_{cm}} \delta U_{cu} . \tag{7'}$$

Hence, the errors in self-compensation caused by the drift of output signals of the indicator and the control unit,* all other conditions being equal, are all the smaller, the smaller the rigidity of the sensitive element and the greater the transmission factors of the measuring circuit components. For a pressure gage for which K_{se} = 200 g force/mm, $K_{ind} = 10^3$ v/mm, K_{cu} = 10 for $\delta U_{ind} = \delta U_{cu}$ = 1 v, the error in self-compensation, on the basis of (7), is equal to

$$\delta P = 0.22$$

or

$$\delta P = 0.0007 \text{ мм Hg} \quad (\text{for } S = 20 \text{ cm}^2)$$

The errors δK_{cm} and δP of the compensating mechanism arise due to magnetic hysteresis, heating, aging of magnetic material, and other processes. These errors will cause the shift $\delta \Delta W$ of the sensitive element and the corresponding change in U_{ind} and U_{cu}. Then, the compensating force will change by δP^c. The measured change of the compensating force will be equal to

$$\delta P^x = \delta P - \delta P^c .$$

* The drift of output signals of the indicator and the control unit arises also due to a change in the feed source voltage (voltage variations in the city power supply). This source of errors does not basically differ in any respect from the drift of parameters of electronic parts and tube characteristics and is, therefore, not discussed in the article.

But, on the basis of (1), taking into account that

$$K_{se}\ \delta\Delta W=\delta P^{x},$$

we have

$$\delta P^{x}=\frac{(K_{cm}+\delta K_{cm})\ K_{ind}\ K_{cu}}{R}\ \delta\Delta W=$$

$$=K\left(1+\frac{\delta K_{cm}}{K_{cm}}\right)\delta P^{x}$$

and therefore,

$$\delta P^{x}=\frac{\delta P}{1+K\left(1+\frac{\delta K_{cm}}{K_{cm}}\right)}. \tag{8}$$

The actual variation of the compensating force due to the drift of the compensating mechanism parameters is $\left[1+K\left(1+\frac{\delta K_{cm}}{K_{cm}}\right)\right]$ times less than the variations which would be liable to occur if negative feedback circuits were not provided. Correspondingly,

$$\delta P^{x}=\frac{\delta P}{(K_{cm}+\delta K_{cm})\left[1+K\left(1+\frac{\delta K_{cm}}{K_{cm}}\right)\right]}. \tag{8'}$$

The error in the pressure gage output signal reduced by $(K_{cm}+\delta K_{cm})\left[1+K\left(1+\frac{\delta K_{cm}}{K_{cm}}\right)\right]$ times is equal to the absolute change of the compensating force if feedback is not provided.

It is characteristic that for a pressure gage for which $K = 10^4$, $\frac{\delta K_{cm}}{K_{cm}} = 0.1$, and $\delta P = 100$ g force, δP^{x} does not exceed 0.01 g force, i.e., for $S = 20\ cm^2$, $\delta P^{x} = 15 \times 10^{-4}$ mm Hg.

The changes in the surrounding medium temperature exert an influence on the operation of a self-compensating pressure gage mainly through the sensitive element and that part of the indicator where the mechanical displacement is converted to the capacitance change effect. In order to oppose the thermal expansion of the sensitive element, the system develops an definite force which actually is the error in the compensating force. The thermal expansion of the volume clearance of the indicator and the change in rigidity of the sensitive element can be neglected in the first approximation, as the volume clearance is not large in itself, and the variation of K_{se} can only change the small constant error in self-compensation. It is easy to show that for a sensitive element in the form of bellows the change of length with temperature is equal to

$$S\Delta W_{c}=l_{0}\ (\alpha_{c}-\alpha_{\partial})\ \Delta T$$

and in the case of a membrane sensitive element

$$S\Delta W_{M}\simeq r_{0}\sqrt{2\ (\alpha_{M}-\alpha_{K})\ \Delta T}.$$

Here, α_c and α_k are the respective coefficients of linear thermal expansion of the bellows and supports, supporting the condenser and the data transmitter plates (see description of the instrument, for instance, in [3]); α_m and α_k are the same coefficients for a membrane sensitive element; ΔT is the temperature change; l_0 and r_0 are the length and the radius of the membrane at normal temperature respectively.

When a self-compensation system is included, the displacement of the sensitive element due to temperature will be reduced by (1 + K) times. For this, it is necessary that the compensating force increases by the quantity

$$\delta P = K_{se} \frac{K}{K+1} \delta \Delta W; \tag{9}$$

and correspondingly, the current passing through the compensating mechanism winding will change by:

$$\delta I = \frac{K_{se}}{K_{cm}} \cdot \frac{K}{K+1} \delta \Delta W. \tag{9'}$$

Thus, in order to reduce the pressure gage errors due to temperature, it is desirable to have a sensitive element of minimum rigidity and to strive to compensate to the fullest possible extent its expansion with temperature by the expansion of the attached parts. It should be noted that for the developed pressure gages [1, 2, 3], the uncompensated movement of the sensitive element due to temperature was reduced to the amount of $7\text{-}8 \cdot 10^{-4}$ mm without special difficulties.

Analyzing (3), (4), (5), (6), (7), (8), and (9), relating the compensation errors with errors originated by individual pressure gage parts, we see that the errors acting on the system can be roughly divided into two categories, attributing to the first all those external factors which act on the pressure gage from outside through the sensitive element (here, apparently, are also included the friction in the sensitive element, vibrations and shocks, convection fluctuations, the microphone effect, etc., which we did not consider), and to the second, all the indicated internal instability factors of electrical components of the pressure gage. The influence of disturbances of the first category cannot be controlled or reduced by negative feedback circuits. The influence of disturbances of the second category can be controlled and reduced by feedback, and this all the more so, the farther the unstable element is located from the pressure gage input, if the direction "sensitive element – indicator – compensating mechanism" is taken as the positive direction of bypass. The error in measurements due to the instability of the farthest component – the compensating mechanism – is reduced (1 +K) times by feedback. The indicated circumstances should be taken into account when determining the tolerances for the operational instability of separate components of the instrument.

The given analysis of errors shows that if the electrical circuit of the pressure gage is 100% compensated by negative feedback, with a transmission coefficient of 10^4, ordinary components can be used; there is no necessity for using additional stabilizing devices in the circuit, including a stabilized feed source. It can be recommended that the powerful cascade of the control unit be fed directly from a 220 v power supply through a selenium rectifier and also that semiconductor devices and magnetic amplifiers be used in the measuring circuit. The size and the weight of the mechanical part of the pressure gage are mainly determined by those of the compensating mechanism. The smallness of compensation errors due to magnetic hysteresis makes it possible to replace the heavy and bulky magnetoelectric systems by miniature direct current electromagnets, where the pulling force is measured according to the degree of magnetization of the magnetic circuit by the induction method. In manufacturing the mechanical unit of the pressure gage, a sufficiently rigid construction with minimum clearances should be provided. It is necessary to provide devices for the limitation and regulation of the stroke, coaxiality, and the initial pull of the sensitive element. The threshold capacity of the measuring instrument is directly related to a careful compensation of the temperature expansion of the sensitive element by means of an equivalent expansion of attached components. Calculations showed that for a sensitive element in the form of a membrane, one should not strive for an extremely thin membrane, as it is better to install a somewhat thicker and reliable membrane, together with an additional electronic amplifier tube in a circuit which is 100% stabilized by negative feedback.

The results of investigating the basic errors of the self-compensation measurement principle justify the development of pressure gages constructed on the basis of this principle with the aim of introducing them in industry.

LITERATURE CITED

[1] V. I. Bakhtin, Priborostroenie No. 10 (1957).

[2] V. I. Bakhtin, Pribory i Teknika Eksperimenta No. 1 (1958).*

[3] V. I. Bakhtin, Ismeritel'naya Tekhnika No. 3 (1957).

[4] V. I. Bakhtin, Priborostroenie No. 1 (1959).

EQUIPMENT FOR HIGH PRECISION INVESTIGATION OF ANEROID SYSTEMS

K. P. Bychkovskii

The performance of aneroids is checked by means of an equipment consisting of a domed glass vacuum chamber with the aneroid element placed inside the chamber together with a manometer for measuring the pressure, and a cathetometer for determining the displacement of the mobile center of the aneroid element as a function of pressure.

Sometimes, instead of the cathetometer, a mechanical indicator with a scale division of 2 μ is used. Optical cathetometers have a scale division of 1.5-2.0 μ.

The mercury manometers used for measuring air pressure in the chamber provide an accuracy of 0.1 mm Hg.

The measurement errors of low-pressure gages with a balanced piston depend on the construction of the instrument. It is possible to measure pressure by means of such a gage with an error of 0.05% of the atmospheric pressure. Recently, a special low-pressure piston gage was produced whose error does not exceed 0.003% of the atmospheric pressure; the achievement of such accuracy is, however, beset with great difficulties.

In order to ensure such accuracy of measurements in all the pressure ranges the whole sensitive unit, including the multiplying mechanism drive and the thermocompensating system, must attain this accuracy in addition to the aneroid element itself. For checking the operation of such a sensitive unit and adjusting its thermocompensating device a special equipment was designed and constructed.

The equipment consists of a miniature thermobarometric chamber with a collimator device for observing the tested unit, a device with optical sighting, and a thermocompensation system for placing in it the aneroid elements under test, as well as a pressure gage system and an electrical supply circuit.

Such an equipment provides a measure of the pressure changes inside the chamber on the order of tenths of a millimeter of a water column, which corresponds to differences of fractions of a meter in height in the pressure of atmospheric layers close to the earth's surface. The aneroid elements tested in the equipment are designed to measure pressures corresponding to barometric heights of 0-10, 0-12, 0-15 and 0-20 km. When the aneroid elements are used for high precision measurements their errors are not usually required to be smaller than 50-100 m in differences of height at any height within a given range. Therefore there is no need to preserve high accuracy of pressure measurements throughout the range. It is sufficient to determine the height level with an error of 1 or 0.5 mm Hg and the deviations from that figure within the specified limits with the accuracy of the proposed measurements. Such measurements are carried out by means of two manometers,

*See English translation.

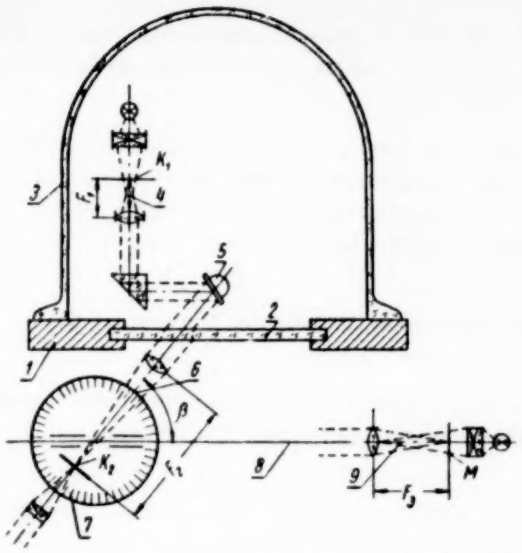

Fig. 1. 1) Base plate of the thermobarometric chamber, 2) glass of the chamber window, 3) glass dome, 4) illuminator which provides the sighting point, 5) glass on the axis of the crank-shaft-rocker mechanism, which is rotated by the aneroid element, 6) theodolite tube, 7) theodolite dial, 8) theodolite guiding rail, 9) collimator setting tube; F_1, F_2 and F_3 are the principal focal distances respectively of the illuminator, the theodolite and the setting collimator tube.

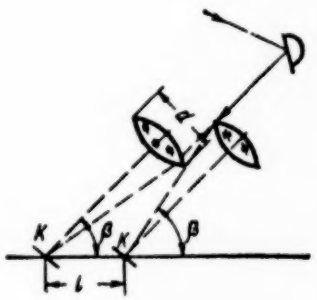

Fig. 2.

a mercury and a water manometer. For studying the operation of the sensitive device with the thermo-compensating arrangement continuously over the entire range only the mercury manometer is used with an additional device for increasing the accuracy of its readings. The fixed center of a modern aircraft aneroid element is displaced by only 0.12μ for a pressure change of 1 mm water column. This displacement produces a rotation of its crankshaft-rocker mechanism axle of about 4". This angle is measured in the instrument described by means of a theodolite. The angle measured by the theodolite is equal to twice the angle of rotation of the axis, which doubles the sensitivity of the device. The collimation method of observation with parallel rays outside the tube, and the small distance between the theodolite and the observed point provide a very accurate sighting for a comparatively rough centering of the instrument and a set focus of the tube. The glass of the chamber observation window must be plane – parallel. Any deviations in the flatness and a parallelism of its faces must correspond to the given accuracy of the angular measurements.

The optical arrangement of the system is shown in Fig. 1.

When the turning angle of mirror 5 is measured, the illuminator tube, the theodolite, and the collimator setting tube are all focused to infinity. Pane 2 is made of an optical glass plate with plane-parallel faces.

With a setting tube the accuracy of the guiding rail 8 of the slide to which the theodolite is fixed need not be very high, since in this case the device for moving the instruments isn't used for measuring the angle; if, however, it is made with the required accuracy, there is no need for the setting tube.

Since in the space between the tube objectives the image is transmitted by parallel rays, an accurate positioning of the theodolite on its guide is not required. The instrument functions in any part of the section determined by the effective diameter of the tube objective and the angle between the direction of the guide and the line of sighting $l = f(d, \beta)$ (Fig. 2).

Angle β is measured by making cross hairs K_2 of the theodolite coincide with setting point M of the collimator and the cross hairs K_1 of the illuminator (Fig. 1).

The coincidence of cross hairs K_1 and K_2 will hold in any position of the theodolite along the guide within the limits of l, if the guide is made with the required degree of accuracy, otherwise angle β must be measured at one point only.

The limiting angle between the direction of the guide and the optical axis of the setting tube is

$$\delta = \arcsin \frac{d}{z},$$

where d is the effective diameter of the theodolite objective, and z is the working length of the guide.

The manometric arrangement of the equipment and the electrical supply circuit is shown in Fig. 3.

Pressure in the vacuum chamber is checked by manometer 9. In order to preserve the vacuum tap No. 1 must be closed. If tap No. 2 across the U-shaped water manometer is opened, small pressure variations in the chamber with respect to cylinder 8 can be measured by the water manometer.

By operating the pump and taps 1 and 3 it is possible to establish the required pressure difference in magnitude and sign between the chamber and cylinder 8. By opening tap 2 the pressure between the chamber and the cylinder is equalized. Thus pressure variations in the chamber can be measured at various pressure levels. The large volume of cylinder 8 ensures a stable pressure in the chamber despite the movement of water in the manometer over the whole measuring range.

In order to decrease the effect of vapor on the accuracy of measurements, manometer 7 is covered with dibutylphthalate.

So as to increase the accuracy of the mercury manometer reading a sight is mounted on micrometer spindle 10. The latter is fixed to a clamp which is hinged to a collar which moves along rod 15. The micrometer thimble division is 0.01 mm.

The temperature inside the chamber can be reduced to −40 to −50°C by means of dry ice packed between the glass dome 4 and the walls of the removable thermostat 3.

For even distribution of temperature over the glass dome it is covered with a sheet of copper. The temperature inside the chamber is measured by a normal spirit thermometer with scale division of 1°C; the temperature is read through the window of the chamber.

The device for fixing the aneroid element and the illuminators is attached to a special table inside the chamber.

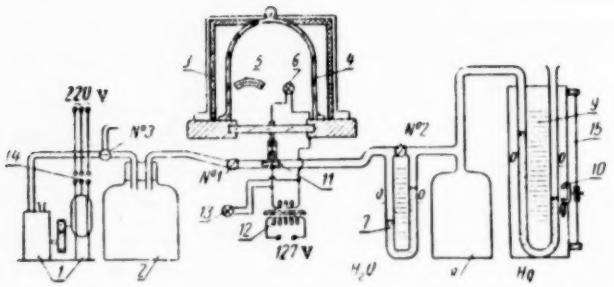

Fig. 3. 1) Vacuum pump with an electric motor, 2) cylinder for controlling the pressure of the system, 3) thermostat, 4) glass dome of the vacuumchamber , 5) thermometer, 6) illuminator lamp, 7) water manometer, 8) cylinder which stabilizes the pressure, 9) mercury manometer, 10) micrometer reading device, 11) metal T-joint for electric supplies to the chamber, 12) stepdown transformer, 13) lamp for lighting the theodolite scale, 14) motor switch, 15) rod; Nos. 1, 2 and 3 operating taps.

Figure 4 shows the movement of the aneroid unit for pressure variations of ± 50 mm of the water column from the initial pressure corresponding to a height of 1000 m. The curve has been plotted from the mean values of the direct and reverse movements. The rotation of the axis of the crankshaft-rocker mechanism was measured by means of a theodolite calibrated in degrees.

The difference between the angles read in the forward and reversed directions at intervals of 10 mm of the water column did not exceed 0.15% of the angle corresponding to that pressure difference.

H m	$\Delta\alpha^c$	$\frac{\Delta\alpha}{\Delta H}$, c/m
+55	2.5	0.5
+50	5.0	0.5
+40	4.85	0.48
+30	5.25	0.52
+20	5.25	0.52
+10	5.0	0.50
0	5.5	0.55
−10	5.25	0.52
−20	5.25	0.52
−30	5.15	0.52
−40	5.4	0.54
−50		
	Mean	0.52

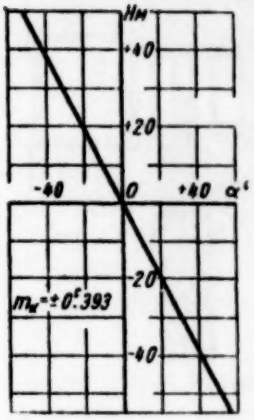

Fig. 4.

On the basis of the mean square values of errors m_α (in centigrade) and the data of the crankshaft-rocker mechanism it was established that the flexure of the unit corresponding to 10 m of height difference was measured with a mean square error of ± 0.5 μ, which amounts on an average to 1 m of barometric difference in height.

On an average in the three levels of measurement (1000, 4000 and 8000 m) the mean square error of the sensitivity coefficient of the unit $K_H = \Delta\alpha / \Delta H$, obtained in a test installation, amounted to ± 0.02 cm/m. It means that, if the error of the multiplying mechanism be neglected, barometric difference in height of 1 m will be measured by this instrument with a mean error of 4 cm.

The accuracy of measurements for differential investigations can be increased relatively easily; for this purpose it is necessary to raise the accuracy of reading of the water manometer (in the experimental installation this manometer provided an accuracy of 1 mm of the water column) and use a more accurate theodolite. In our experiments this, however, was not necessary since the errors in barometric meter height difference due to atmospheric causes are always greater than 4 cm.

PIEZOELECTRIC ACCELERATION TRANSDUCERS

V. P. Nenyukov, A. S. Zhmur and G. L. Lyapin

The piezoelectric quartz transducer described below is designed for recording acceleration of shock nature. The transducer is assembled in a cylindrical steel body whose bottom end has a conical thread for fixing the transducer to the object under test. The upper part of the body has a hexagonal shape.

Inside the transducer body there is a cylindrical channel (Fig. 1) into which a plexiglas sleeve is pressed which insulates the piezoelectric plates from the steel body. For a more even distribution of pressure a hardened and carefully ground-in steel lining is placed under the bottom plate.

An intermediate plate which provides inertia is placed between the quartz plates. Both faces of the intermediate plate are also ground down and tested against a glass gage. A hardened steel cover is placed over the top plate. The bottom surface of the cover is ground flat, but the top one is made spherical to provide a more even distribution of the initial pressure, attained by a threaded plug. For the convenience of tightening up, the thread should be fine.

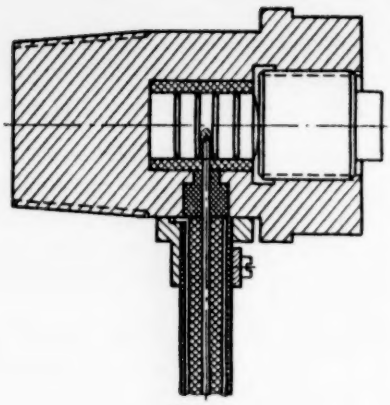

Fig. 1.

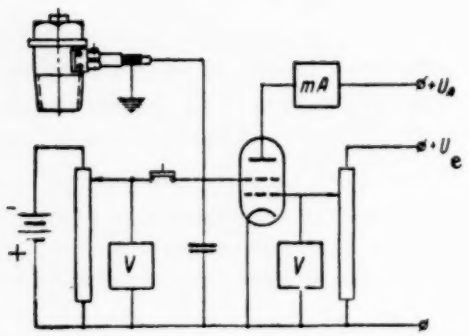

Fig. 2.

In order to avoid losing contact between the intermediate and the quartz plates the initial compressing force should be greater than the maximum force of inertia of the intermediate plate. Moreover, the initial compressing force should be chosen not to exceed, together with the force of inertia, the maximum permissible load on the piezoelectric plates.

The permissible mechanical compressing force for piezoelectric plates depends to a great extent on the quality of the grinding of faces. With above construction of the transducer and the use of well-ground quartz plates it is possible to recommend a compressing force of 1200 kg, which corresponds to a pressure of 1500 kg/cm².

Such a transducer provides measurements of acceleration from 20 to 200000 g. The sensitivity of the transducer is practically the same over the whole range.

For an increased sensitivity, barium titanate plates can be used. In connection with the marked affect of temperature on the piezoelectric properties of barium titanate its range of application is limited to laboratory conditions.

The simplest method of eliminating the temperature effect is by calibration immediately before each measurement. By means of this method it becomes often possible to use barium titanate transducers under industrial conditions.

When barium titanate elements are used in above transducer it is recommended to adjust the initial compressing force to 500 kg, which corresponds to a pressure of 700 kg/cm².

The natural frequency of a transducer with barium titanate elements will be a little lower than that of quartz transducers.

The assembly of piezoelectric transducers required great care. Before assembling, the polished surfaces of quartz plates are washed with alcohol and then dried. After this treatment it is not recommended to touch them by hand.

In assembling the plates it is necessary to place them in such a way that the intermediate plates should receive a negative potential. The positive charges which arise at the opposite ends of the quartz plates are taken to ground via the body of the transducer.

In the piezoelectric transducer circuit it is possible to use an electrometer tube (Fig. 2). In this circuit the grid of the electrometer tube is connected to the intermediate plate of the transducer and also to the scale capacitor.

Before starting measurements the control grid is supplied (by throwing the switch) through a special potentiometer with a voltage equal to that on the free grid. This minor complication of the circuit is necessary for greater stability of operation of the electrometer tube.

A measuring instrument which shows the value of the anode current is connected in the anode circuit of the tube. By adjusting the voltage on the cathode-grid the anode current of the tube is set to its maximum value. The deflection of the pointer is noted. Next, a load corresponding to the required compression force is placed on the transducer by means of a universal test machine or weights.

With the compressive load the grid of the electrometer tube becomes charged negatively and the current in the anode circuit is reduced. The value of the scale capacitor is chosen in such a manner that the difference

between the anode current for the loaded and unloaded conditions is large enough for a convenient reading without blocking the tube.

The transducer plug is tightened until the instrument pointer reading becomes the same as for the corresponding load.

By means of a dynamometer wrench the compression force of a piezoelectric transducer can be measured from the impression of steel ball in a brass crusher. For this purpose a brass core is placed inside the transducer with a a steel ball over it. To prevent the ball slipping during compression it is placed in a centering socket. The appropriate load is conveyed to the ball by means of hardened rod. After an exposure (30 sec) the load is removed and the imprint on the brass crusher measured. Next,the force which produces a similar imprint is measured (by means of the dynamometer wrench). In tightening subsequent transducers only the readings of the dynamometer wrench are used.

When the construction of the transducer has been established,the tightening is done by means of an ordinary wrench. After each tightening movement of the wrench the natural frequency of the transducer is measured. The tightening is considered to be completed when the natural frequency of the tested transducer becomes the same as that of a reference transducer assembled by one of the two methods described above.

Since the quartz transducer is designed to work in field conditions, it is filled with paraffin before tightening.

Experimental investigation established that the natural frequency of the transducer is equal to 39000 cps. The transducer oscillations were shock excited. A cathode-ray oscillograph with mechanical scanning was used for recording.

Since the transducer damping coefficient is close to zero, it can be recommended for recording periodic sinusoidal oscillations with a maximum frequency of 10000 cps.

For a number of shock processes it is possible to evaluate the applicability of the acceleration transducer from the duration of the contact and the shape of the curve. If as a first approximation it is assumed that the rise and fall of the deformation in a shock vary along a curve resembling a sine wave, the contact duration can be determined as half a period. Owing to the bad damping of the piezoelectric transducers,above instruments can be recommended for recording acceleration of shock phenomena only if their natural period of oscillation is about one-tenth of the contact time.

Experiments have confirmed the small effect produced on the quartz transducer by temperature and humidity. This circumstance provides the possibility of calibrating once for a complete series of experiments.

The capacity of a quartz plate 10 mm in diameter and 4 mm thick is 0.8 $\mu\mu$f. With two plates the total capacity of the system will be 1.6 $\mu\mu$f. This low capacity requires an amplifier with a very large input impedance. Experience has shown that the use of an electrometer tube is not always convenient and efficient. In order to make the input time constant sufficiently large,the input capacity is increased by connecting in parallel with the transducer a scaling capacitor. The scaling capacitor decreases the input signal amplitude, but at the same time improves the characteristic of the input circuit at low frequencies. Since the signal received from the piezoelectric quartz transducer is sufficiently large, the connection of the scaling capacitor does not create additional difficulties in designing the amplifier.

The capacity of the scaling capacitor is usually chosen between several hundred and 5000 $\mu\mu$f.

When the transducer is far removed from the amplifier and the recording instrument the capacity of the leads can replace the scaling capacitor. If a coaxial cable is used for connecting the transducer to the amplifier their separation can be as large as 100 m, without a need for cathode followers installed at the transducer end.

The use of coaxial cables type RK-1, RK-2,or RK-3 is recommended in view of their good shielding against interference coming from electrical installations.

It is very important for the reliable operation of transducers designed to measure large accelerations to provide a sufficiently strong fixture for the output cable. In the above equipment the output cable is fixed by means of a steel clip fastened to the body of the transducer with two screws.

The weight of the inert body in this transducer is 1.2 g. With an acceleration of W = 1000 g the voltage which is formed on the surface of the quartz plates and fed to the amplifier grid is 0.1 v with the scaling capacity of 500 μμf. In view of the high sensitivity of the piezoelectric transducer the amplifiers working with them have, usually, a low gain.

A good insulation of the output cable with respect to ground is a great importance for reliable operation of the piezoelectric transducers. The best materials for this purpose are polished amber, polystyrene, and plexiglas.

DETERMINING THE NATURAL FREQUENCY OF VIBRATORS

Yu. P. Dobrolenskii

In order to determine the dynamic errors of a vibrator oscillograph, it is necessary to know the natural frequency of a damped vibrator and the degree of damping, which is not listed in the vibrator certificate.

The experimental determination of the natural frequency of a vibrator is difficult and in practice only the amplitude error is determined from an experimentally obtained amplitude-frequency characteristic of the vibrator. Phase errors are ignored and this is often inadmissible.

A method of determining the natural frequency of a vibrator is briefly described below and the results of determining the natural frequencies of various vibrators are given.

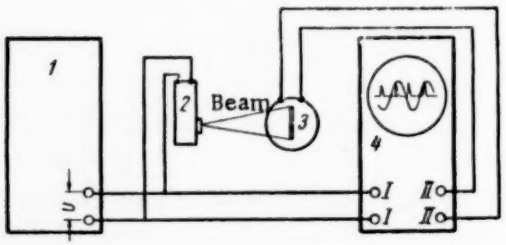

Fig. 1.

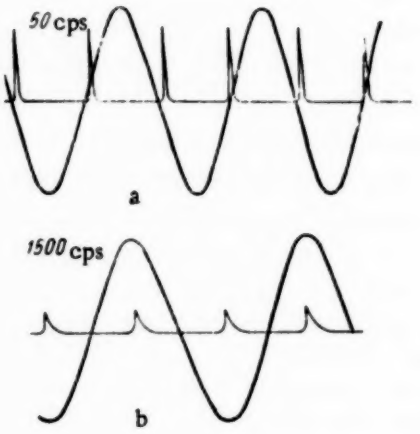

Fig. 2.

The idea of the method consists in measuring the phase difference between the sinusoidal voltages fed to the input of the vibrator and the angular oscillations of its mirror. By means of this method a complete phase-frequency characteristic of a vibrator can be obtained. For the determination of the natural frequency, however, it is only necessary to find on this characteristic a point which corresponds to a phase difference of 90° (condition of resonance).

The block schematic of the installation for determining the natural frequency of a damped vibrator is given in Fig. 1.

Voltage U is fed from an audio frequency oscillator 1 to vibrator 2 and terminals I of the dual beam oscilloscope 4. The voltage induces oscillations in the moving part of the vibrator which is fixed in its holder to the oscillograph. In each cycle the beam passes twice across the slit in the screen in front of photomultiplier 3; the photomultiplier used was of the FÉU-19 type, which generated for each period two voltage pulses transmitted to terminals II of the dual beam oscilloscope.

Vibrator type	Sensitivity mm/ma	Natural frequency in air f_0, cps	Natural frequency of a damped vibrator fy, cps	$\frac{f_0}{f_y}$
I	1,5	5500	3300	0.6
II	6,0	10000	6200	0.62
III	2,2	2500	1500	0.6
IV	0,3	3000	2000	0.67
V	0,11	2000	1200	0.6
VI	1,3	500	300	0.6

If at a very low frequency (10-20 cps) the above pulses are made to coincide with the zero line of the voltage U sine-wave on the oscilloscope screen, they will lag increasingly behind the sine-wave with rising frequency.

The frequency at which this phase difference reaches 90° will be, as already stated, the natural frequency of the vibrator. The frequency is read off the oscillator scale.

Figure 2 shows the picture seen on the oscillograph screen at a low frequency (a) and at resonance (b).

The table above gives data obtained in testing by this method six types of vibrators.

MEASURING EQUIPMENT FOR INVESTIGATING THE PROCESS OF ROCK COMPRESSION FILLING

G. F. Lyubenko

The equipment here described was used for measuring pressure on the floor and the roof of strata layers being filled in by a ZMD machine, and the residual pressure after compression.

The hydraulic compression filling machine ZMD of the DonUGI (Fig. 1) is made in the shape of a cylinder with a propelling piston inside it; a loading hole, for a hopper, is made in the side of the cylinder, and at the end an unloading hole. In operation the machine is placed across the working, which is being cut so that the mouth of the load chamber opens out into the cleared space. The filling material is brought to the hopper by a conveyor, a loading machine, a transporter, or by hand. In the idle stroke of the ramming piston, the loading window is opened and the rock fills the chamber. In the working stroke, the rammer compresses the rock under heavy pressure into the loading space.

The reaction to the effort exerted in embedding the rock is taken up by a thrust base. The machine is moved by means of a special winch.

For investigating the compression process the DonUGI workshops in conjunction with the tensometric and electrical measurements laboratory produced special electrical dynamometers of the DonUGI design with sensitive resistance type transducers which provide a recording of signals directly on an oscillograph without an amplifier or their indication by pointer instrument for visual observation.

The operation of the electrical dynamometer DonUGI is based on the property of wire to change its ohmic resistance due to strains in it within the elastic limit. The operating transducers R_1 and R_3 and the compensating ones R_2 and R_4 are interconnected in a bridge circuit (Fig. 2). Voltage U measured on a voltmeter is connected from a battery to the supply diagonal of the bridge. The supply circuit of the bridge contains a switch and a fuse.

The loop of oscillograph L and a microammeter are connected in parallel to the measuring diagonal of

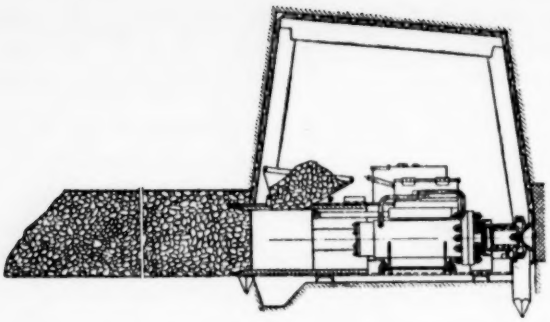

Fig. 1.

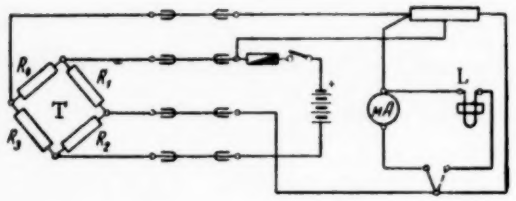

Fig. 2.

the bridge. The measuring instruments are connected through a switch, which provides the use of either the oscillograph for recording or the microammeter for observing the signals. A potentiometer is connected in parallel with the measuring diagonal, its resistance is 10-15 kilohms and it is designed to balance the bridge.

The dynamometer transducers are connected to an amplifier. It is possible by means of oscillograph MPO-2 to record on a film at definite intervals the pressure in the filling rock or that of the filling rock against the floor and roof of the layer (the transducers are calibrated for pressure).

During filling, pressure is continuously recorded on a film as a function of time (the film moves at a definite speed). The speed of the ZMD machine rammer can be considered, sufficiently accurately for our purpose, as constant. Hence the recording can be represented as a function of the rammer's movement.

The oscillograms obtained on a film are then enlarged on photographic paper. The rammer movement is plotted horizontally and the pressure vertically. The area bounded by the pressure curve and the Y-axis (movement) represents, if taken to a certain scale, the work done by the rammer loaded with the rock. This area is measured by means of a planimeter.

In the course of investigating the filling machine in the pit, pressure was measured on the roof and floor, the end and side walls of the filling space, inside the filling mass itself, and on the supports left in the filling space.

The DonUGI has developed a special stand with electrodynamometers for measuring pressure on the roof and floor during pressing-in of the rock. These dynamometers work in conjunction with electronic indicators ÉI-1. The basic component of the dynamometer is a plate; it stands freely on a hard welded frame and is placed together with the frame flush with the surface of the floor of the working (with the stand base). Four tensometric transducers are suspended underneath it in the strain zone. The transducers are hermetically sealed by means of carbinol paste (carbinol adhesive with cement) and bitumen lacquer. The tensometric transducers are interconnected in a bridge circuit, the two operating transducers are placed in the middle of the plate and the compensation transducers on a special bracket.

When the rock is being pressed-in, the lower strands of the plate become extended, producing a strain in the wires of the operating transducers. This produces a total resistance change which is proportional to the strain. The change in the resistance unbalances the bridge. The unbalance voltage is compensated by means of a balancing device which has a scale calibrated in relative units. The bridge is balanced either by means of earphones or an indicating instrument. At balance the reading of the compensating device scale is noted.

Calibration of the instrument provides the required factors for converting the scale readings into values of force. The calibration chart compiled from this data shows a linear relationship between the applied load and the compensator scale reading.

Several types of bodies were used for the transducers.

A channel iron was the simplest of them. Steel strips were welded to the inner walls of the channel iron, and square plates with transducers fixed to them were freely placed on the strips at regular intervals. The transducers were isolated from dust and moisture by means of a glycerin bath inside a special cover screwed to the main plate.

The dynamometers were placed parallel to the direction of the movement of the material from the point at which it left the machine.

The leads from the transducers and the potentiometers with their scales were led out to a place where an observation point was installed.

At each meter of the filling separate transducers were placed. In order to ensure safety of operation the equipment was placed in an explosion-proof covering which also provided good waterproofing for the transducers. As the result of tests it was established that the dynamic pressure of the rock at the end of compression of one discharge of the ZMD machine attains at the first meter of the filling 130 t/m^2, and as the machine stops the pressure suddenly drops to 120 t/m^2. This pressure is maintained for a long time almost without change, dropping slightly in the first ten days and increasing again in the next thirty days due to the pressure of the strata on the filling. Similar pressure measurements were made at the 2nd, 3rd, 4th and 5th meters of the filling space. At the last (5th) meter the pressure dropped to 50 t/m^2. The nature of the changes measured by the transducers at the 2nd, 3rd, 4th and 5th meters was the same as that of the first transducer.

The nature of the caving in of the roof and the floor of the filling was also studied by means of the ZMD. In two weeks, the roof caved in at one of the props by 2.1 cm and at another by 1.8 cm.

These very useful measurements show that the pressed-in filling block during and after laying exerts considerable pressure on the roof and floor of the layer owing to its compression, i.e., it performs the function of a prop; moreover the caving in of the roof is very small.

AN ASPECT OF THE EFFECT OF TEMPERATURE ON THE RESISTANCE OF A CONDUCTOR COVERING A SURFACE

B. I. Puchkin

It is often necessary in the course of physical experiments to study the electrical properties of thin conducting layers fixed to a hard surface, and obtained by means of sputtering, deposition in vacuum, galvanically or otherwise. In this study an important part is occupied by the effect of temperature on the electrical resistance of these layers. The work published on this question does not mention, however, the effect on the resistance of different coefficients of linear expansion of the layer and the underlay.

Let us use the expression representing the effect of temperature on the resistance of the conductor (C) rigidly connected to the surface (S) of an underlay which is not mechanically loaded [1]:

$$\frac{dR}{R_0}=\left\{\left(\frac{1}{\rho_0}\cdot\frac{\partial\rho}{\partial T}\right)_C-\left(\frac{1}{l_0}\cdot\frac{\partial l}{\partial T}\right)_C+\right.$$
$$\left.+\kappa^+\left[\left(\frac{1}{l_0}\cdot\frac{\partial l}{\partial T}\right)_S-\left(\frac{1}{l_0}\cdot\frac{\partial l}{\partial T}\right)_C\right]\right\}dT,$$

where R is the resistance of the conductor; l is its length; ρ is its resistivity; k^+ is its strain-response coefficient; T is temperature.

Subscript 0 denotes that the variable is taken at its initial temperature T_0.

In studies at a certain degree of accuracy it is obviously desirable to consider temperature changes due to above cause, especially for substances with a small resistance temperature coefficient and a large temperature strain response. Despite the importance of this question its solution is made more difficult owing to the fact that the data on strain response is given in the technical literature only for wires*. It seems therefore most expedient to develop on a wide scale the study of the temperature strain response of various thin conducting layers. This work is becoming increasingly important at present since the study of the temperature strain response of thin layers is finding practical application in measurement techniques.

LITERATURE CITED

[1] W. Sotman, Archiv für Technische Messen, 260, 197-200, 249-252, 1957.

[2] G. K. Kuchinsky, Phys. Rev. No. 1, 1954.

REPRODUCIBILITY OF THE BOILING TEMPERATURE OF OXYGEN

M. P. Orlova

The low reference point of the international temperature scale is the temperature of equilibrium between liquid oxygen and its saturated vapor at an atmospheric pressure derived from the formula

$$t_p = t_{760} = 1.26 \cdot 10^{-2} \cdot (p - 760) - 0.065 \cdot 10^{-4} \cdot (p - 760)^2,$$

where p is the pressure of the saturated vapor of pure oxygen.

With the development of work at low temperatures the requirement of accuracy of calibration at the temperature of liquid oxygen increased and thus arose the problem of revising the method of reproducing this temperature.

Secondary thermometers are usually calibrated against a condensation thermometer filled with pure oxygen. The basic errors in this method of calibration are due to the instability of the temperature of the oxygen bath filled with industrial liquid oxygen which contains nitrogen (up to 0.7%) as its main admixture. In the course of evaporation the content of nitrogen decreases and changes the boiling temperature of the bath, which acquires a temperature "drift." Moreover, the bottom layers of the oxygen bath acquire a considerably higher temperature (up to 1.5°) than that of liquid oxygen equilibrium under atmospheric pressure. The excess temperature is periodically equalized by the formation of a large number of vapor bubbles, which produces temperature fluctuations in addition to the even "drift." Since the condensation thermometers have a considerably greater inertia than the platinum resistance thermometers (the inertia of a platinum thermometer of P. G. Strelkov's design approaches 9 sec, whereas that of a condensation thermometer from 18 to 20 sec) the calibration of these secondary thermometers by means of such a bath is not sufficiently accurate.

In 1948-1949 the MGIMIP* laboratories developed, for producing the oxygen point, the required method and equipment, which were subsequently widely applied in precision measurements carried out in the same laboratory, and which proved to be satisfactory.

Below we describe the design of the equipment and give the results of calibrating platinum thermometers at the oxygen point.

Oxygen Condensation Thermometer. The construction of the oxygen condensation thermometer was slightly changed as compared with the previous model (its schematic diagram is shown in Fig. 1). In order to be able to check the purity of oxygen of various fillings by the difference in vapor compressibility, two oxygen condensation thermometers a and b protected by vacuum jackets were used. The protection was provided in order to prevent possible condensation of oxygen at the upper level of the bath. The beaker of the condensation thermometer is made of platinum foil in order to improve heat exchange between the thermometer and the bath. The manometer is connected to the thermometers by means of flexible copper capillary tubes. The capillary tube (internal diameter – 1 mm) is connected to a glass manometer by means of a copper-glass joint. The flexible connection by means of capillary tubes provides the possibility of lowering the condensation thermometer into various containers to different depths (for instance, makes it possible to measure the temperature distribution in an oxygen bath).

*MGIMIP = Moscow State Institute of Mechanical and Measuring Instruments.

The manometer mercury oxidizes readily and the meniscus surface becomes covered with an oxide film, which under the pressure of the mercury sticks to the inside surface of the manometer tube and makes the observation of the mercury level extremely difficult. The oxide film is removed by means of a device c, described by R. Scott in 1940, which clears the mercury surface of the film and keeps the manometer clean. The manometer tubes d, e, f and g are made of chemical glass. Since their diameters are 20 mm the correction for the height of the meniscus is negligibly small.

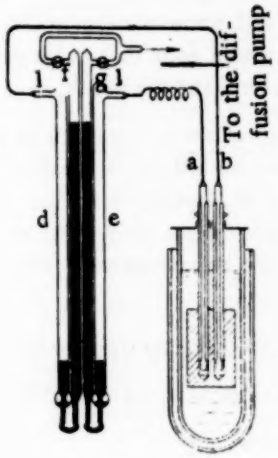

Fig. 1.

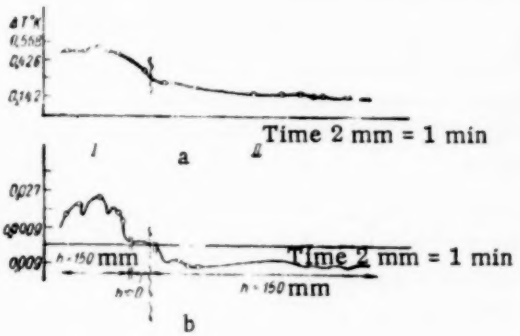

Fig. 2.

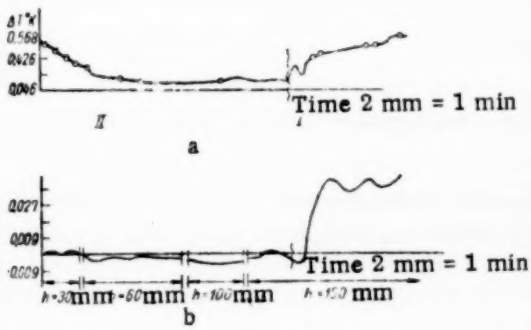

Fig. 3.

The manometer bends f and g are interconnected; through tap h they can be evacuated using a diffusion pump. This is necessary, since the mercury of the condensation thermometer absorbs oxygen which can destroy the vacuum in these bends and introduce an additional measurement error. When the manometer of the oxygen thermometer is filled with mercury and oxygen, care should be taken that no traces of air penetrate into the oxygen. Before filling, the whole system should be conditioned during 48 hours by heating the glass and metal parts up to 200-300°C under constant evacuation. Following this operation they are filled with mercury. The mercury is pumped in under vacuum, and then the system is filled with pure oxygen at a small pressure, 20-30 mm Hg, obtained by decomposition by heat of potassium permanganate. Oxygen is evolved at 230-245°C and its purity is subsequently checked by means of two condensation thermometers. It was established that possible impurities produced a difference in the thermometer readings not exceeding $2 \cdot 10^{-3}$ °C.

Investigation of an oxygen bath temperature operating conditions. It is very difficult to obtain in liquid oxygen baths a constant temperature and an absence of temperature gradients. We obtained favorable results by decreasing heat exchange between the bath and the ambient medium.

For this purpose we increased lagging by an additional external Dewar flask filled with oxygen (Fig. 1). Figures 2-4 show the test results of the oxygen bath temperature operating conditions. Figures 2 and 3 show the variations with time of the liquid oxygen overheating, i.e., the difference of the temperature measured in the oxygen and the temperature of equilibrium under atmospheric pressure.

The upper and the lower curves of Fig. 2 show the variations of the temperature difference between two condensation thermometers lowered into the inner oxygen bath at a vertical distance from each other of h = 150 and h = 0 mm. The lower curve b shows the condition prevailing when the bath is boiled by means of a heater placed under Dewar flask. Curve a shows the condition when the bath is not boiled. Section I corresponds to tests without the external Dewar flask. Section II shows the results obtained with the flask. The vertical temperature distribution in the bath with and without the external lagging is different. Lagging decreases the vertical temperature gradient and at the same time increases the internal temperature stability of the bath. Figure 3 shows curves similar to Fig. 2. The vertical distance h between the condensation thermometers is equal to 30, 60, 100, and 150 mm. Figure 4 shows the bad effect due to the boiling device most commonly

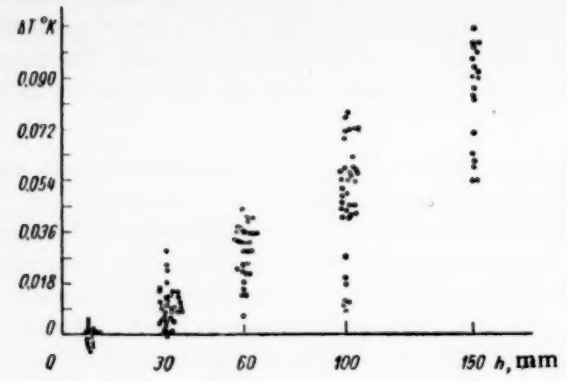

Fig. 4.

used in stabilizing the temperature of oxygen baths; the groups of points indicate the temperature differences of the condensation thermometers at various time intervals.

In order to equalize the vertical temperature gradient in the bath, both the condensation and the platinum thermometers were placed in holes in a copper block and covered with vacuum cement (Fig. 1). The frozen cement provides a good thermal contact between the thermometers and the block.

Reproducibility of the calibrations at the oxygen point. We calibrated a platinum resistance thermometer No. 21/1 of P. G. Strelkov's design. The thermometer has a helical quartz body. The sensitive element is made of platinum wire of 0.050 mm in diameter. The resistance of the thermometer at the temperature of melting ice is on the order of 100 ohms.

Pure platinum, brand IONKh-3, with a ratio of $R_{100}/R_0 \geq 1.39191$ was used for making the wire.

The temperature was measured with such a thermometer which had an error of about 0.0001°C.

The results of calibration at the oxygen point are given in the table below.

No. of experiment	W_{O_2}	v	v^2
1	0.245500	$+4.5 \cdot 10^{-6}$	$20 \cdot 10^{-12}$
2	0.245002	$+6.5 \cdot 10^{-6}$	$42 \cdot 10^{-12}$
3	0.245497	$+1.5 \cdot 10^{-6}$	$2.2 \cdot 10^{-12}$
4	0.245487	$-8.0 \cdot 10^{-6}$	$64 \cdot 10^{-12}$
5	0.245502	$+6.5 \cdot 10^{-6}$	$42 \cdot 10^{-12}$
6	0.245495	$-0.5 \cdot 10^{-6}$	$0.25 \cdot 10^{-12}$
7	0.245491	$-4.5 \cdot 10^{-6}$	$20 \cdot 10^{-12}$
8	0.245490	$-5.5 \cdot 10^{-6}$	$30 \cdot 10^{-12}$

In addition to the experimental values of errors their calculation means of formulas and tables given in [1] is also provided.

$$S_r = \kappa(\alpha, n)\sigma_r \text{ and } S_i = \kappa(\alpha, n)\sigma,$$

where σ and σ_r are the mean square errors; S_i is the error of a single measurement in calibration; S_r is the error obtained as the result of calibration.

Coefficient k which depends on the probability α and the number of observations n is determined from the table [1]. The probability that the value of the error in question does not exceed the given value is taken to be 90%.

$$\Sigma v = 0.5 \cdot 10^{-6}\ ;\ \Sigma v^2 = 220 \cdot 10^{-12};$$

$$\sigma = \pm\sqrt{\frac{\Sigma v^2}{n-1}} = \pm 5.6 \cdot 10^{-6}\ ; \qquad (\kappa = 1.895);$$

$$\frac{\Sigma W_{O_2}}{n}=0.245495;$$

$$\sigma_r=\pm\frac{\sigma}{\sqrt{n}}=\pm 2\cdot 10^{-6};$$

$S_r = \pm\ 4\cdot 10^{-6}$ which amounts to $\pm$ 0.001°; $S_1 = \pm\ 11\cdot 10^{-6}$ which amounts to $\pm$ 0.003°; $W_{O_2} = 0.245395 \pm 0.000004$, where $W_{O_2} = R_{O_2} / R_0$.

The reproducibility of the oxygen point in degrees amounts to $\pm$ 0.003°.

LITERATURE CITED

[1] V. I. Romanovskii, Basic Problem of the Theory of Errors (Moscow and Leningrad, 1947).

SELECTION AND CALIBRATION OF TUNGSTEN AND MOLYBDENUM WIRE FOR THERMOCOUPLES

S. K. Danishevskii

The wide application of tungsten-molybdenum thermocouples in industry made it necessary to calibrate large quantities of these thermocouples. In this connection special equipment and methods were developed for calibrating tungsten-molybdenum thermocouples[1].

It should be noted that the present technique of manufacturing tungsten and molybdenum wire does not provide for thermoelectric uniformity and hence makes it impossible to obtain a standard calibration characteristic for tungsten-molybdenum thermocouples made of wire which comes from different coils.

In order to obtain from a given quantity of coils of wire the maximum number of thermocouples with similar calibrations, it is necessary to use a considerable amount of labor in sorting out and matching coils of tungsten and molybdenum wire. Moreover the experimental matching of coils does not always lead to a reduction of the number of thermocouples with different characteristics to a minimum [1]. It is therefore necessary to develop a method of sorting and matching coils which would provide thermocouples with predictable calibration characteristics and at the same time would considerably speed up and facilitate the selection of coils.

This problem has been solved and at present the new method is being successfully used in the automation laboratory of the RSFSR Ministry of Communications for mass-production calibration of tungsten-molybdenum thermocouples.

The proposed method of selecting and matching of tungsten and molybdenum coils of wire amounts to the following operations.

Checking the wire for homogeneity. Each coil of tungsten and molybdenum wire is checked for thermoelectric homogeneity (evenness) at 1500 $\pm$ 20°C. For this purpose thermocouples are made from wire samples (0.5-1 m) taken from the "beginning" and "end" of each coil of tungsten and molybdenum wire (TB_i, TE_i; MB_i and ME_i).* A kaolin end-piece is placed into the effective area of the heater and heated up to about 1500°C. Then the sensitive end of the thermocouple under test is placed inside the kaolin and the produced emf is measured. The electrodes inside the end-piece are insulated by means of double kaolin tubes.

* TB_i, TE_i, MB_i and ME_i thermocouples are made from the "beginning" and "end" of the i-th coil of tungsten and molybdenum wire, respectively.

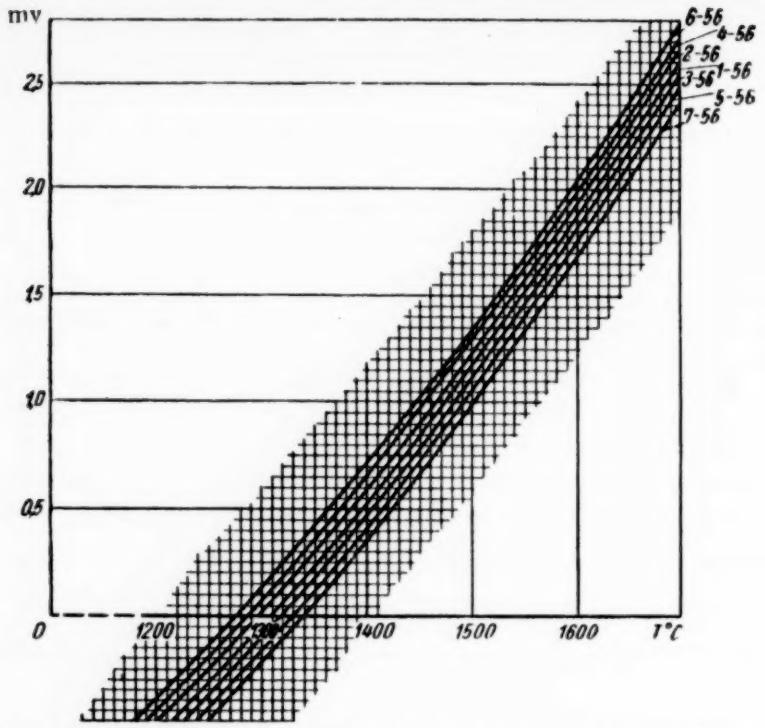

Fig. 1. Relationship between the emf of tungsten-molybdenum thermocouples and the temperature.

The value of the emf difference for which any given coil is considered to be homogeneous must not exceed 0.03 mv at 1500°C. If the emf difference is greater than this value the coil is not used for making thermocouples. The rejected coil may be used for making stationary or portable compensation leads.

When the thermocouple emf is measured, it is necessary to note the sign. The positive value in the adopted technique corresponds to the connection of the wire sample marked TB_1 and MB_1 ("beginning" of the coils) to the "+" terminal of the potentiometer.

Making a reference tungsten-molybdenum thermocouple. Out of the coils which have been checked for homogeneity those with the minimum difference emf (not greater than 0.005 mv) are selected from the tungsten and molybdenum coils. The wire of these coils is considered to be standard (thermocouples made of such reference wire used in Central Automation Laboratory were labeled as 1-56). Thermocouple electrodes made from these coils are marked respectively T and M. From the selected reference tungsten and molybdenum coils a thermocouple (TM) is made and its characteristic is measured between 1200 and 1700°C. The temperature is read and emf measured at every 100°C [1].

Next, thermocouples are made from the "beginnings" of each coil of tungsten (molybdenum) and the reference molybdenum (tungsten) coil. The thermocouples are marked TB_1T (MB_1M). These thermocouples are measured as for the check of nonhomogeneity at 1500°C ± 20°C and the sign of their emf is noted. The positive emf value corresponds to connecting the wires marked TB_1 or MB_1 (the "beginning" of the coils) to the terminal marked "+" on the potentiometer.

Matching of tungsten and molybdenum wire for thermocouples. When the thermocouples are matched they are divided into several groups according to their calibration characteristics (Fig. 1). Individual characteristics of thermocouples within one of the groups can differ from the characteristic of this group by no more than the adopted limit (according to the temperature or emf). We adopted a limit of (± A), equal to ± 0.03 mv which amounts to ± 5° for the operating region of the thermocouple (1500-1700°C). It was found in practice that thermocouples made of different coils of the same brand of tungsten (VRN) or molybdenum (MCh) can have different calibration characteristics, which will all be parallel to each other, however, in the range of 1200 to

TABLE 1

No. of graph / No. of coil	Thermal emf of the thermocouples (in mv)						
	$E_{MB_iME_i}$	E_{MB_iM}	$E_{TB_iTE_i}$	E_{TB_iT}	$E_{TB_iT} - E_{TB_iTE_i}$	$E_{MB_iME_i} - E_{MB_iM}$	E_{MB_iM}
	(1)	(2)	(3)	(4)	(4–3)	(1–2)	(–2)
1	$\pm n$	$\pm n_1$	$\pm m$	$\pm m_1$	$\pm m_1 \mp m$	$\pm n \mp n_1$	$\mp n_1$
2	. . .	. . .	. . .	. . .	. . .	. . .	. . .
. . .	. . .	. . .	. . .	. . .	. . .	. . .	. . .
i	. . .	. . .	. . .	. . .	. . .	. . .	. . .

TABLE 2

Limiting values of the sum of indexes		Notation of the thermocouple calibration characteristic groups
in tolerance units	in mv	
$+A \div -A$	$+0.03 \div -0.03$	1-56
$+3A \div +A$	$+0.09 \div +0.03$	2-56
$-3A \div -A$	$-0.09 \div -0.03$	3-56
$+5A \div +3A$	$+0.15 \div +0.09$	4-56
$-5A \div -3A$	$-0.15 \div -0.09$	5-56
$+7A \div +5A$	$+0.21 \div +0.15$	6-56
$-7A \div -5A$	$-0.21 \div -0.15$	7-56

1700°C (Fig. 1).* This circumstance was used in developing the technique of matching coils. The calibration characteristic of the reference tungsten-molybdenum thermocouple was given the number 1-56. All the remaining characteristics of groups (considering the adopted tolerance of 0.03 mv) differ from the reference characteristic by a value in millivolts which is a multiple of 0.06.

All the groups which have a characteristic with a lower value of the emf than the reference characteristic at the same temperature have been given an odd number; all those with a higher value an even number. (see Fig. 1).

In order to make the characteristics of various combinations of any tungsten and molybdenum coils (M_iT_i) with different combinations of "beginnings" and "ends" fall within the limits of the reference characteristic (TM) of ± A mv (± 0.03 mv) of the reference curve it is necessary to observe the following conditions.

$$0 \leq E_{TB_iMB_i} - E_{TM} \leq A$$

or

$$0 \geq E_{TB_iMB_i} - E_{TM} \geq -A; \quad (1)$$

$$0 \leq E_{TE_iMB_i} - E_{TM} \leq A$$

or

$$0 \geq E_{TE_iMB_i} - E_{TM} \geq -A; \quad (2)$$

$$0 \leq E_{TB_iME_i} - E_{TM} \leq A$$

or

$$0 \geq E_{TB_iME_i} - E_{TM} \geq -A; \quad (3)$$

$$0 \leq E_{TE_iME_i} - E_{TM} \leq A$$

or

$$0 \geq E_{TE_iME_i} - E_{TM} \geq -A. \quad (4)$$

*In the temperature range 1400-1700°C temperature variations of 10° correspond to emf changes of a tungsten-molybdenum thermocouple of 0.07 mv. A change in the emf of 0.03 mv corresponds to a temperature change of about 5°.

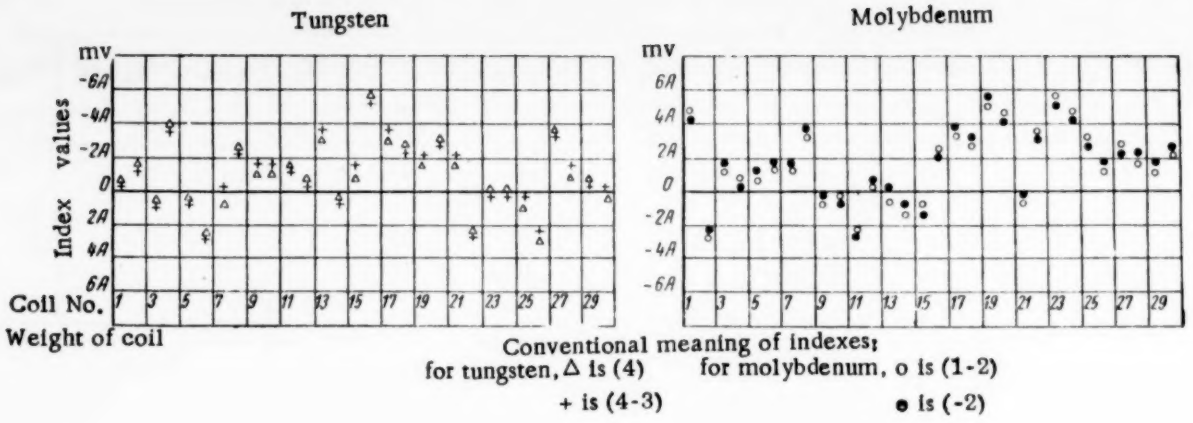

Fig. 2.

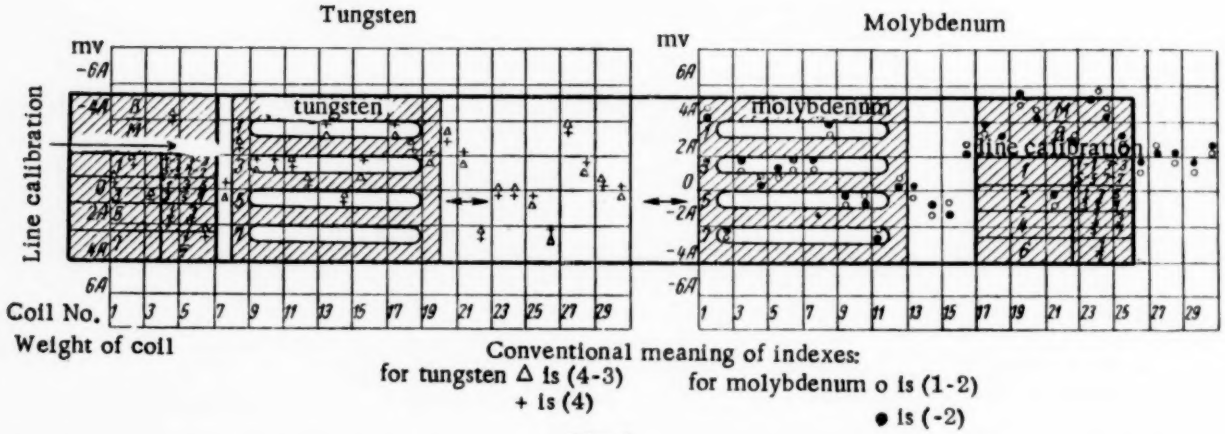

Fig. 3.

Since the calibration curves are parallel it is sufficient that these conditions be fulfilled at a single temperature. We choose 1500°C as a suitable temperature, since it lies approximately in the middle of the range for which the thermocouples are calibrated (1200-1700°C).

Above conditions can be written in a different form. Let us represent the value of the emf of thermocouple TB_iMB_i in terms of the emf of thermocouples consisting of electrodes TB_i and MB_i and the reference electrodes T and M:

$$E_{TB_iMB_i} = E_{TB_iT} - E_{MB_iT} = E_{TB_iT} - E_{MB_iM} + E_{TM}.$$

Substituting the right hand side of above equation into (1) we have

$$0 \leq E_{TB_iT} - E_{MB_iM} + E_{TM} - E_{TM} \leq A$$

or

$$0 \geq E_{TB_iT} - E_{MB_iM} + E_{TM} - E_{TM} \geq -\leq.$$

Then (1) will assume the form:

$$0 \leq E_{TB_iT} - E_{MB_iM} \leq A;$$

$$0 \geq E_{TB_iT} - E_{MB_iM} \geq -A. \qquad (1')$$

After similar transformations of (2), (3) and (4) we have:

$$0 \leq E_{TB_iT} - E_{TB_iTE_1} - E_{MB_iM} \leq A,$$

$$0 \geq E_{TB_iT} - E_{TB_iTE_1} - E_{MB_iM} \geq -A; \qquad (2')$$

$$0 \leq E_{TB_iT} + E_{MB_iME_1} - E_{MB_iM} \leq A,$$

$$0 \geq E_{TB_iT} + E_{MB_iME_1} - E_{MB_iM} \geq -A, \qquad (3')$$

$$0 \leq E_{TB_iT} - E_{TB_iTE_1} + E_{MB_iME_1} - E_{MB_iM} \leq A$$

$$0 \geq E_{TB_iT} - E_{TB_iTE_1} + E_{MB_iME_1} - E_{MB_iM} \geq -A. \qquad (4')$$

The values of the thermocouple emf's included in (1'), (2'), (3') and (4') are determined when the wire is checked for homogeneity and when the emf's of the thermocouples consisting of the "beginning" of each coil and the reference wire are measured.

These values of the emf are entered into a table in the course of measurements taking into consideration their respective signs (Table 1).

Values of $E_{MB_iME_1}$, E_{MB_iM}, $E_{TB_iTE_1}$ and E_{TB_iT} in various combination form part of inequalities (1'), (2'), (3') and (4'). These values are entered in Table 1 into columns (1), (2), (3) and (4), respectively.

Using the numbering of Table 1 and grouping the expressions referring to molybdenum and tungsten coils, it is possible to write the inequalities (1'), (2'), (3') and (4') in the form:

$$0 \leq (\ 4\ ) + (-2) \leq A;$$
$$0 \geq (\ 4\ ) + (-2) \geq -A.$$
$$0 \leq (4-3) + (-2) \leq A;$$
$$0 \geq (4-3) + (-2) \geq -A.$$
$$0 \leq (\ 4\ ) + (1-2) \leq A;$$
$$0 \geq (\ 4\ ) + (1-2) \geq -A.$$
$$0 \leq (4-3) + (1-2) \leq A;$$
$$0 \geq (4-3) + (1-2) \geq -A^3.$$

Thermocouples whose characteristics differ from that of the reference couple 1-56 by more than ± A mv are sorted out into groups each with its own calibration characteristic (Table 2).

For convenience of matching the index values of the tungsten and molybdenum coils are transferred from Table 1 onto graph paper (Fig. 2) where each tungsten and molybdenum coil has its own column. For tungsten coils the negative values of indexes are plotted above, and for the molybdenum coils below the zero index. If thermocouples are made up of tungsten and molybdenum coils whose indexes lie on the same line and within the tolerance (A = 0.03 mm), the calibration characteristics of thermocouples made out of these coils will have the standard characteristic 1-56 with an error not exceeding ± A mv (± 0.03 mv).

Thermocouples of other groups are selected in a similar manner.

For speeding up the selection of coils a special rule is used consisting of two stationary and two sliding plates. Each of the moving plates has 4 slots 15 mm wide, where one corresponds on the scale to 0.03 mv i.e., to the tolerance (A). The figures in front of the slots denote the number of the line, counting those missed by the slots.

It can easily be seen (from Figs. 2 and 3) that if thermocouples are made out of tungsten wire coils whose indexes are found in lines higher than those of the molybdenum coils (which is denoted on the left plate by T/M), the thermocouples will have odd calibration numbers. If, on the other hand, the tungsten coil indexes are found in a line lower than those of molybdenum coils (which is denoted on the right hand plate by M/T),

the thermocouples will have even calibration numbers. This is due to the fact that in the first instance the indexes' sums will always be negative, and in the second, always positive. The stationary plates of the rule bear inscriptions showing in what lines the tungsten and molybdenum coils should be for the thermocouples made from corresponding wire to have a required characteristic. When the wire coils are selected, the rule is placed over the graph paper which bears the tungsten and molybdenum indexes (see Fig. 3).

If new reference wire has to be used the following procedure is adopted.

From newly selected reference tungsten and molybdenum coils with a good thermoelectrical homogeneity (between 0.00 and 0.005 mv) a thermocouple is made up and its calibration characteristic measured [1].

Next, the emf is measured of thermocouples made of coils passed for homogeneity against reference coils, according to the technique described above.

The measurement results and subscripts are entered in a table similar to Table 1.

When the indexes are entered in the table, their position should now be counted from the new axis of coordinates, whose position is determined by the difference between the emf's of the new and original reference thermocouples at 1500°C.

As an example, let us take the case when the characteristic of the new reference thermocouple coincides with the old characteristic 3-56, i.e., it differs from the original reference characteristic (1-56) by -0.06 mv. In this instance the horizontal axes for tungsten and molybdenum must be separated by 0.06 mv. Moreover, since the new control thermocouple has an odd calibration number, the axis of the zero tungsten index must be drawn higher than the corresponding axis of molybdenum.

One of the possible ways of placing the axis is that of making the new tungsten zero axis coincide with the old zero axis and making the new zero molybdenum axis coincide with the old −0.06 mv molybdenum axis.

The indexes of the new tungsten and molybdenum coils to be matched are taken from the new values of the zero coordinates according to the value of the indexes (see Table 1).

The matched tungsten and molybdenum coils are placed in boxes which are supplied with a calibration table and graph suitable for thermocouples made out the wire in this box.

Special attention should be paid to the inadmissibility of making thermocouples from wire taken out of different boxes even if both boxes have the same calibration number. This is due to the fact that characteristics of thermocouples depend on the sum of the tungsten and molybdenum index numbers and not on the numbers themselves. The neglect of this condition may lead to considerable errors in measurements.

Above calibration technique was tried out at the Central Automation Laboratory on several consignments of wire. The results proved to be quite satisfactory.

The mean square error of thermocouple group calibration is determined by the error of individual calibrations (± 9°) [1] in conjunction with the additional error due to the averaging of characteristics (± 5°) and can be evaluated as $\pm \sqrt{9^2 + 5^2} = 10$ to 11°.

At present the Central Automation Laboratory is making thermocouples of two calibrations only, namely 5-56 and 7-56 out of a large quantity of tungsten and molybdenum wire.

The new method has facilitated and speeded up the sorting out of tungsten and molybdenum coils into groups with predictable calibration characteristics, thus reducing the number of different calibrations to a minimum.

LITERATURE CITED

[1] S. K. Danishevskii, Zavodskaya Lab. 22, 10 (1956).

CALCULATION OF A PHOTOELECTRIC FLUXMETER

S. G. Rabinovich and A. N. Tkachenko

The sensitivity of fluxmeters even with silk thread suspensions and mirror indication does not exceed $2\text{-}5\cdot10^{-6}$ Wb·turn/div with a stabilization time of 3-10 sec per division; this sensitivity is often insufficient [1].

Photoelectric fluxmeters (PEF) [2-5] have far better operational characteristics. Since they use a torsion suspension galvanometer they provide a greater sensitivity with a speedier operation than the best fluxmeters of other designs. Their sensitivity is independent of the measuring coil resistance over a wider range.

Principle of operation and circuit of a PEF. The schematic circuit of a PEF is shown in Fig. 1. The difference between voltage e_x across the terminals of the measuring coil MC, due to changes in flux Φ_x, and the feedback voltage e_{fb} produces current i which flows in the moving coil mirror galvanometer G. The galvanometer mirror deflection caused by current i produces a displacement of the light beam provided by the illuminating lamp L along the differential photoresistors P1 and P2. This causes a change in voltage U_2 at the grid of tube T, and in its anode current I, which provides a differentiated negative feedback for balancing out voltage e_x. Differentiated feedback is attained either by means of mutual induction coupling [2] or, as shown in Fig. 1, by means of a differentiating RC network.

Analysis of the block schematic and dynamic properties of a PEF when measuring single-pulse variations of the flux. Figure 2 shows the block schematic of the PEF.

Let us write the transfer functions of the elements in operational form, by means of Laplace transforms (initial conditions are everywhere zero).

The transfer functions of the elements of the closed system

$$\frac{I(p)}{\Phi_x(p)}=\frac{\psi KS\,\frac{1}{\Sigma r}\,y_{st}\;(p)p}{(1+T_y p)\cdot(1+\tau p)\cdot(Jp^2+Pp+W_{\text{м}})+\frac{\psi KS}{\Sigma r}\,y_{st}\;\;(p)K_{fb}(p)p},$$

will be:

Measuring coil:

$$\frac{e_x(p)}{\Phi_x(p)}=p;$$

converter of voltage into current:

$$\frac{i\,(p)}{e\,(p)}=\frac{1}{\Sigma r\,(\tau p+1)};$$

galvanometer:

$$\frac{\alpha(p)}{i(p)} = \frac{\Psi}{Jp^2 + Pp + W_M};$$

photooptical amplifier:

$$\frac{U_1(p)}{\alpha(p)} = \frac{K}{1 + T_y p};$$

stabilizing element:

$$\frac{U_2(p)}{U_1(p)} = y_{st}(p)$$

(it is assumed that the stabilizing element does not load the photoresistance, i.e., it is an element of directional discrimination);

electron amplifier:

$$\frac{I(p)}{U_2(p)} = S;$$

feedback link:

$$\frac{e_{fb}(p)}{I(p)} = K_{fb}(p)\, p.$$

The following notations were adopted: Σr is the sum of the galvanometer circuit resistances; τ – galvanometer circuit constant ($\tau = \frac{L}{\Sigma r}$, where L is the galvanometer circuit inductance); α the angle of rotation of the galvanometer coil; coefficients J, P, Ψ and W_M which characterize a moving coil galvanometer are: J – the moment of inertia of the galvanometer moving part; $P = \Psi^2 / \Sigma r$ – the damping coefficient of the galvanometer; where $\Psi = B s \omega$, B being the induction in the galvanometer air gap, s the area of the coil, ω the number of turns in the coil and W_M the moment constant of the torsion suspension. K is the conversion factor of the photooptical amplifier; T_y – the photoresistors' time constant; S – the mutual conductance of the electronic amplifier; K_{fb} – the transfer function coefficient of the differentiating element. Let us assume that the flux changes instantaneously from 0 to Φ_M, i.e., let us assume the PEF input to be a step function. Then $\Phi_x(p) = \Phi_M/p$. Let us introduce notation $\Psi KS/\Sigma r = K_p$.

As the result we have:

$$\frac{I(p)}{\Phi_M} = \frac{y_{st}(p) K_p}{(1 + T_y p)\cdot(1 + \tau p)\cdot(Jp^2 + Pp + W_M) + K_p y_{st}(p)\, K_{fb}(p)\, p}. \qquad (1)$$

Let us at first for simplicity's sake assume the photoresistors to have no inertia ($T_y = 0$), the induction of the input circuit to be negligibly small ($\tau = 0$), and coefficient $K_{fb}(p)$ of the differentiating circuit transfer function to be constant. Let us also assume that $Y_{st}(p) = 1$.

Applying the expansion formula to expression (1) we obtain for this case:

$$\frac{I(t)}{\Phi_M} = \sum_{i=1}^{i=2} \frac{K_p}{F'(p_i)}\, e^{p_i t} = K_p \left(\frac{e^{p_1 t}}{2p_1 J + K_{fb} K_p + P} + \frac{e^{p_2 t}}{2p_2 J + K_{fb} K_p + P} \right),$$

where p_1 and p_2 are the roots of the characteristic equation:

$$Jp^2+(K_{fb}K_p+P)\,p+W_M=0.$$

Quantity P can be neglected since in practice it amounts to a few percent of $K_{fb}K_p$. One can also neglect on the basis of the same considerations $4JW_M$ as compared with $(K_{fb}K_p)^2$.

Thus we shall obtain:

$$p_1\simeq-\frac{W_M}{K_{fb}K_p};\quad p_2\simeq-\frac{K_{fb}K_p}{J}.$$

Considering that $2JW_M < K_{fb}K_p$ we finally obtain:

$$\frac{I(t)}{\Phi_M}=K_p\left(\frac{e^{-\frac{W_M t}{K_{fb}K_p}}}{P+K_{fb}K_p}-\frac{e^{-\frac{K_{fb}K_p t}{J}}}{K_{fb}K_p-P}\right). \tag{2}$$

The first term of (2) represents the slow decrease of the output current with a time constant of θ_d:

$$\theta_a=\frac{K_{fb}K_p}{W_M}. \tag{3}$$

The second term of the expression determines the growth of the output current with the time constant τ_{st}:

$$\tau_{st}=\frac{J}{K_{fb}K_p}.$$

It is obvious that in an ideal fluxmeter $\theta_d = \infty$ and $\tau_{st} = 0$. For this purpose one of the conditions a) $J = 0$, $W_M = 0$ or b) $K_{fb}K_p = \infty$ must be fulfilled.

If the stable state value of the output current I_M be now examined (assuming that $\theta_d = \infty$) we shall obtain:

$$\frac{I_M}{\Phi_M}=\frac{K_p}{K_{fb}K_p+P}=\frac{1}{C_\Phi}, \tag{4}$$

where C_Φ is the PEF constant.

For $K_{fb}K_p >> P$

$$\frac{I_M}{\Phi_M}\simeq\frac{1}{K_{fb}}. \tag{5}$$

The value of C_Φ can be calculated in advance from (4) and (5). If, however, K_p should change, for instance, due to changes in the mutual conductance of electronic amplifier, a small error will appear which can be determined from:

$$\frac{dC_\Phi}{dK_p}=-\frac{P}{K_p^2},$$

$$\text{or}\quad \frac{dC_\Phi}{C_\Phi}=-\frac{dK_p}{K_p}\cdot\frac{P}{K_{st}K_p+P}=-\frac{dK_p}{K_p}\gamma, \tag{6}$$

$$\text{where}\quad \gamma=\frac{P}{K_{st}K_p}.$$

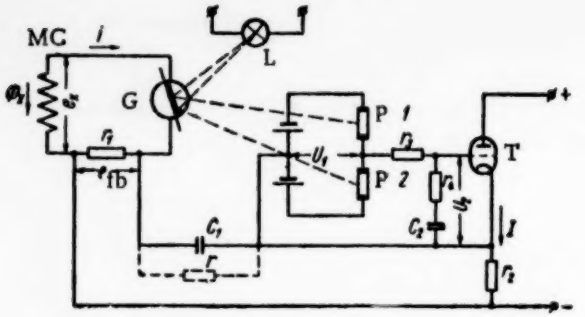

Fig. 1.

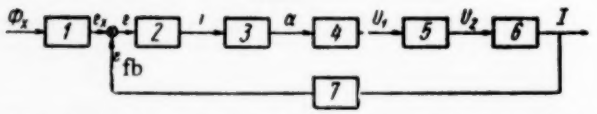

Fig. 2. 1) Measuring coil; 2) converter of the voltage difference e into current; 3) galvanometer; 4) photo-optical amplifier; 5) stabilizing element; 6) electronic amplifier; 7) a differentiating negative feedback link.

Let γ indicate the unbalance error due to the lack of compensation of the measured flux by the output current through the differentiating negative feedback.

Above expression (2) does not always characterize the dynamic properties of an actual PEF. Oscillations often arise in the circuit. They probably occur when one of the assumptions made above that the time constants T_y or τ is small does not hold.

Often the primary reason is the inertia of the photoresistors themselves. When vacuum photoelectric resistance elements are used with external excitation a considerable lag is experienced, even with a small input capacity of the tube, due to a large dynamic resistance of the photoresistors

Moreover, the feedback coefficient of the differentiating link depends in actual practice on p.

Let us assume in future that the RC circuit is used as a differentiating link in the fluxmeter. This is due to the difficulty of constructing a coil with accurately specified mutual induction. The inaccuracy of the mutual induction necessitates a special adjustment of the PEF during manufacture. The use of RC network as a differentiating circuit with capacitors of a 0.1% accuracy (for instance of the PGT type) makes it possible to dispense with this adjustment.

The transfer function for the RC differentiating network has the form:

$$\frac{e_{fb}(p)}{I(p)} = \frac{T_2 r_2 p}{1+T_1 p} = \frac{K_{fb} P}{1+T_1 p}, \tag{7}$$

where $T_1 = (r_1 + r_2)C_1$; $T_2 = r_1 C_1$. It is also assumed for the sake of simplicity that the internal impedance of the electronic amplifier is considerably larger than r_2.

Taking into consideration (7), formula (1) can be written:

$$\frac{I}{\Phi_M}(p) = \frac{K_p (1+T_1 p)}{(1+T_y p)(1+\tau p)(Jp^2+Pp+W_M)(1+T_1 p)+K_p T_2 r_2 p}. \tag{8}$$

The moment constant W_M of the torsion suspension can be considered equal to zero, since the stability of the circuit, obviously, does not depend on it. It is also possible to neglect the induction of the input circuit, since in practice as a rule $\tau \ll T_y$.

Let us examine the characteristic equation obtained after these assumptions:

$$p(Jp+P)(1+T_y p)(1+T_1 p)+K_p T_2 r_2 p = 0.$$

Taking into consideration that

$$P < K_p K_{fb} \quad \text{or since} \quad K_{fb} = T_2 r_2, \text{then} P < K_p T_2 r_2,$$

we obtain:

$$JT_y T_1 p^3 + [PT_y T_1 + J(T_y + T_1)]p^2 + [J + P(T_y + T_1)]p + K_p T_2 r_2 = 0.$$

The circuit is stable providing the inequality of Hurwitz is observed:

$$[PT_yT_1+J(T_y+T_1)]\,[J+P(T_y+T_1)]>JT_yT_1K_pr_2T_2. \tag{9}$$

From (9) it follows that there exists a $K_p = K_{p\,crit.}$ at which the circuit becomes unstable. The circuit also becomes unstable with an increasing depth of feedback, i.e., $K_{fb} = T_2r_2 = r_1r_2C_1$. Since $K_{fb} = C\,\Phi$, the PEF circuit stability increases with its sensitivity.

Any self-oscillations arising in the circuit can be eliminated by connecting into the grid circuit of the tube a stabilizing network (Fig. 1).

Its transfer function is

$$\frac{U_2(p)}{U_1(p)} = \frac{1+T_4p}{1+T_3p}, \tag{10}$$

where $T_4 = r_4C_2$; and $T_3 = (r_3 + r_4)\,C_2$.
Resistance r_3 includes the internal resistance of the bridge and photoresistors.

The transfer function of the PEF, in conjunction with (10) assumes the form:

$$\frac{I(p)}{\Phi_M} = \frac{K_p(1+T_1p)\,(1+T_4p)}{(1+T_yp)\;(Jp^2+Pp+W_M)\,(1+T_1p)\,(1+T_3p)+(1+T_4p)\;K_pT_2r_2p}. \tag{11}$$

Considering that

$$P<K_pT_2r_2;\ (J+PT_y)<T_4K_pT_2r_2;$$
$$P(T_1+T_3)<T_4K_pT_2r_2;\ W_M=0,$$

we obtain in a similar manner the characteristic equation:

$$\begin{aligned}&JT_yT_1T_3p^4+[JT_y(T_1+T_3)+T_1T_3(J+PT_y)]\,p^3+\\&+[JT_y+(J+PT_y)\,(T_1+T_3)]p^2+T_4K_pT_2r_2p+K_pT_2r_2=0.\end{aligned} \tag{12}$$

The condition of stability is:

$$\begin{aligned}&[JT_y(T_1+T_3)+T_1T_3(J+PT_y)]\,\{[JT_y+(J+PT_y)\,(T_1+\\&+T_3)]\,T_4-[JT_y(T_1+T_3)+T_1T_3\,(J+PT_y)]\}-\\&-JT_yT_1T_3K_pT_2r_2T_4^2>0.\end{aligned} \tag{13}$$

In this case by suitably selecting T_3 and T_4 it is possible to stabilize circuits with any values of K_p and K_{fb}.

It can be assumed that there exists an optimum value for T_3 and T_4 at which the output current of the PEF rises with greatest speed, i.e., it is possible to synthesize the PEF circuit with the view of obtaining the maximum speed of operation. This problem is of great importance if the PEF is to be used for recording rapid continuous changes of flux. The detailed examination of this question, however, falls outside the scope of this article.

Calculation and choice of parameters of sensitive PEF for measuring single pulse variations of flux. Let us assume we are given: Φ_M – the nominal value of flux, I_M – the nominal value of the output current, r_{mc} – the maximum value of the measuring coil resistance, θ_d – the time constant of the drift, and γ – the error due to lack of compensation. The design of the galvanometer is also assumed to be given, i.e., we assume that the values of B, s and l_v (where l_v is the mean length of the galvanometer coil turn) are known. Let us also consider that the moment constant of the torsion suspension W_M is also known, since it is determined by considerations of the mechanical strength of the instrument, and with a given construction of the galvanometer cannot be made smaller than a certain value.

Parameters K, S and ω have to be determined; K is the coefficient of transformation of the photooptical amplifier, S – the mutual conductance of the electronic amplifier and ω the number of turns in the coil.

Let us derive the required design formulas.

From (4) we have:

$$C_\Phi = \frac{\Phi_M}{I_M}. \tag{14}$$

Equations (4-6) provide:

$$\frac{dC_\Phi}{C_\Phi} \cdot \frac{K_p}{dK_p} = -\frac{P}{K_{fb} K_p} = -\frac{\frac{(Bs\omega)^2}{\Sigma r}}{C_\Phi \frac{Bs\omega KS}{\Sigma r}} = -\frac{Bs\omega}{C_\Phi KS} = -\gamma.$$

From (3) we have:

$$\Theta_a = \frac{K_{fb} K_p}{W_M} = \frac{C_\Phi \frac{Bs\omega}{\Sigma r} KS}{W_M}.$$

From here it is easy to obtain:

$$KS = \frac{1}{C_\Phi} \sqrt{\frac{\Theta_d W_M \Sigma r}{\gamma}}; \tag{15}$$

$$\omega = \frac{1}{Bs} \sqrt{\Theta_d W_M \Sigma r \gamma}. \tag{16}$$

The galvanometer coil resistance is

$$r_g = \frac{\rho l_v \omega}{q},$$

hence

$$q = \frac{\rho l_v \omega}{r_g}, \tag{17}$$

where ρ is the resistivity of copper; q is the winding wire cross-sectional area.

From the power point of view it is advisable to have $r_g \simeq r_{mc} + r_1$. It is also advisable to have r_1 as small as possible. However a decrease in r_1 with the fluxmeter constant remaining unchanged leads to a rise in capacity C_1 or resistance r_2. The size of the capacitor is limited by constructional considerations. The increase of resistance r_2 is limited by the internal impedance of the electronic amplifier.

It is convenient to use in calculations the notion of the "drift time constant" (θ_d). However it is more obvious to denote the drift by the time required for the fluxmeter indicator to traverse a division of the scale, θ. Let us find the relation between the two quantities.

According to (2) the drift is expressed by the equation:

$$\frac{I_M}{\Phi_M} = \frac{1}{K_{fb}} e^{-\frac{t}{\theta}} = \frac{1}{C_\phi} e^{-\frac{t}{\theta}},$$

where $I_M = \frac{\Phi_M}{C_\varphi} e^{-t/\theta}$, or differentiating,

$$\frac{dI_M}{dt} = -\frac{\Phi_M}{C_\phi \theta} e^{-\frac{t}{\theta}}$$

Assuming t = 0, since the speed of drift is maximum at the beginning of the time interval, and taking finite increments instead of the differentials we obtain:

$$\Delta I_M = \frac{\Delta t}{\theta} \cdot \frac{\Phi_M}{C_\phi} = \frac{I_M}{\theta}.$$

Hence, $\Delta t = \frac{\Delta I_M}{I_M} \cdot \theta = \frac{\Delta_n}{n} \cdot \theta$, where n is the number of scale divisions of the fluxmeter indicator. Assuming $\Delta n = 1$, we have:

$$\Theta = n\theta. \tag{18}$$

Relationships (14-18) are the basic design formulas of the PEF.

Let us give a numerical example. Let it be required to calculate a PEF with two values of constants: $15 \cdot 10^{-8}$ Wb · turn/div and $300 \cdot 10^{-8}$ Wb · turn/div suitable for a measuring coil of 100 ohm. The drift of the indications of an output instrument with a scale of 100 divisions must not exceed one division in 7 sec.

The fluxmeter error of measurement must not exceed 0.5% when its parameters K, S and Σr change by 25%. A fluxmeter with such parameters is superior to the best mirror galvanometers both in its sensitivity and and its operating time. Moreover this instrument provides for a measuring coil of a considerably higher resistance, which results in a still higher sensitivity. Let us note that the sensitivity of the PEF is limited mainly by the level of thermoelectric emf's in the galvanometer circuit.

At the beginning of calculations let us assume an output current of $1.5 \cdot 10^{-3}$ amp. Such a current will provide the possibility of connecting simple instruments, and even a recorder.

Now let us obtain the values of the instrument parameters:

$$C_{\phi\,min} = \frac{15 \cdot 10^{-8} \cdot 100}{1.5 \cdot 10^{-3}} = 10^{-2} \text{ Weber/amp}$$

$$C_{\phi\,max} = \frac{300 \cdot 10^{-8} \cdot 100}{1.5 \cdot 10^{-3}} = 20 \cdot 10^{-2} \text{ Weber/amp}$$

Let us determine the error due to lack of compensation:

$$\gamma = \frac{dC_\phi}{C_\phi} \cdot \frac{K_p}{dK_p} = \frac{0.5}{25} = 0.02.$$

Let us calculate the specified value of the drift time content:

$$\Theta_d = n\theta = 100 \cdot 7 = 700 \text{ sec}.$$

On the basis of the reasoning outlined above and considering that the measuring coil resistance is 100 ohm let us take r_g = 100 ohm and r_1 = 50 ohm.

Then $\Sigma r = 100 + 100 + 50 = 250$ ohm.

Let us choose a torsion suspension galvanometer with B = 0.45 Wb/m^2, $s = 1.6 \cdot 10^{-4}$ m^2, $l_s = 6.5 \cdot 10^{-2}$ m, and $W_M = 1.13 \cdot 10^{-7}$ N·m/rad.

Next from (15) we find

$$KS = \frac{1}{10^{-2}} \sqrt{\frac{700 \cdot 1.13 \cdot 10^{-7} \cdot 250}{0.02}} = 100 \text{ amp/rad}.$$

The required value of KS can be best attained by changing the mutual conductance S of the electronic amplifier.

From (16) we find the number of turns in the galvanometer coil:

$$\omega = \frac{1}{0.45 \cdot 1.6 \cdot 10^{-4}} \cdot \sqrt{700 \cdot 1.13 \cdot 10^{-7} \cdot 250 \cdot 0.02} =$$

= 280 turns.

From the resistance of the galvanometer we determine the wire cross-sectional area:

$$q = \frac{175 \cdot 10^{-10} \cdot 6.5 \cdot 10^{-2} \cdot 280}{100} = 318 \cdot 10^{-11} \text{ m}^2.$$

The wire with a diameter of 0.06 mm ($q = 283 \cdot 10^{-11}$ m^2) has the nearest cross-sectional area to the required value, and can be used.

Having selected the wire for the coil it is necessary to ascertain that it will fit into the air space of the galvanometer magnetic system. If the coil does not fit into the space it means that with the given construction of the galvanometer it is impossible to attain the desired fluxmeter parameters.

C_1 and r_2 remain to be calculated. From (7) we find:

$$r_2 C_1 = \frac{C_\varphi}{r_1} = \frac{10^{-2}}{50} = 2 \cdot 10^{-4} \text{ sec}.$$

From constructional consideration the capacity of C_1 is limited to $2 \cdot 10^{-6}$ f. Then,

$$r_2 = \frac{2 \cdot 10^{-4}}{2 \cdot 10^{-6}} = 100 \text{ ohm}.$$

In order to obtain $C_{\varphi\ max} = 20 \cdot 10^{-2}$ Wb/amp, it is necessary to make $r_2 = 20 \cdot 100 = 2000$ ohm.

Let us note that in this instance theoretically Θ_d will be a little smaller owing to the decrease of the mutual conductance S of the electronic amplifier due to a rise in r_2.

Let us check the stability of the PEF circuit for: $C_{\varphi\ min} = 10^{-2}$ Wb/amp; $r_2 = 100$ ohm;

$$P = \frac{(Bs\omega)^2}{\Sigma r} = \frac{(0.45 \cdot 1.6 \cdot 10^{-4} \cdot 280)^2}{250} = 16 \cdot 10^{-7} \text{ m} \cdot \text{sec}.$$

The moment of inertia of the chosen galvanometer moving part is $0.12 \cdot 10^{-7}$ kg·m². The time constant T_y of cadmium sulfide photoresistors type FS-K7 is 0.01 sec, $T_1 = (100 + 50) \cdot 2 \cdot 10^{-6} = 3 \cdot 10^{-4}$ sec, and $T_2 = 50 \cdot 2 \cdot 10^{-6} = 10^{-4}$ sec.

$$K_\mu = \frac{Bs\omega}{\Sigma r} KS = \frac{0.45 \cdot 1.6 \cdot 10^{-4} \cdot 280 \cdot 100}{250} = 8 \cdot 10^{-3} \text{ N·m/ohm.}$$

Thus we obtain in conjunction with (9):

$$[16 \cdot 10^{-7} \cdot 0.01 \cdot 3 \cdot 10^{-4} + 0.12 \cdot 10^{-7} (0.01 + 3 \cdot 10^{-4})] [0.12 \cdot 10^{-7} + 16 \cdot 10^{-7} (0.01 + 3 \cdot 10^{-4})] > 0.12 \cdot 10^{-7} \cdot 0.01 \cdot 8 \cdot 10^{-3} \cdot 3 \cdot 10^{-4} \cdot 10^{-4} \cdot 100.$$

The inequality holds and the circuit is stable.

For $C_{\varphi\ max} = 20 \cdot 10^{-2}$ Wb/amp, $r_2 = 2000$ ohm, $T_1 = (2000 + 50) \cdot 2 \cdot 10^{-6} \approx 4 \cdot 10^{-3}$ sec:

$$[16 \cdot 10^{-7} \cdot 0.01 \cdot 4 \cdot 10^{-3} + 0.12 \cdot 10^{-7} (0.01 + 4 \cdot 10^{-3})] [0.12 \cdot 10^{-7} + 16 \cdot 10^{-7} (0.01 + 4 \cdot 10^{-3})] < 0.12 \cdot 10^{-7} \cdot 0.01 \cdot 8 \cdot 10^{-3} \cdot 10^{-4} \cdot 4 \cdot 10^{-3} \cdot 2000.$$

Hurwitz' inequality does not hold and the circuit is unstable. In order to obtain a stable operation it is sufficient, as it will be seen from (13), to introduce a stabilizing network with the following parameters: $r_3 = 3 \cdot 10^6$ ohm, $r_4 = 10^4$ ohm and $C_2 = 2 \cdot 10^{-6}$f.

In conclusion it is useful to note that for capacity C_1, only a high insulation capacitor can be used.

The finite value of insulation leads to the appearance of a direct, in addition to a differentiated, feedback. This makes a stable electrical moment W_{el} appear at the galvanometer, the moment acting in exactly the same way as a torsion suspension [6]. It is desirable to make the drift due to the imperfect insulation of the capacitor smaller than that due to the torsion suspension. It can be shown that for $r_{in} \gg r_1 + r_2$ (see Fig. 1) we have:

$$W_{el} = \frac{Bs\omega}{\Sigma r} \cdot \frac{r_1 r_2}{r_{in}} KS. \qquad (19)$$

If it is assumed that the permissible value of $W_{el} = W_M = 1.13 \cdot 10^{-7}$ N·m/rad we have:

$$r_{in} = \frac{0.45 \cdot 1.6 \cdot 10^{-4} \cdot 280 \cdot 100 \cdot 50 \cdot 100}{250 \cdot 1.13 \cdot 10^{-7}} = 3.6 \cdot 10^9 \text{ ohm}$$

It is obviously desirable to have a capacitor insulation higher than 10^{10} ohm.

Conclusions. Above relationships provide the possibility of designing a highly sensitive photoelectric fluxmeter with given constants for measuring single pulse variations of flux. Above design data were fully tested out on a model fluxmeter constructed to that design.

LITERATURE CITED

[1] E. Meuer and C. Moerder, Spiegel galvanometer und Lichtezeigerinstrumente, A.V.Y.P.K.Y. (Leipzig, 1957).

[2] S. P. Kapitsa, J. Tech. Phys. 25, 7 (1955).

[3] P. P. Cioffi, A recording fluxmeter of high accuracy and sensitivity, Rev. Sc. Inst. 21, 7 (1950).

[4] I. G. Gutovskii, DAN SSSR 116, 2 (1957).

[5] R. R. Kharchenko, "Special problems in the dynamic of moving coil instruments" Author's report of his dissertation for the degree of Dr. Tech. Sci. [in Russian] (MEI, 1956).

[6] B. A. Seliber and S. G. Rabinovich, Automation and Remote Control 17, 8 (1956).*

PHOTOELECTRIC AMPLIFIERS F17

A. M. Kasperovich

Only in the last few years have photocompensation systems acquired recognition as simple and reliable means of obtaining high sensitivityin measuring voltage or current with a small zero drift. These systems can be used for solving many a problem of measurement and control in technology, physics, chemistry, biology, etc.

However, in manufacturing various photocompensation systems difficulties arise in making the unit consisting of the galvanometer, the optical system and the photosensitive elements (this unit is usually known as the photoelectric amplifier). Above difficulties in practice limited the application of the photocompensation system.

In this connection the "Vibrator" plant has since 1957 started producing universal photoelectric amplifiers type F17 for use with other equipment.

Construction and unit parameters. The photoelectric amplifier F17 consists of three basic units: the galvanometer, illuminator and the photoresistors.

The amplifier galvanometer is carefully sealed and protected from the effects of ambient air temperature. Lagging is achieved by a plastic screen. Inside the lagging cover there is a copper screen which equalizes temperature differences around the galvanometer.

The moving part of the galvanometer is fixed on torsion suspensions. The magnetic system has small stray fluxes and is well protected against external fields.

The position of the lamp in the illuminator is adjustable. A CTs-78 (7.5 v 0.5 amp) lamp is used which should be run at lower voltage than specified in order to increase its life. The powerful illuminator condenser is fitted with a diaphragm containing three slits whose image is projected onto the photoresistances by means of the objective placed in front of the galvanometer mirror. The condenser includes an infrared filter which decreases considerably the amount of heat penetrating inside the galvanometer.

The cadmium sulfide photoresistors were developed for the F17 amplifier by B. T. Kolomiets and A. O. Olesk. These photoresistors similar to type FS-K2 possess a high specific sensitivity, a high resistance factor, and a low temperature coefficient. They have a long life and are stable [1].

Figure 1 shows the appearance of these resistors.

According to the purpose for which the amplifier is designed the photoresistors are made in two types: the low resistance five-electrode ones for working directly with indicating or recording instruments,or the high resistance three-electrode ones for working with electronic amplifiers.

Their construction is as follows. A light-sensitive layer of cadmium sulfide is glued to a glass disc 25 mm in diameter. Current-carrying electrodes are fixed to the surface of this layer by means of the metal pulverization process. In order to decrease the effect of humidity on the photoresistors they are hermetically sealed inside a metal container. On the photoresistor side the container has a shield with windows cut in it.

The external appearance of the shield with the three slits of the diaphragm projected onto it is shown in Fig. 2.

* See English translation.

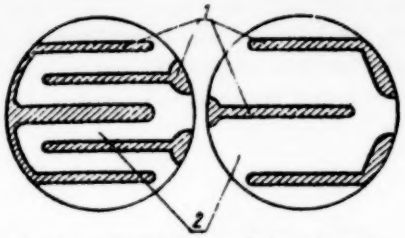

Fig. 1. Appearance of the photoresistors. 1) Electrodes, 2) sensitive surfaces.

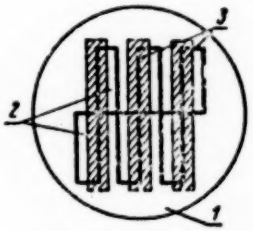

Fig. 2. Appearance of the shield with the image of the diaphragm. 1) Shield, 2) openings in the shield, 3) image of the diaphragm.

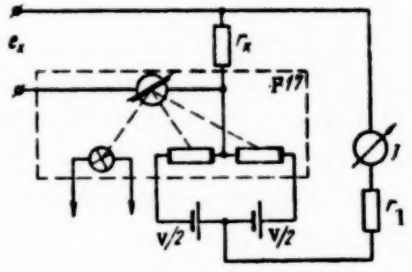

Fig. 3.

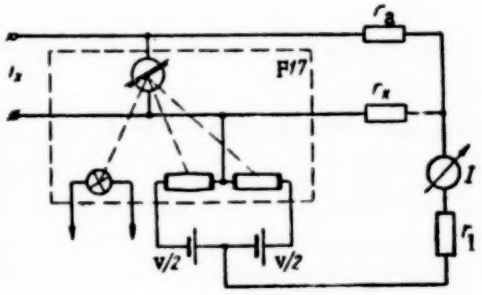

Fig. 4.

When the galvanometer mirror is rotated, the image of the diaphragm moves over the shield and the light is redistributed with respect to the upper and lower halves of the photoresistor changing their respective resistances. The latter change can be transformed into a voltage or current variation, for instance as shown in Figs. 3, 4, 5 or 6.

At present, three types of amplifiers are being produced, which differ by their galvanometer coil windings: F17/1 is voltage sensitive, F17/2 is current sensitive, and F17/3 is made for voltage stabilizers.

The constructional parameters of these galvanometers are given in the table below.

The conversion factor is an important constructional parameter of any photoelectric amplifier, and it is defined as the derivative of the output current with respect to the turning angle of the galvanometer moving part.

$$K_I = \frac{dI}{d\alpha}.$$

In a circuit without an additional amplifier the conversion factor is represented by the formula:

$$K_I = 2U\frac{1-a}{1+a}\cdot\frac{f}{b}\cdot\frac{1}{r_{in}+r_1},$$

where a is the resistance ratio of the lighted half of the photoresistor to its shaded half; r_1 – the amplifier load resistance; r_{in} – the internal resistance of the photoresistor; f – the distance between the mirror and the diaphragm (50 mm); b – the width of the slit (2 mm) in the diaphragm.

The value of a depends but little on the heating of the incandescent lamp and amounts to 0.2-0.3.

The internal resistance of the photoresistor is represented by:

$$r_{in} = \frac{r_c}{1+a},$$

where r_c is the resistance of the lighted half of the photoresistor.

The internal resistance of the photoresistor is inversely proportional to the width b of the slit, so that at low resistance loads the conversion factor will depend but little on b.

With 6 v across the incandescent lamp the value of r_c amounts to 5500 ohm. Taking numerical values, the conversion factor formula becomes:

$$K_I = \frac{30\,U}{4400+r_1}.$$

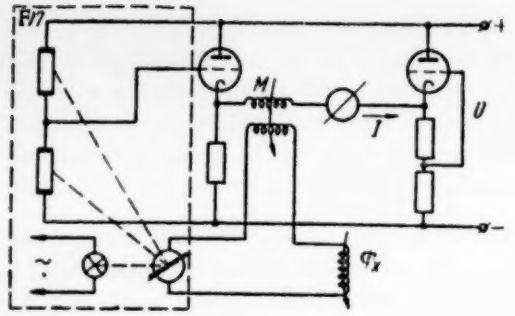

Fig. 5.

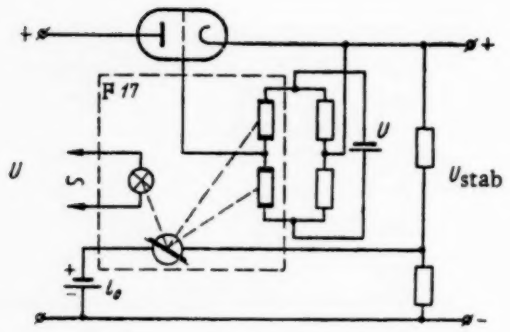

Fig. 6.

If an additional electronic amplifier is used it is convenient to divide the photoelectric amplifier circuit conversion factor into two factors: the photoamplifier voltage conversion factor and conversion factor of the additional amplifier

$$K_I = \frac{dU}{da} \cdot \frac{dI}{dU}.$$

The voltage conversion factor is determined from the expression:

$$K_U = 2U \frac{1-a}{1+a} \cdot \frac{f}{b}$$

or with numerical values:

$$K_U = 30\,U.$$

It is usually desirable to make the conversion factor as large as possible. Its limit is determined by the power dissipated in the photoresistor.

It can be considered that maximum power is dissipated in the photoresistor when both its halves are equally lighted. Experience shows that it must not exceed 0.6 w.

The conversion factor dI /dU of the electronic amplifier is determined in the normal way.

Possible circuits and basic relationships. Figures 3, 4, 5 and 6 show typical methods of connecting photoelectric amplifiers type F17 to various photocompensating circuits. Components included in the amplifier F17 are enclosed by a dotted line.

Figure 3 shows a photocompensation circuit for measuring voltage by means of the F17 amplifier alone. In this circuit ex is related to the output current I by the following expression:

$$I = \frac{e_x}{r_k}(1-\gamma),$$

where r_k is the compensating resistance; γ is the lack-of-compensation error caused by the counteracting moment of the torsion suspensions (the method of its calculation is given below).

The circuit for measuring current i_x also without an additional electronic amplifier is shown in Fig. 4. For this case we have:

$$I = i_x \frac{r_k + r_a}{r_k}(1-\gamma),$$

where r_a is the additional resistance (see Fig. 4).

If a higher value is required for the conversion factor (for instance for the photo-fluxmeter circuit) it is normal to use an additional electronic amplifier.

A schematic of such a fluxmeter with a photoelectric amplifier F17 is shown in Fig. 5. In this circuit

Type \ Parameters	Flux linkage ψ, maxwell/turns	Moment WM of the torsion suspension dyne·cm/rad	Monent of inertia J, g·cm²	Coil resistance, ohm	Frame resistance, ohm
F17/1	10^6	0.74	0.085	60	–
F17.2	10^7	0.84	0.095	5100	–
F17/3	$4.7 \cdot 10^6$	3.3	0.22	1000	$8 \cdot 10^{-4}$

the measured flux Φ_X is related to the output current in the following manner:

$$\Phi_x = MI(1+\gamma_0),$$

where

$$\gamma_0 = \frac{\psi}{KM}.$$

(This circuit uses as a differentiating link a coil with a mutual induction M. For this purpose, however, an RC network can also be used).

If even a higher gain is required it is advisable to supply the photoresistors from a separate voltage source. An example of such a connection is given in Fig. 6, which shows a schematic of one photocompensation voltage stabilizer.

Design formulas. When designing photocompensation amplifiers or stabilizers it is possible to use [2] and [3] where a detailed analysis is made of the theory of designing and calculating such instruments.

However, when photoelectric amplifiers F17 with given constructional parameters are available, it is more convenient to use simplified calculations.

In this instance design parameters Ψ, W_M, r_2, J and K are known and it is required to determine the operational parameters of a photoelectric amplifier. They normally consist of the range of the amplifier, decay time τ, the lack of compensation error γ (with a given resistance of the source r_s) and the input impedance γ_{in}. Some of the operational parameters are usually specified.

Let us now calculate an amplifier circuit for measuring voltage when the limiting voltage e_x and the internal resistance of the source are known.

The value of the compensation resistance r_k is determined from the equation:

$$r_\kappa = \frac{e_x}{I_N}.$$

The value of the nominal output current should not, as a rule, be chosen smaller than 50 μa, since otherwise fluctuations of the instrument's zero may become noticeable.

When a photoelectric amplifier is connected to a photocompensation circuit the latter acquires due to feedback new dynamic properties very different from those of a photoelectric galvanometer. In order to account for these properties it is usual to represent the photocompensation amplifier as an equivalent galvanometer, whose moment of inertia is equal to the moment of inertia of the amplifier galvanometer, and the specific restoring moment W_{el} is determined from the formula [2]:

$$W_{el} = \frac{\psi}{10} \cdot \frac{r_\kappa K}{\Sigma r},$$

where Σ_r is the total impedance of the galvanometer circuit.

The accuracy of the amplifier is characterized by the lack-of-compensation error γ, which is determined from the formula:

$$\gamma=\frac{W_{\kappa}}{W_{el}}.$$

The lack-of-compensation error of the amplifier can be decreased by balancing or by taking into account its value [2].

The period of free oscillations of the photocompensation amplifier T_{0el} is determined from the formula:

$$T_{0el}=2\pi\sqrt{\frac{J}{W_{el}}}.$$

The degree of damping is found from the expression:

$$\beta=\frac{\psi\cdot 10^{-9}}{2\Sigma r\sqrt{J W_{el}}}.$$

Quantity β should not be made less than 0.5 to avoid self-oscillations [3].

With the knowledge of the period of free oscillations T_{0el} and the degree of damping β, it is easy to determine by means of known relationships the decay time τ.

With a degree of damping exceeding 0.8 and inaccuracies of reading of 2% it is convenient to use for calculating the damping time formula:

$$\tau=1.2\,\beta T_{0el}.$$

The input impedance of the amplifier (static) is determined from:

$$r_{in}=\frac{\Sigma r}{\gamma}.$$

The calculation of a photocompensation amplifier for measuring current with a given range and internal resistance of the source is made in a similar manner.

In this instance the only difficulty is the determination of the compensation resistance r_k and the additional resistance r_a, since only the ratio between them is known:

$$r_a=\frac{I-i_x}{i_x}r_{\kappa}.$$

In this case quantities r_k and r_a should be chosen on the basis of conditions for the best damping and minimum error.

The value of the electrical restoring moment for the photocompensation current amplifier is calculated from formula:

$$W_{el}=\frac{\psi}{10}\cdot\frac{r_{\kappa}K}{r_g+r_a+r_{\kappa}+\frac{r_g}{r_{st}}(r_{\kappa}+r_a)}.$$

The input impedance is determined from:

$$r_{in}=\gamma\frac{(r_\kappa+r_a)\,r_g}{r_\kappa+r_a+r_g}.$$

An example of calculating parameters of a photocompensation amplifier. Let us calculate the parameters of a photocompensation amplifier with a sensitivity of 40 μv and an output microammeter M24 of 100 μa and internal resistance of 3000 ohm. Let the internal resistance of the voltage source be 40 ohm. Since the instrument will have to work in this case from a low resistance source we should choose amplifier F17/1. No additional amplification will be required.

Let us determine the conversion ratio of the amplifier. Let us assume the voltage across the incandescent lamp to be 6 v and across the photoresistors 100 v.

The conversion factor will then be:

$$K=\frac{30\,U}{4400+r_1}=\frac{30\cdot100}{4400+3000}=0.4\ \text{amp/rad}$$

and the compensation resistor:

$$r_\kappa=\frac{e_\kappa}{I_N}=\frac{40\cdot10^{-6}}{100\cdot10^{-6}}=0.4\ \text{ohm}.$$

Next we find the electrical restoring moment:

$$W_{el}=\frac{\psi}{10}\cdot\frac{r_\kappa K}{\Sigma r}=\frac{10^6}{10}\cdot\frac{0.4\cdot0.4}{60+0.4+40}=160\ \text{dyne}\cdot\text{cm}.$$

The lack-of-compensation error will be

$$\gamma=\frac{W_M}{W_{el}}=\frac{0.74}{160}=0.5\%.$$

and the input impedance:

$$r_{in}=\frac{\Sigma r}{\gamma}=\frac{100}{0.005}=20\,000\ \text{ohm}.$$

The period of free oscillations:

$$T_{0el}=2\pi\sqrt{\frac{J}{W_{el}}}=6.28\sqrt{\frac{0.085}{160}}=0.14\ \text{sec}.$$

The degree of damping:

$$\beta=\frac{\psi^2\cdot10^{-9}}{2\Sigma r\sqrt{JW_{el}}}=\frac{10^{12}\cdot10^{-9}}{2\cdot100\cdot\sqrt{0.085\cdot160}}=1.4.$$

and the amplifier decay time:

$$\tau = 1.2\ \beta T_{\text{sel}} = 1.2 \cdot 1.4 \cdot 0.14 = 0.25\ \text{sec}.$$

Thus the decay time and the error of the amplifier are determined primarily by the parameters of the output microammeter.

Examples of use of the F17 photoelectric amplifiers. At present the F17 photoelectric amplifiers are already being used to a certain extent.

Thus the ZIP plant is making ink recorders N373 incorporating an F17 amplifier and possessing 23 ranges, starting with 0.5 mv and 0.5 μa full scale deflections. The decay time of the recorders does not exceed 2 sec.

In the "Vibrator" plant several instruments are produced which incorporate the F17 amplifier. They include the photocompensation voltage stabilizers U1136. These stabilizers have 8 ranges from 0 to 3–450 v and 300 to 30 ma, respectively. The stability of the output voltage provided by these stabilizers is 0.01%.

The development has been completed of multirange thermoelectric voltmeters T17 which have a range up to 1 Mc measuring down to 75 mv; they have a large overload capacity (ten times the scale for transients).

The development of a sensitive photocompensation fluxmeter is proceeding. The photocompensation instruments already produced are completely serviceable under laboratory and field conditions, thus disproving the opinion that these instruments are very shock-sensitive. Only when especially sensitive instruments are made does it become necessary to place them on specially massive tables or main walls.

Conclusions. The photoelectric amplifiers F17 have no electronic tubes, they are simple and reliable. Their output power is sufficient to work normal indicating and ink recording instruments. When this power is inadequate other amplifying devices can be connected to them (electronic, magnetic and other amplifiers including electric motors) thus providing any output power that may be required in practice. The zero drift in such cases remains, as it was originally insignificant.

The F17 photoelectric amplifiers should extend the use of photocompensation systems to various spheres of science and technology.

LITERATURE CITED

[1] B. T. Kolomiets and A. O. Olesk, Élektrichestvo No. 6 (1956).

[2] B. A. Seliber and S. G. Rabinovich, Automation and Remote Control 23, 8 (1957).**

[3] S. G. Rabinovich, Measurement Techniques No. 1 (1957).

ZERO INDICATOR FOR HIGH RESISTANCE MEASURING CIRCUITS

T. B. Rozhdestvenskaia and G. F. Pankratov

In measuring high resistances or small continuous voltages in high resistance circuits it is becoming increasingly common to use null indicators which consist of ac amplifiers with dc to ac converters (vibrator choppers, dynamic capacitors) [1, 2, 3].

In the VNIIM* electrical measurements laboratory a null indicator was developed which can be classed as dc to ac converter. The indicator is designed for use in bridge or compensation circuits for measuring high resitances.

* VNIIM = All-Union Scientific Research Institute of Metrology.

** See English translation.

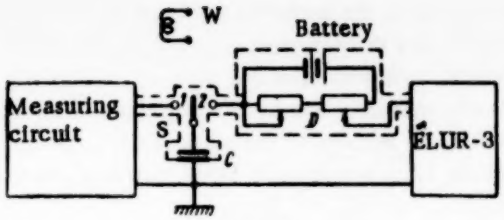

Fig. 1.

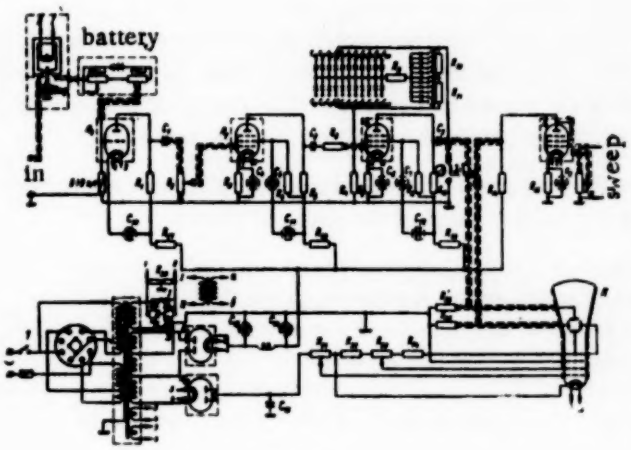

Fig. 2.*

The block schematic of the null indicator is shown in Fig. 1. A small capacity well-insulated air capacitor C is switched by means of a special switch S alternately from the measuring to the input circuit of an ac amplifier which has a C-ray tube connected to its output. If the measuring circuit is not balanced, each time switch S is in position 1 the capacitor has the unbalance voltage connected across it. When the capacitor C is switched to the input resistance of the amplifier a pulse is produced on the cathode-ray tube screen owing to the discharge of the capacitor. The amplitude and polarity of the pulse depend on the amplitude and polarity of the unbalance voltage. Switch S is energized by means of winding W which is fed with an alternating current.

The sensitivity of the amplifier is only limited in practice by the instability of the contact potential difference of switch S and the noise level of the ac amplifier. The contact potential difference can be limited with appropriate construction, to several microvolts and the noise level of the amplifier lies in the region of 10^{-6} to 10^{-7} v [1].

The inertness of the amplifier is determined by the time constants of the two circuits: "capacitor-measuring circuit output" and "capacitor – amplifier input." Since the output resistance of circuits for measuring high resistances is usually of the order of 10^{7}-10^{8} ohm, the time constant of the capacity charging circuit with a capacitor of a few $\mu\mu$f is sufficiently small (of the order of 10^{-5} to 10^{-4} sec). The capacity discharging circuit time-constant is, with an input resistance of the amplifier of 10^{6} - 10^{7} ohm, of the order of $10^{-5} - 10^{-7}$ sec. At a switching frequency of 50 cps a capacitor of 6-7 $\mu\mu$f with above circuit parameters has time to charge and discharge practically completely.

The mean value of the consumed current of the measuring circuit is

$$i_{av} = Qf = Cuf, \qquad (1)$$

where Q is the charge received by the capacitor when switched to the measuring circuit; C – the capacity of the capacitor; u – the unbalance voltage of the measuring circuit; f – the switching frequency.

Since at the instant switch S makes in position 1 capacitor C is discharged, the current taken from the measuring circuit at that instant is relatively large. When the instrument is used as a null indicator, however, the initial value of the current is due to a small unbalance voltage in a high output resistance of the measuring circuit. Therefore the current pulse as the capacitor is connected to the measuring circuit, is not large.

Voltage u at output of the measuring circuit in a near balance condition depends on the sensitivity of the null indicator, i.e., on the minimum voltage across capacitor C that will cause a noticeable pulse at the amplifier output.

If we take C = 5 – 6 $\mu\mu$f, u - 10^{-5} v, f = 10 – 50 cps, the mean current will be $i_{av} = 5 \cdot 10^{-16}$ to $3 \cdot 10^{-15}$ amp. With an output resistance of the measuring circuit of $r_m = 10^{7} - 10^{8}$ ohm, the current at the instant the capacitor is connected will be $i_{max} \leq 10^{-12}$ amp. Thus both the i_{av} and i_{max} are very small.

Pulses can appear at the output of the amplifier even without any voltage in the measuring circuit. They are due to the contact potential differences of switch S and a possible thermal emf. The contact potential

* л = tube.

difference and thermal emf's depend on the type of contact materials used, the material of the capacitor vane, the cleanliness of the vane surfaces and the contacts, their uniformity and the construction of the entire input circuit. If above components are properly made the contact potential difference and the thermal emf do not exceed a few microvolts. Their effect can be reduced still further by means of a special compensation circuit D which eliminates pulses at the output of the amplifier when there is no voltage at the output of the measuring circuit. Experience has shown that the compensation circuit need not be adjusted more often that every 30-60 min.

The circuit comprises an amplifier with a cathode-ray tube at its output (type ÉLUR-3 of the "Étalon" plant) whose schematic is given in Fig. 2. For convenience of observation horizontal scanning is used. A polarized relay is used as switch S. The relay armature, which carries the moving contact, is made of polystyrene in the shape of a strip; a steel plate is fixed at the end of the armature which is placed between the poles of a magnet. The relay is fed by 50 cps current. The magnetic circuit of the relay with its coils is placed inside a steel screen but the stationary and moving contacts are placed in a separate brass cover. The contacts are made of silver and mounted on a polystyrene plate in order to obtain the required high insulation [4].

In order to ensure a high insulation of the capacitor it is mounted on amber supports. The zero adjustment compensator consists of two variable nonwire resistors. A dry battery supplies the required voltage.

An experimental model of the null indicator, which in fact was a laboratory hook-up, did not have a sufficiently high sensitivity and therefore could not be used for measuring resistances above 10^{11} ohm. When a special amplifier with a lower noise level and a higher gain was developed and the switching frequency lowered to 5 cps, it became possible to measure resistors of the order $10^{13} - 10^{14}$ ohm.

LITERATURE CITED

[1] L. I. Baida and A. A. Semenkovich, DC Amplifiers [in Russian] (1953).

[2] A. H. Scott, Measurements of multimegohm resistors, J. Nat. Bureau of Standards, 56, 3 (1953).

[3] H. Palevsky, R. K. Swank and Grenchik, Rev. Sci. Instr. 18, 5 (1947).

[4] B. S. Sinitsyn, "The effect of leakage currents on the errors of measurements in dc circuits" Scientific Notes of the L'vov Polytechnic Institute, Electrotechnical Series [in Russian] issue 8, No. 4 (1949).

A NULL INDICATOR FOR DC MEASURING DEVICES

M. Kh. Shliomovich and M. Sh. Kapnik

It is often difficult to find null indicators (galvanometers) suitable in current and voltage sensitivity for dc bridges or potentiometers. This usually happens in circuits where high resistance null indicators are required, while high-resistance galvanometers with a sufficiently high current sensitivity are not available. A circuit for measuring high resistances of the order of 10^7 ohm can serve as an example.

Sometimes it becomes necessary to use a galvanometer in conjunction with a dc amplifier or to convert dc into ac and feed it to an ac amplifier (see for instance [1]), which has at its output an ac indicating instrument. Such devices are comparatively complicated and a dc amplifier cannot always be made sufficiently reliable and stable. Hence, sometimes in the cases mentioned above, it is recommended to use [2, 3] as a dc null indicator a device consisting of a capacitor, galvanometer and a switch.

This device operates in the bridge circuit (Fig. 1) in the following manner. The voltage from the measuring diagonal of the bridge U_{xx} is fed through switch S_1 to capacitor C which is charged if the bridge is unbalanced. Next the capacitor is disconnected by means of the switch from the bridge and is discharged into galvanometer G. The galvanometer moving coil is deflected by the discharge current pulse.

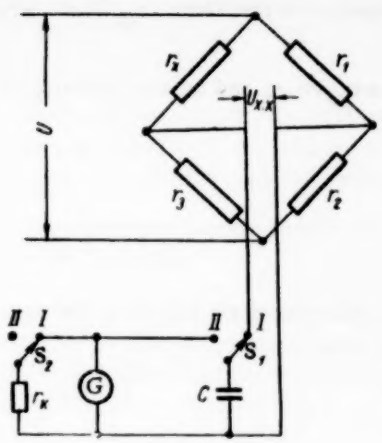

Fig. 1.

The device is arranged to produce a periodic charging and discharging of the capacitor, i.e., a periodic series of pulses through the galvanometer. A variation in the bridge arms will produce a corresponding change in the pulses. By the increasing or decreasing of these pulses as observed on the galvanometer it is possible to judge whether the bridge is approaching balance or not. Moreover it is not necessary to charge the capacitor completely. It is sufficient to note the charging time t_1 of the capacitor. If the circuit is approximately balanced beforehand or if the time constant of the charging circuit is small, the time t_1 can be fixed approximately and the capacitor switched manually.

In some of the null indicators of this type [2] the time interval t_1 is fixed by means of switching contacts of a relay controlled by a thyratron. In the version described below the switching is made by means of a mechanical drive which carries a cam on its axis. When the axis is rotated the cam operates the contacts.

Below we give an example of the use of the indicator in a high-resistance bridge and provide the specification of the circuit components.

In this device it is desirable to discharge the capacitor completely in order not to aggregate in the capacitor charges from each incomplete discharge and thus complicate the single value relation between charge on the capacitor and the kick of the galvanometer.

The time t_2 in which the capacitor discharges completely and the galvanometer is deflected is also determined by closing appropriate contacts by means of the drive.

The use of such a null indicator provides a higher sensitivity for the bridge than an ordinary galvanometer. The high sensitivity is due to the fact that even an insignificant voltage, which produces across the measuring bridge diagonal a very small charging current, will provide the capacitor in the first part t_1 of the period with enough energy for a sufficiently large current pulse in the second part t_2 of the period to make the galvanometer deflection noticeable.

Its second advantage is its high input resistance.

Its third advantage consists in the elimination of the requirement for matching in the usual manner the bridge and indicator resistances for an optimum bridge operation.

Sensitivity. The increased sensitivity of the suggested indicator as compared with a galvanometer connected in the usual manner directly across the bridge diagonal can be explained in the following way.

Let us compare the deflection dc of the galvanometer, when it is connected directly to the bridge diagonal, with its kick α_m for the conditions under discussion. Let us connect the galvanometer to a resistance near its critical value.

When the galvanometer is connected directly to the bridge diagonal we have:

$$\alpha_c = S_I I, \tag{1}$$

where S_I is the galvanometer current sensitivity; I is the current in the galvanometer coil.

The current through the galvanometer is determined from:

$$I = \frac{U_{xx}}{r_g + \frac{r_g r_к}{r_g + r_к}} \cdot \frac{r_к}{r_g + r_к}, \tag{2}$$

where r_g is the galvanometer resistance; r_k is the external critical galvanometer resistance; r_{gg} is the bridge resistance across the indicator terminals.

Since in the case of the high resistance bridge under consideration $r_{gg} \gg r_g$ and for the majority of galvanometers $r_k \gg r_g$, we finally obtain:

$$I \simeq \frac{U_{xx}}{r_{gg}}. \tag{3}$$

When the galvanometer is connected to the circuit in question its parameters are chosen in the manner described below so as to make the galvanometer work in a ballistic condition:

Then:

$$\alpha_m = S_{bk} Q = S_I \frac{2\pi}{T_0 e} Q, \tag{4}$$

where S_{bk} is the ballistic sensitivity in a critical operating condition; Q is the charge on the capacitor; T_0 is the period of the galvanometer free oscillations.

The voltage across the capacitor is:

$$U_c = U_{xx}\left(1 - e^{-\frac{t_1}{r_{gg}C}}\right). \tag{5}$$

Then

$$Q = U_c C = U_{xx}\left(1 - e^{-\frac{t_1}{r_{gg}C}}\right)C. \tag{6}$$

From (1) and (4) we obtain the relation between the galvanometer indications in either case.

$$\frac{\alpha_m}{\alpha_c} = \frac{2\pi}{T_0 e}\left(1 - e^{-\frac{t_1}{r_{gg}C}}\right) r_{gg} C. \tag{7}$$

It is obvious that for a high resistance bridge circuit with a suitably chosen C it is possible to obtain a ballistic throw of the indicator greater than the deflection of a galvanometer connected directly to the bridge diagonal, although this may require a greater time for measurements.

It should be noted that it is easy to increase the value of α_m by a factor of e:

$$\alpha_m = S_I \frac{2\pi}{T_0} Q. \tag{8}$$

For this purpose it is only necessary to discharge the capacitor into an open circuited galvanometer. Then the ballistic sensitivity of the galvanometer will increase by a factor of e and its operation time will rise but little.

While the capacitor is being charged, however, the galvanometer is connected by switch S_2 to a critical resistance in order to decrease the time of its return to zero. When these conditions are fulfilled (7) becomes:

$$\frac{\alpha_m}{\alpha_c} = \frac{2\pi}{T_0}\left(1 - e^{-\frac{t_1}{r_{gg}C}}\right) r_{gg} C. \tag{9}$$

The choice of circuit parameters. It will be seen from the above that the time intervals t_1 and t_2 and the value of capacity C are determined in relation to the galvanometer sensitivity S_I, the period of its free oscillations T_0, and the specified bridge sensitivity and the resistance of its arms.

In choosing optimum values for t_1, t_2 and C it is necessary to consider the following sometimes contradictory requirements.

1. The intervals t_1 and t_2 must not be large so that measurements do not last too long. The minimum t_1 however, should be large enough for the galvanometer to return to zero while the capacitor is being charged. Since the galvanometer takes about 1.5 T_0 to return to zero when it is connected to a resistance near its critical value, t_1 should be chosen so that

$$t_1 \geqslant 1.5\ T_0. \tag{10}$$

2. On the other hand t_1 should be large enough to produce a substantial charge Q on the capacitor (the charge $Q\text{-}CU_C$ increases with t_1). A large charge provides a large galvanometer deflection.

3. For the same considerations C should be made as large as possible; but an electrolytic capacitor has across its terminal a random voltage which may exceed the signal voltage.

4. On the other hand a small capacity C is required for a small discharge time constant $\tau_{ds} = Cr_g$. A small value of τ_{ds} is necessary to make the galvanometer operate under conditions close to the ballistic ones. In fact, so as to obtain proportionality between charge Q and the throw of the galvanometer it is necessary to make the duration of the capacitor discharge t_{ds} considerably smaller than that of the galvanometer throw t_t. In practice it is sufficient to make $t_{ds} \simeq 3\tau_{ds} = 3Cr_g$ to obtain a complete discharge of the capacitor.

On the other hand for a galvanometer in a state of free oscillations:

$$t_t \simeq 0.25\ T_0. \tag{11}$$

This provides the condition of operation used in ballistic galvanometer circuits:

$$t_{dc} \ll t_t$$

or

$$3Cr_g \ll 0.25\ T_0. \tag{12}$$

An example of calculating indicator circuit components. The bridge designed to measure resistances r_x up to 10^9 ohm consists of ratio arms 10^5 and 10 ohm and a measuring arm of 10^5 ohm. For these values $r_{gg} = 10^5$ ohm. The bridge is fed from a 100 v battery. The type M21 galvanometer has the following characteristics: $r_g = 500$ ohm, $r_k = 20000$ ohm, $C_I = 1.5 \cdot 10^{-9}$ amp/mm/m and $T_0 = 4$ sec. The error of measuring r_x must not exceed 1% with a bridge sensitivity of approximately 0.3%.

It is first necessary to find the value of voltage U_{xx} at the measurement diagonal of the bridge when it is unbalanced.

It is obvious that with the specified bridge parameters a change of the resistance of one of the bridge arms

$\Delta r/r$ by 0.3 will produce:

$$U_{xx} = 30 \cdot 10^{-6} \text{ V}.$$

From (1) we have:

$$\alpha_c = \frac{I}{C_I} \simeq \frac{U_{xx}}{C_I r_{gg}} = \frac{30 \cdot 10^{-6}}{1.5 \cdot 10^{-9} \cdot 10^5} = 0.2 \text{ mm/m}$$

Let us now determine the ballistic throw under the condition that during the discharge the galvanometer is in a free oscillating condition and during charging is connected to its critical resistance.

It is obvious from (8) that:

$$\alpha_m = \frac{2\pi Q}{C_I T_0} = \frac{2\pi U_{xx} C}{C_I T_0}\left(1 - e^{-\frac{t_1}{r_{gg} C}}\right).$$

From (10) we obtain the minimum time:

$$t_1 = 1.5 \cdot 4 = 6.0 \text{ sec}.$$

Selecting (with a margin) $t_1 = 8.5$ sec and C = 100 μf we obtain:

$$\alpha_m = \frac{2\pi \cdot 30 \cdot 10^{-6} \cdot 10^2 \cdot 10^{-6}}{1.5 \cdot 10^{-9} \cdot 4}\left(1 - e^{-\frac{8.5}{10^5 \cdot 10^2 \cdot 10^{-6}}}\right) =$$

$$= 1.8 \text{ mm/m}.$$

The throw of the galvanometer is increased by a factor of 9 as compared with its deflection when it is connected directly to the circuit.

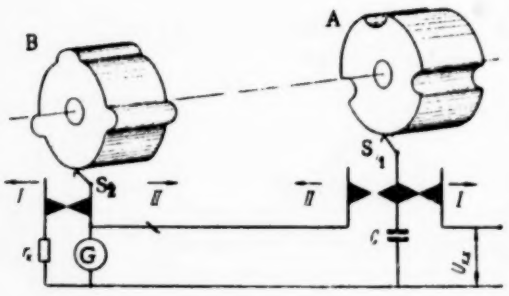

Fig. 2.

Let us check the fulfilment of condition (12). It is obvious] that $t_{ds} = 3.5 \cdot 10^2 \cdot 10^{-4} = 0.15$ sec. On the other hand $t_t = 0.25$ $T_0 = 0.25 \cdot 4 = 1$ sec.

Hence the condition of the ballistic state of the galvanometer is fulfilled in this case.

Naturally a larger ballistic throw could be obtained with a larger t_t or C, but this would lead to a longer measuring time or the breaking of condition (12). The inadvisability of increasing C is demonstrated in the table below, which shows values of α_m/α_c and t_{ds} obtained from (9) for this example at $t_1 = 8.5$ sec for various values of C. The impossibility of using 1000 μf becomes apparent from the table, since it infringes condition (12).

The experimental model was driven by a Warren motor with a reduction gear whose axis turned at 2 rpm and had three cams mounted on it. The contact through which the capacitor discharges remains closed for time $t_2 = 1.5$ sec. The discharge itself is completed in 0.15 sec after the closing of the contact, but the galvanometer throw lasts 1 sec. The time of one complete cycle of operations of a null indicator is $T = t_1 + t_2 = 8.5 + 1.5 = 10$ sec.

In order to achieve an increase in the ballistic sensitivity of the galvanometer by a factor of e it is necessary to disconnect from the galvanometer resistance r_k during discharging. For this purpose a more intricate cam is used (Fig. 2). It consists of two parts A and B(for clarity they are shown separately on the drawing). Part A serves to switch over capacitor C from the bridge diagonal to the galvanometer by means of a double

C, μf	$\frac{r_m}{r_c}$	$t_{ds} = 3\tau_{ds}$, sec
1000	12.5	1.5
100	9.0	0.15
10	1.56	0.015
1	0.16	0.0015

throw switch S_1. Part B serves to connect to and disconnect from the galvanometer resistor r_k. This is performed by switch P_2 driven by cam B. The time t_3 during which the galvanometer is not connected to r_k is made slightly longer than t_2 and time t_4 during which r_k is connected to the galvanometer is found from the relation:

$$t_4 = T - t_3.$$

In our example the following values of t_3 and t_4 were found convenient

$$t_3 = 2 \text{ sec} \qquad t_4 = 8 \text{ sec}$$

LITERATURE CITED

[1] T. B. Rozhdestvenskaya, and G. F. Pandratov, Measurement Techniques, No. 5 (1959).•

[2] A. E. Hawkins, J. Sci. Instr. No. 12 (1956).

[3] J. I. Carasso and R. W. Pittman, J. Chem. Soc., April, 1956.

• See English translation.

MEASUREMENTS AT HIGH AND ULTRAHIGH FREQUENCIES

FREQUENCY ERRORS IN MEASURING CAPACITY BY MEANS OF Q METERS

G. M. Strizhkov

An attempt is made in this article to find the frequency errors which arise when capacity is measured at high frequencies on Q meters type KV-1 and UK-1.

Q meter equivalent circuit. In studying the properties of Q meters KV-1 and UK-1 it is convenient to replace their circuits by equivalent ones (Fig. 1) which consists of reactances only, since the active resistances affect but little the measurement of capacity.

The type KV-1 Q meter trimming capacitor reactances are small enough to be omitted on the equivalent circuit. We shall also assume that capacitors have no calibration errors at low frequencies.

Let us find the absolute error ΔC in the normal method of measuring capacity by means of Q meters. For this purpose let us connect instead of C_X a known capacity C_0. Such a capacity can be obtained in type KVCh-1 capacitors developed by the NGIMIP.

The value of capacity C_0 measured by the instrument is determined as the difference between two scale readings of capacitor C_k, i.e., as $C_{ms} = C_{k_1} - C_{k_2}$.

On the basis of series resonance we obtain for the equivalent circuit in Fig. 1:

$$C_{K_2} = \frac{C_{K_1} - C_0 - (L_B - L_K)\,\omega^2 C_{K_1} C_0}{1 - \omega^2 C_0 (L_B + L_K) + \omega^4 C_0 C_{K_1} L_K^2}. \tag{1}$$

The absolute error of measurement will be:

$$\Delta C = C_{ms} - C_0 = C_{K_1} - C_{K_2} - C_0. \tag{2}$$

Substituting the values from (1) we have:

$$\Delta C = (C_{K_1} - C_0)\left[1 - \frac{1 - \omega^2 C_0 \dfrac{L_B - L_K}{C_{K_1} - C_0} C_{K_1}}{1 - \omega^2 C_0 (L_B + L_K) + \omega^4 C_0 C_{K_1} L_K^2}\right]. \tag{3}$$

The formula thus obtained accounts for the error caused by the distributed inductances L_b and L_k. It follows therefore, that an omission of inductance L_b from the equivalent circuit will lead to errors in estimating the accuracy of capacity measurements.

Analysis of the absolute error. It follows from (3) that error ΔC depends on several variables. The object of the analysis consists in establishing the nature of functions

$$\Delta C=\psi_1 (C_{k_1}) \text{ for } C=\text{const} \;\&\; \omega=\text{const},$$
$$\Delta C=\psi_2 (C_0) \text{ for } C_{k_1}=\text{const} \;\&\; \omega=\text{const},$$
$$\Delta C=\psi_3 (\omega) \text{ for } C_{k_1}=\text{const} \;\&\; C_0=\text{const}.$$

Let us note that error ΔC does not depend on either the total inductance L of the connecting leads or the source of the current, since this inductance is included both in the first and second tuning to an equal extent.

Effect of the first tuning capacity C_{k_1} on the absolute error ΔC of capacity measurements. Let us first examine function $\Delta C = \Psi_1(C_{k_1})$ for the type KV-1 Q meters.

Assuming ω, C_0 = const and denoting:

$$A=C_0\,\omega^2\,(L_k-L_a),$$
$$B=C_0\,\omega^2\,(L_k+L_a),$$
$$D=C_0\,\omega^4\,L_k^2,$$

let us write error ΔC in the form:

$$\Delta C=\psi_1 (C_{k_1})=(C_{k_1}-C_0)\left(1-\frac{1+A\dfrac{C_{k_1}}{C_{k_1}-C_0}}{1-B+DC_{k_1}}\right). \tag{4}$$

By a simple analysis we find the characteristic points of expression (4).

The analysis of expression (4) and the graphical relation $\Delta C = \Psi_1(C_{k_1})$ plotted from it leads to the conclusion that in the region of operation absolute error ΔC is in the first place negative and in the second increases with C_{k_1}.

The absolute error becomes zero, i.e., C = 0 for values of C_{k10}, which are right outside the range of possible values of C_{k_1} (for set KV-1, C_{k_1} max = 450 μμf and for set UK-1, C_{k_1} max = 65 μμf).

Now let us examine relation $C = \Psi_1(C_{k_1})$ for type UK-1 Q meter.

Denoting

$$A=C_0\,\omega^2\,(L_a-L_k),$$
$$B=C_0\,\omega^2\,(L_a+L_k),$$
$$D=C_0\,\omega^4\,L_k^2,$$

we obtain for ω and C_0 = const :

$$\Delta C=(C_{k_1}-C_0)\left(1-\frac{1-A\dfrac{C_{k_1}}{C_{k_1}-C_0}}{1-B+DC_{k_1}}\right). \tag{5}$$

The only difference between (4) and (5) is the sign in front of $A\,\dfrac{C_{k_1}}{C_{k_1}-C_0}$. It can be shown that this sign depends on the relation between the values of L_b and L_k, which differs for UK-1 and KV-1.

The analysis of expression (5) and the graph of function $C = {}_1(C_{k_1})$ show that for set UK-1 the error is positive and decreases with a rise in C_{k_1}, i.e., a reversed effect is observed to that of set KV-1. The absolute error ΔC in set UK-1 will equal zero when $C_{k_1} = C_{k_{10}}$.

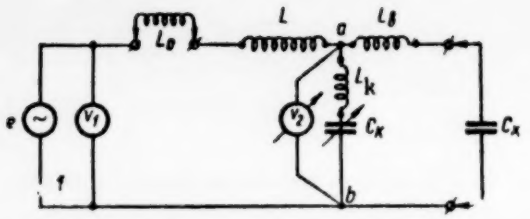

Fig. 1. L_0 is the inductance of the outside coil; L is the total inductance of connecting leads; L_k and C_k are the inductance and capacity of the measuring capacitor; L_b is the inductance of lead-in wires; and C_x is the capacity being measured.

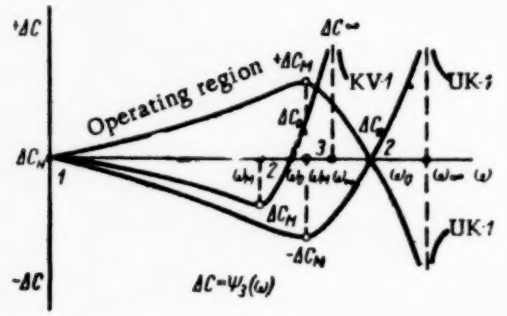

Fig. 2.

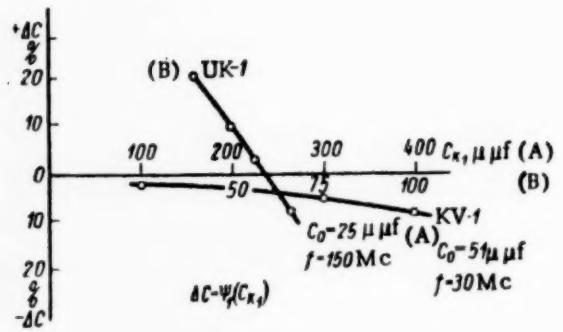

Fig. 3.

Effect of the value of the measured capacity C_0 on the absolute error ΔC of capacity measurements. For this purpose let us examine $\Delta C = \psi_2(C_0)$ for type KV-1 instruments. Denoting:

$$A = C_{K_1}\,\omega^2\,(L_K - L_a),$$
$$B = \omega^2\,(L_K - L_a),$$
$$D = \omega^4\,C_{K_1}\,L_K^2,$$

we obtain

$$\Delta C = \psi_2\,(C_0) = (C_{K_1} - C_0)\left(1 - \frac{1 + A\dfrac{C_0}{C_{K_1} - C_0}}{1 - BC + DC_0}\right). \quad (6)$$

Assuming that in expression (6) $A\,\dfrac{C_{00}}{C_{k_1} - C_{00}} = DC_{00} - BC_{00}$, we will obtain $\Delta C_0 = 0$ for

$$C_{00} = C_{K_1} + \frac{C_{K_1}\,(L_K - L_a)}{L_K + L_a - \omega^2\,C_{K_1}\,L_K^2}. \quad (7)$$

An analysis of expression (6) shows that between the values of $C_0 = 0$ and $C_0 = C_{k_1}$ the error ΔC has a maximum value and that the maximum is in the region of C_0 = 5 and 20 μμf, i.e., in the operating region of set KV-1.

For sets of the UK-1 type let us denote:

$$A = \omega^2\,C_{K_1}\,(L_a - L_K),$$
$$B = \omega^2\,(L_a + L_K),$$
$$D = \omega^4\,C_{K_1}\,L_K^2,$$

we have

$$\Delta C = (C_{K_1} - C_0)\left(1 - \frac{1 - A\dfrac{C_0}{C_{K_1} - C_{K_0}}}{1 - BC_0 + DC_0}\right). \quad (8)$$

An analysis of expression (8) shows that for $C_0 = C_{k_1} = C_0'$ we have:

$$\Delta C' = \frac{AC_0'}{1 - BC_0' + DC_0'}. \quad (9)$$

If $A\,\dfrac{C_0''}{C_{k_1} - C_0''} = 1$ the error is:

$$\Delta C'' = C_{K_1}\left(1 - \frac{1}{1 + A}\right) \quad (10)$$

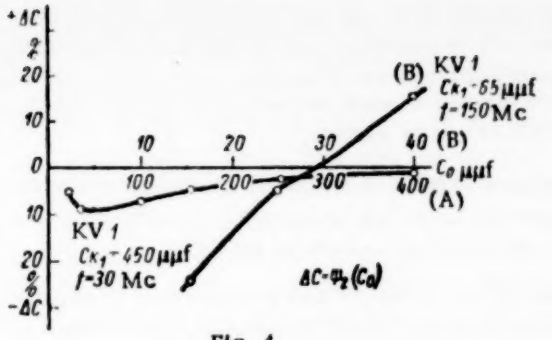

Fig. 4.

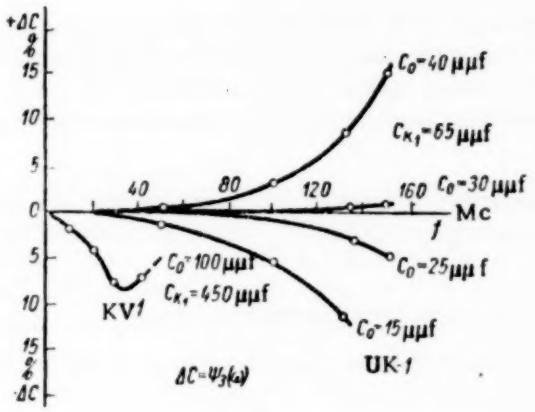

Fig. 5.

with $C_0^* = \dfrac{C_{k_1}}{1 + \omega^2 C_{k_1}(L_b - L_k)}$.

It is characteristic that $\Delta C = 0$ for $C_0 < C_{k_1}$.

Effect of the operating frequency on the absolute error ΔC of capacity measurements. For set KV-1 we have:

$$\Delta C = A\left(1 - \frac{1 - \omega^2 B}{1 - D\omega^2 + E\omega^4}\right). \qquad (1)$$

where

$$A = C_{k_1} - C_0,$$

$$B = \frac{C_{k_1} C_0 (L_k - L_a)}{C_{k_1} - C_0},$$

$$D = C_0 (L_k + L_a),$$

$$E = C_0 C_{k_1} L_k^2.$$

From equation (11) it is easy to plot a graph of function $\Delta C = \psi_3(\omega)$ (Fig. 2) which has a maximum at $0 < \omega < \omega_0$.

Both for UK-1 and KV-1 Q meters function $\Delta C = \psi_3(\omega)$ has a maximum between the values of $\omega = 0$ and $\omega = \omega_0$. Contrary to the KV-1 set the error ΔC in set UK-1, however, can have both a positive and negative sign depending on the value of B being larger or smaller than unity. In turn the value of B depends on the measured value of C_0. This condition is shown in Fig. 2.

Test results. The formula for the absolute error ΔC and relations for the characteristic points of function $\Delta C = \psi(C_k, C_0, \omega)$ include the distributed L_k and L_b. It is however, difficult to determine their values accurately. It is therefore impossible to calculate by means of this formula the absolute error and correct the measurement of capacity. Hence corrections must be obtained experimentally by means of a known capacity. High-frequency coaxial capacitors type KVCh developed by the NGIMIP were the reference capacities. They are made in the form of open-circuited coaxial lines working at frequencies below their 1/4 wave resonance. A short circuited coaxial line was used as the external induction L_0.

Test results are given in Figs. 3-5.

On the basis of these data it is possible to arrive at the following conclusions:

1. For Q meters type KV-1 the error of measurement decreases with a decreasing first tuning capacity C_{k_1} (Figs. 2, 5).

2. For the UK-1 instruments the minimum error occurs when the first tuning capacity C_{k_1} is equal to 50-60 μμf (Figs. 2, 5).

3. With the normal method of capacity measurement the following errors will arise at the highest guaranteed frequency: for the KV-1 sets from −6 to −8% at f = 30 Mc; for the UK-1 sets from +5 to −10% at f = 100 Mc.

4. With a decreasing frequency the error of capacity measurements decreases.

5. In order to decrease this error it is advisable to change the method of measurements for set KV-1, namely to obtain the first tuning with the capacity under test and the minimum capacity C_{k_1} of the measuring capacitor, C'_{k_1} and the second tuning without the capacity under test and the measuring capacitor at C'_{k_2}.

Then the measured capacity will be $C_x = C'_{k_2} - C'_{k_1}$.

As far as UK-1 type Q meters are concerned the former method of measurement can be preserved, but the capacity for the first tuning should be chosen as near to 50-60 $\mu\mu f$ as possible.

6. Taking into consideration that with the present design of sets KV-1 and UK-1 deviations of the distributed inductances from the above-mentioned values will occur, the following limiting capacity measurement errors should be established for these instruments: -10% for set KV-1 and $\pm 10\%$ for set UK-1.

Let us note that at present these errors are not specified at all. It should also be noted that in addition to errors in capacity measurements due to distributed constants there are also errors including those caused by the tube voltmeter circuit, the reaction of the oscillator supplying the measuring circuit, etc. The study of these errors, however, is outside the scope of the present investigation.

Variations of the self-inductance of the measuring capacitor. It is known that the self-inductance of the measuring capacitor is one of the causes of the ΔC error and the entire analysis on which formula (3) is based was made with the assumption that this induction does not vary during measurement. Experience has shown however, that square-law capacitors whose vanes have a noncircular shape change their inductance with respect to the angle of rotation of the moving vanes.

By connecting a known inductance in series with the capacitor, it is possible to determine from the resonant frequency and the value of the capacitor the additional inductance $L_a = L + L_k$, which includes the varying inductance L_k of the capacitor.

On the basis of the results thus obtained it is possible to arrive at the following conclusions:

1. Measuring capacitors with noncircular vanes change their self-inductance with respect to the angle of rotation of the moving vanes (instruments type KV-1).

2. Linear capacitors do not change their inductance with respect to the angle of rotation of the moving vanes (instruments type UK-1).

3. In view of the above results it is advisable to fit the KV-1 sets with linear capacitors.

Conclusions. The theoretical and experimental data obtained above may serve as a basis for establishing error tolerances in measuring capacity with KV-1 and UK-1 sets at high and ultrahigh frequencies.

FREQUENCY DEVIATION METER ERRORS AND A METHOD OF CHECKING THEM

I. M. Sorkin

The wide application of frequency modulation in communications and broadcasting led to the construction of deviation meters, instruments designed for checking frequency deviations.

According to specification the deviation meters should provide frequency deviation measurements with an overall accuracy of 5-10%. These tolerances in deviation meter errors are to a certain extent tentative and are based on the calculation of component errors. An experimental determination of these errors is difficult owing to the lack of specification for checking deviation meters approved by the Committee of Standards, Measures and Measuring Instruments.

Hence the development of a technique for determining experimentally components of the total deviation meter error has become a pressing matter.

The principle of operation and block-schematic of a deviation meter. The principle of operation of the deviation meter is based on the conversion of the frequency-modulated signal into a low frequency voltage whose amplitude is proportional to the deviation frequency.

Figure 1 shows the block schematic of the deviation meter. The voltage of the measured signal is amplified and fed to the mixer together with the local oscillator voltage. At the output of the mixer the intermediate frequency is filtered out, amplified and fed to the voltage limiter, which eliminates the parasitic amplitude modulation of the signal and provides a constant voltage signal fed to the frequency discriminator. The frequency discriminator converts the frequency modulated signal into a low frequency voltage (of the modulating frequency) whose amplitude is proportional to the frequency deviation of the input frequency-modulated signal. This voltage is measured by means of a tube voltmeter whose scale is calibrated in kc of the deviation frequency.

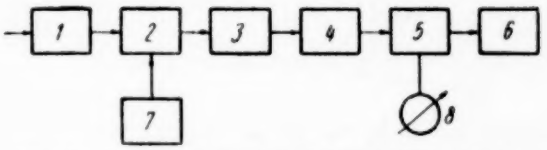

Fig. 1. Block schematic of the deviation meter. 1) High frequency amplifier, 2) mixer; 3) intermediate frequency amplifier; 4) limiter; 5) frequency discriminator; 6) tube voltmeter (kc); 7) local oscillator; 8) tuning indicator.

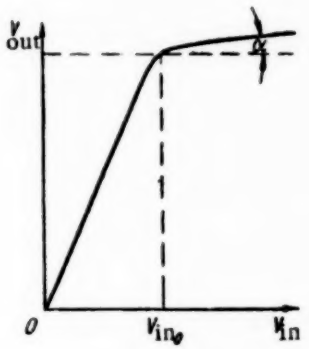

Fig. 2.

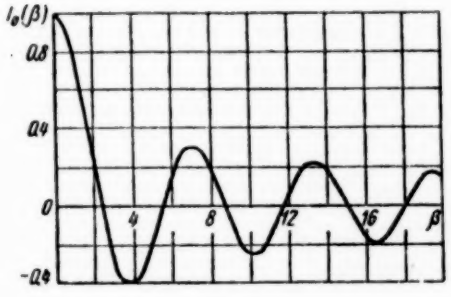

Fig. 3.

Deviation meter errors. The total deviation meter error is composed of the error of the amplifying channel, the limiter error, the frequency discriminator error and the error of tube voltmeter calibration.

Amplifying channel error. The basic theoretical error of the deviation meter is due to the transitional period in the amplifying channel of the instrument. Usually the instrument is calibrated on the assumption that its static and dynamic characteristics are the same. In reality, however, due to the change in the signal frequency, self oscillations arise in the amplifying channel of the instrument and the duration of these oscillations is determined by their decay time.

Hence a frequency modulated signal of frequency Δf, with an amplitude deviation impressed on the input of the instrument will produce at the output of the amplifying channel a signal with a maximum frequency deviation Δf, which will differ from Δf by an amount determined by the transient period. In this instance the reading of the frequency deviation on the instrument scale, which is calibrated in the static condition when all the transient processes in the amplifier have been completed, will contain a certain error:

$$\gamma_1 = \frac{\Delta f - \Delta f'}{\Delta f} \qquad (1)$$

The transition of a frequency modulated signal through an amplifying channel has been studied in a number of papers and formulas characterizing signal distortion for a general case produced, these expressions are too complicated, however, for practical application.

Let us make the following simplifying assumptions which usually hold in practice:

1) the frequency characteristic of an amplifying channel be represented by a single-hump resonance curve of an equivalent tuned circuit,

2) the bandwidth of the amplifying channel at a level 0.7 of the maximum gain is more than twice as great as the amplitude of the deviation frequency

thus providing the transmission of the greater part of the frequency-modulated signal spectrum, which corresponds to the case of small distortions,

3) the phase characteristic of the amplifying channel is linear.

Let the input of such an amplifying channel be fed with a frequency modulated signal whose carrier frequency is equal to the resonance frequency of the amplifying channel:

$$U_1 = U_m e^{j(\omega_0 t + \beta \sin \Omega t)}, \tag{2}$$

where ω_0 is the carrier frequency, β is modulation index, Ω – the angular velocity of the modulating voltage.

The frequency spectrum of this signal can be represented by the expression:

$$U_1 = U_m e^{j\omega_0 t}\left\{I_0(\beta) + \sum_{n=1}^{\infty} I_n(\beta)\left[e^{jn\Omega t} + (-1)^n e^{-jn\Omega t}\right]\right\}. \tag{3}$$

where $I_0(\beta)$, $I_1(\beta)$, $I_2(\beta)$.... $I_n(\beta)$ are Bessel functions of the first kind and zero, 1st, 2nd,...., n-th order with an argument equal to the index of modulation.

In passing through the amplifying channel each component will be amplified by $Q\cos\Psi_n$ and shifted in phase by angle $\frac{\pi}{2} \pm \varphi_n$. Where $Q = \frac{f_0}{B}$; B being the bandwidth of the amplifying channel and Q the Q factor of the circuit, equivalent to the amplifying channel; $\varphi_n = \tan^{-1} \frac{2F}{B} n$; where F is the modulating frequency. Thus the output voltage can be written as:

$$U_2 = U_m e^{j\left(\omega_0 t - \frac{\pi}{2}\right)}\left\{I_0(\beta) + \sum_{n=1} I_n(\beta)\cos\varphi_n\left[e^{j(n\Omega t - \varphi_n)} + (-1)^n e^{-j(n\Omega t - \varphi_n)}\right]\right\}. \tag{4}$$

Considering that

$$\left[e^{j(n\Omega t - \varphi_n)} + (-1)^n e^{-j(n\Omega t - \varphi_n)}\right] = \begin{cases} 2\cos(n\Omega t - \varphi_n) \\ \text{with an even n} \\ 2j\sin(n\Omega t - \varphi_n) \\ \text{with an odd n} \end{cases}$$

we obtain the final expression for the output voltage:

$$U_2 = U_m Q e^{j\left(\omega_0 t - \frac{\pi}{2}\right)}\left\{I_0(\beta) + 2\sum_{n=2;\,4...}^{\infty} I_n(\beta)\cos\varphi_n\cos(n\Omega t - \varphi_n) + 2j\sum_{n=1;\,3;\,5...}^{\infty} I_n(\beta)\cos\varphi_n\sin(n\Omega t - \varphi_n)\right\}. \tag{5}$$

From (5) we have the phase of the output voltage:

$$\Phi = \tan^{-1} \frac{2\sum_{n=1;\,3;\,5...}^{\infty} I_n(\beta)\cos\varphi_n\sin(n\Omega t - \varphi_n)}{I_0(\beta) + 2\sum_{n=2;\,4..}^{\infty} I_n\cos\varphi_n\cos(n\Omega t - \varphi_n)} \tag{6}$$

The maximum error will occur at small modulation indexes β, i.e., at high modulating frequencies F when the transitional period is comparable with that of the modulating frequency.

For $\beta \ll 1$ the frequency spectrum of a frequency-modulated signal can be considered as consisting of the carrier and the first pair of side-bands only: $I_0(\beta) = 1$ and $I_1(\beta) = 0.5\beta$.

Hence

$$\Phi = \operatorname{arctg}[\beta \cos\varphi_1 \sin(\Omega t - \varphi_1)], \tag{7}$$

whence the instantaneous value of the output frequency

$$\omega = \frac{d\Phi}{dt} = \frac{\beta\Omega \cos\varphi_1 \cos(\Omega t - \varphi_1)}{1 + [\beta \cos\varphi_1 \sin(\Omega t - \varphi_1)]^2}. \tag{8}$$

Since $\beta \ll 1$ the second term in the denominator can be neglected

Then

$$\omega = \beta\Omega \cos\varphi_1 \cos(\Omega t - \varphi_1) \tag{9}$$

or by substituting $\beta\Omega = \Delta\omega$ & $\cos\varphi_1 = \frac{1}{\sqrt{1+a^2}}$.

$$\text{where } a = \frac{2F}{B}$$

we finally obtain:

$$\omega = \frac{\Delta\omega}{\sqrt{1+a^2}} \cos(\Omega t - \varphi_1). \tag{10}$$

Thus the frequency amplitude deviation $\Delta\omega$ will correspond to the instrument reading:

$$\Delta\omega' = \frac{\Delta\omega}{\sqrt{1+a^2}}. \tag{11}$$

For the assumptions made, usually $a \ll 1$; hence by developing in a series it is possible to find an expression for the error of the amplifying channel:

$$\gamma_1 = \frac{\Delta\omega - \Delta\omega'}{\Delta\omega} = 1 - \frac{1}{\sqrt{1+a^2}} \simeq \frac{a^2}{2}. \tag{12}$$

Whence substituting the value of a from (12) we obtain:

$$\gamma_1 = 2\left(\frac{F}{B}\right)^2. \tag{13}$$

Thus in a deviation meter with a maximum measurable deviation frequency $\Delta f = 75$ kc and a bandwidth of B = 15 kc the error of the amplifying channel due to the transitional period will be 2%.

It follows from (13) that the error of the amplifying channel can be decreased by increasing its bandwidth.

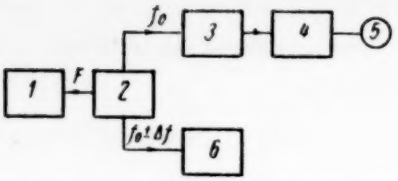

Fig. 4. Block schematic for checking deviation meters in dynamic condition. 1) Audio oscillator; 2) frequency modulation oscillator; 3) receiver; 4) filter; 5) telephone; 6) deviation meter.

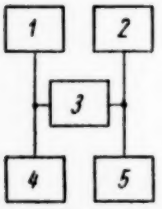

Fig. 5. Block schematic of the deviation meter static condition checking circuit. 1) Standard signal generator GSS-7; 2) audio-frequency oscillator ZG-10; 3) frequency modulation meter IChM-5; 4) heterodyne wavemeter GVShD; 5) voltmeter VLU-2.

The limiter error is due to the incomplete elimination of the parasitic amplitude modulation, which can occur either in the transmitter or in the amplifying channel.

The incomplete voltage limitation is due to the limiter characteristic (Fig. 2) having in the operating region a slope $S = \tan\alpha$.

Moreover, the output voltage of the limiter can change due to the variation of its supply conditions or a change in tubes, which can also produce errors.

In order to avoid errors due to the limited deviation, meters are usually provided with a means of checking the voltage supplied to the discriminator on a scale which shows the working voltage range of the limiter.

The readings of a well designed deviation meter are practically independent of the input voltage, i.e., the limiter error can be neglected.

The frequency discriminator error is due to changes in its characteristic with changing parameters of its components and also to the transient period.

The first component of the error determines in the main the accuracy of the frequency discriminator operation. The second component can be made insignificantly small if the frequency discriminator is used whose linear characteristic corresponds to a frequency range larger than the bandwidth of the amplifier.

Thus the frequency discriminator error γ_2 and the calibration error γ_3 of the tube voltmeter can be considered as static error contrary to the dynamic error γ_1 due to the transient period in the amplifier.

In this connection two methods of checking deviation meters are being used, the dynamic and the static methods.

By checking the deviation meter in its dynamic condition the total error of measurement γ_d can be determined:

$$\gamma_d = \gamma_1 + \gamma_2 + \gamma_3.$$

The checking of deviation meters in a static condition provides the total error in the static state γ_c:

$$\gamma_c = \gamma_2 + \gamma_3.$$

In a well-designed deviation meter the total error in the static condition constitutes a large part of the dynamic error.

Checking the deviation meter in a dynamic state. The deviation meters can be checked in the dynamic state by Crossby's method of measuring frequency deviations. This method consists in determining, by means of a narrow-band receiver tuned to the carrier frequency of the frequency modulated signal, zero values of the carrier frequency with a changing index of modulation.

It follows from (3) and Fig. 3 which shows the variations of the carrier amplitude $I_0(\beta)$ as a function of the modulation index, that the carrier amplitude passes through zero values at $\beta_1 = 2.4$; $\beta_2 = 5.52$; $\beta_3 = 8.65$; etc.

Knowing the value β_k of the k-th carrier amplitude minimum and the modulating frequency F it is possible to determine the actual value of the deviation frequency: $\Delta f_d = \beta_k F$.

By noting simultaneously the deviation meter reading Δf corresponding to β_k it becomes possible to determine the referred relative dynamic error γ_d:

$$\gamma_d = \frac{\Delta f - \Delta f_d}{\Delta f_{max}} \cdot 100\%,$$

where Δf_{max} is the maximum frequency deviation for the given deviation meter scale.

Figure 4 shows a block schematic for checking deviation meters in a dynamic condition by Crossby's method. The advantage of this method consists in its accuracy. Its disadvantage consists in the limitation of its measurements to certain fixed points only.

Moreover this method can in practice be only used with a stable carrier frequency of the transmitter under test and a precisely sinusoidal modulating voltage. Otherwise the drift of the carrier of a frequency modulated signal makes it difficult to tune by means of a narrow-band receiver,especially at low modulating frequencies when the receiver bandwidth must be especially narrow.

It is also obvious that this method cannot be used for checking deviations with modulation indexes smaller than $\beta = 2.4$, which correspond to the first root of the Bessel function $I_0(\beta)$

Checking the deviation meter in a static state. Checking deviation meters in the static condition has become widespread in industry and it provides sufficiently accurate results by relatively simple means. The popularity of this method is due to the deviation measurements in communications and broadcasting being usually made with large modulation indexes $\beta = \Delta f/F$.

For large modulation indexes which correspond to relatively low modulation frequencies the parameters of the modulated oscillation can be considered constant for any given instant, and hence the modulated oscillation as being sinusoidal. In this so-called quasi-stationary condition the feeding to the deviation meter of frequency-modulated signals can be considered equivalent to feeding of consecutive unmodulated stationary frequencies whose values vary from the mean frequency to the maximum one and the frequency deviation in which the instrument is calibrated can be considered equivalent to the difference between the maximum and mean stationary frequencies. The latter consideration provides the means for checking and calibrating the deviation meter under static conditions.

As an example let us examine the checking of a deviation meter type IChM-5.

The connections of the instruments for checking a IChM-5 set are shown in Fig. 5.

The output IChM-5 voltmeter, which is calibrated in kc of the deviation frequency, is first supplied from the audio-frequency oscillator ZG-10 with a low frequency voltage which is increased until the instrument pointer reaches the graduation on the scale corresponding to the deviation being checked. The value of the voltage corresponding to this graduation is read off the ac voltmeter VLU-2.

Next the IChM-5 set is supplied from a standard signal generator GSS-7 with an unmodulated signal, whose frequency corresponds to the mean frequency of the frequency modulated signal and is measured on a reference wavemeter GVShD. Set IChM-5 is then tuned to this frequency. The resonance point is determined by the tuning indicator pointer being at the mid-scale zero. The VLU-2 voltmeter should then read zero on its dc scale.

Next the IChM-5 set is supplied from generator GSS-7 with a signal whose frequency is equal to the frequency of the maximum deviation. This frequency is checked on the wavemeter GVShD and must produce a VLU-2 voltmeter dc scale reading which when multiplied by $\sqrt{2}$ will correspond to its reading on the ac scale.

The difference between the maximum and mean frequencies determines the actual value of the frequency deviation corresponding to the graduation to which the pointer was at first set. The referred relative calibration error γ_c of the IChM-5 output voltmeter in terms of kc of the deviation frequency is determined from the formula:

$$\gamma_c = \frac{\Delta f_n - \Delta f_d}{\Delta f_{max}} \cdot 100\%,$$

where Δf_n is the normal value of the deviation set on the IChM-5 voltmeter scale; $\Delta f_d = f_{max} - f_{av}$ is the actual value of the deviation frequency equal to the difference between the maximum and mean frequencies set on the wavemeter. Δf_m is the maximum deviation frequency for the given IChM-5 scale (10, 30 or 100 kc).

The accuracy of this method is determined by the error of the heterodyne wavemeter GVShD which amount to 0.001% and that of the reference voltmeter VLU-2 which does not exceed 2.5%.

Since the values of these errors are smaller than the permissible error of the IChM-5 set of 5 to 10%, the accuracy of this method is sufficient.

If necessary the accuracy of checking can be increased by using corrections for the reference voltmeter VLU-2 readings.

MEASURING THE VOLTAGE STANDING-WAVE RATIO OF A GENERATOR BY MEANS OF A PHASE SHIFTER

L. S. Liberman

In super-high frequency measurements it is often necessary to have a matched source of power. The use of a decoupling attenuator does not always produce the required results due to reflections from it or to an excessive loss of power. It becomes therefore, necessary to reduce the actual voltage standing-wave ratio by means of a transformer.

It is also desirable to be able to check the value of the voltage standing-wave ratio of the generator directly during operation.

The usual technique of measuring the v.s.w.r. of a generator by means of a measuring line and a short-circuiting plunger is labor-consuming and unsuitable for checking the v.s.w.r. during operation.

The technique of measuring the v.s.w.r. by means of a phase shifter described in [1] is less labor-consuming, but it requires the use of a probe and does not provide a direct reading of the v.s.w.r. The method here proposed is illustrated by a block-schematic (see figure).

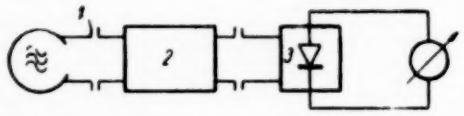

The source of power 1* whose reflection coefficient (or v.s.w.r.) it is required to measure "at the flange" in the direction of the generator, is connected through a phase shifter 2 to a detector head 3. If the detector head is not matched the power supplied by the generator will depend on the phase angle of the load impedance "at the flange" of the generator. Let us find the relation of the power to the phase of the reflection coefficient of the load. Let us use the equation of a generator as an active two-terminal network:

$$B = \Gamma_g A + B_0,$$

where B is the complex amplitude wave travelling in the direction of the load; A is the complex amplitude wave travelling in the direction of the generator; Γ_g is the reflection coefficient of the generator; B_0 is the amplitude wave produced by the generator when a matched load is connected to it.

The load equation with above notation has the form:

$$A = \Gamma_1 B,$$

* It is assumed that the source of power at the "output flange" is a linear generator.

where Γ_1 is the reflection coefficient of the load.*

By solving simultaneously the two equations with respect to B we obtain:

$$B=\frac{B_o}{1-\Gamma_g\,\Gamma_n}.$$

Let us determine the power at the load:

$$P_{le}=\frac{P_{mch}}{|1-\Gamma_g\,\Gamma_n|^2},$$

where P_{mch} is the power supplied by the generator to a matched load.

Thus the power of the incident wave depends on the reflection coefficient of the generator and on the load.

The power consumed in the load is:

$$P_n=P_{le}\ (1-|\Gamma_n|^2)=\frac{P_{mch}}{|1-\Gamma_g\,\Gamma_n|^2}(1-|\Gamma_n|^2).$$

By measuring the phase $\Gamma_n=|\Gamma_n|e^{j}$ by means of a phase shifter when Γ_n = const and φ = var, it is possible to obtain the maximum and minimum power in the load:

$$\left.\begin{aligned} P_{n\ max}&=\frac{P_{mch}}{(1-|\Gamma_g|\cdot|\Gamma_n|)^2}(1-|\Gamma_n|^2),\\ P_{n\ min}&=\frac{P_{mch}}{(1+|\Gamma_g|\cdot|\Gamma_n|)^2}(1-|\Gamma_n|^2)\end{aligned}\right\}. \qquad (1)$$

Assuming that the detector operates in a square law condition it is possible to take the rectified current or voltage as proportional to the power consumed. Then from (1) we have:

$$\frac{I_{max}}{I_{min}}=\frac{V_{max}}{V_{min}}=\frac{P_{n\,max}}{P_{n\,min}}=\left(\frac{1+|\Gamma_g|\cdot|\Gamma_n|}{1-|\Gamma_g|\cdot|\Gamma_n|}\right)^2. \qquad (2)$$

Let us now examine two limiting conditions, namely a badly mismatched generator and a badly mismatched detector. In the first instance we apply the technique of measuring the v.s.w.r. of a detector [2]. In fact, assuming $|\Gamma_g|=1$ we obtain from (2)

$$\frac{I_{max}}{I_{min}}=\left(\frac{1+|\Gamma_g|}{1-|\Gamma_n|}\right)^2=(\text{v.s.w.r.})^2.$$

On the contrary assuming $|\Gamma_n|=1$ we find the s.w.r. in the direction of the generator:

$$\frac{I_{max}}{I_{min}}=\left(\frac{1+|\Gamma_g|}{1-|\Gamma_g|}\right)^2=(\text{v.s.w.r.})^2\text{gen.}$$

Thus in order to measure the v.s.w.r. it is sufficient to determine by means of the phase shifter the maximum and minimum detected current (or voltage) in the detector.

* Both equations are referred to the same plane in front of the phase shifter, for instance, the plane of the generator flange.

A mismatch of the detector can be attained, for instance, by placing in front of the detector head a capacity or induction diaphragm. The error due to an incomplete mismatch of the detector can be easily estimated by means of the precise formula (2), the error decreasing with the value of the reflection coefficient of the generator.

Above method was used for measuring the v.s.w.r. of attenuators and for their matching. In this case the output of the attenuator was connected to a treble line-stretcher matcher by means of which it was possible to reduce the reflection coefficient of the power source from 0.1 to 0.03 and less. Squeeze lines with a waveguide cross-section of 11 × 5.5 and 7.2 × 3.4 were used as phase shifters. It would appear that phase shifters of another type can produce better results [3].

Above method is suitable for measuring the v.s.w.r. over a wide range of waves if everywhere the condition $\Gamma_n \simeq 1$ (or $\Gamma_g \simeq 1$) is made to hold.

LITERATURE CITED

[1] L. N. Bryanskii, Measurement Techniques, No. 2 (1958).*

[2] L. S. Liberman, Radio Engineering and Electronics, v. 2, No. 7 (1957).

[3] M. E. Gertsenshtein and L. N. Bryanskii, Radio Engineering and Electronics, v. 3, No. 5 (1958).

A TRANSISTOR AMPLIFIER FOR OPERATION WITH MEASURING WIRE TRANSDUCERS

P. V. Novitskii and G. N. Novopashennyi

Wire transducers are now widely used for measuring the most diverse mechanical quantities (tensions, strains, forces, pressure, vibration, etc.). They operate as a rule, however [1] with unwieldy electronic equipment fed from ac supplies, which makes their use in field conditions rather difficult.

The article deals with a transistor amplifier developed by the author in the Leningrad Polytechnical Institute for working with wire transducers and supplied from a 12 v storage battery for measuring under field conditions at 16 to 4000 cps.

The measuring amplifier consists of a voltage and a power amplifier providing at the output 100-150 ma ac.

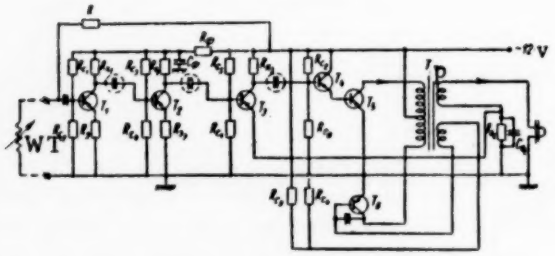

The schematic of the amplifier is shown in the figure attached. The wire transducer WT is connected as a potential divider and fed with dc. Each stage of the voltage amplifier (transistors T_1, and T_2 type P6G) has a negative feedback both dc and ac, for constant operating condition with changing temperature or parameters in the first instance and for a stable gain in the second.

The power amplifier consist of three stages (transistors T_3-type P6G, T_4-P2B and T_5 and T_6-P3B). The voltage generated across resistor $R_{9.c.}$ is fed to the emitter of T_3 thus establishing an envelope feedback across the power amplifier and the output transformer. This method provides with relatively small output transformer dimensions a greatly improved response at low frequencies.

*See English translation.

At higher frequencies the feedback becomes a function of frequency (capacitor $C_{0.c.}$) which compensates for the dropping-off in the vibrator frequency characteristic at higher frequencies up to 4000 cps.

In order to obtain a greater gain from transistor T_3 and the required signal power for the final stage, a matching transistor T_4 is connected between them. The second transistor of the final stage is fed from a special winding of the output transformer. This device provided a much simpler amplifier circuit and a minimum number of transistors and other components for the attainment of the required results.

Over-all tests of the amplifier have shown that with a type II vibrator of type MPO-2 oscillograph the output current amounted to 100 ma with an input of 1 mv. The frequency characteristic of the amplifier from 16 to 4000 cps is flat within ± 3db.

Variations of the ambient temperature from +15 to +45°C produced a variation in the output current of 1%.

The power taken by the set from the storage battery is about 3 w. A change in the supply voltage of ± 10% produces a change in the output current of ± 4%.

LITERATURE CITED

[1] A. M. Turichin and P. V. Novitskii, Wire Transducers and Their Technical Application [in Russian] (Gosénergoizdat, 1957).

EQUIPMENT FOR MEASURING PERMITTIVITY AT SUPER-HIGH FREQUENCIES

A. I. Tereshchenko

In 1957 the author developed in the Khar'kov State University a method [1, 2, 3] and constructed a device (see Figure attached) for measuring permittivity based on the phase sensitive properties of a waveguide discriminator. The discriminator serves to compare the phases of the waves reflected from a sample of the dielectric under test and from a standard resonator. This comparison produces a difference current in the discriminator detectors, which is proportional to the permittivity of the sample.

When the high frequency generator (HFG) is tuned to the natural frequency f_0 of the resonator R the waves reflected from the resonator and the short circuiting plate K arrive at the junction of the T-piece T_2 with a phase difference $\varphi = 90°$. As a result the waves incident to detectors D_1 and D_2 are equal in amplitude and produce equal currents [4]. A series opposing connection of the detectors provides a cancellation of these currents.

If a sample 0 of the dielectric under test is placed in front of the short-circuiting plate, an addition phase shift will appear between waves which are being compared. As the result, the balance of the detector currents will be disrupted and the indicator I pointer will move away from zero.

The range in which a single-valued relation holds between the permittivity of the material under test and phase (which in practice holds in range ϵ of the unit order) can be easily used for establishing a single-valued relation between the values of ϵ and the indicator reading.

Such a calibration can be made by the graphic interpolation method from several reference points obtained from materials with known permittivities. Testing with an adjusted equipment and calibrated scale simply amount to placing the sample in position and reading the appropriate value off the scale.

A mistuning of the generator with respect to the resonator frequency f_0 (or on the contrary the mistuning of the resonator) is equivalent to a change in the ratio of the T-piece arms lengths leading to the resonator

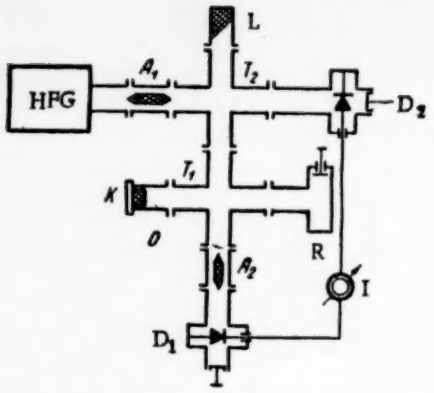

A_1 is an attenuator; A_2 – a detector balancing attenuator; L – matching load; T_1 – the first double T-piece; T_2 – the second double T-piece; D_1 – the second detector head; R – the standard resonator; K – the short-circuiting plate; 0 – the sample of the dielectric under investigation; I – the pointer indicator.

and the short-circuiting plate K. This circumstance provides the possibility of using available standard waveguide components.

By means of this equipment we measured the permittivity of hard dielectric samples in the form of plates of thickness $d = \lambda_a/2$ (where λ_a is the wavelength in the air portion of the waveguide) and dimensions corresponding to the cross section of the waveguide. In order to avoid the possible deviation from the single-value reading of the scale, mentioned above (which becomes possible if the range of the measured values of ϵ becomes too large), samples can be made with a different thickness.

When the current difference was measured by means of a 50 μa microammeter the actual sensitivity of the equipment, i.e., the difference in the indicator readings with known changes of ϵ amounted to 15 for a unity change in ϵ (for instance from 2 to 3). This sensitivity can be greatly increased by means of modulating the high frequency signal with an ac voltage and amplifying the difference current of the detectors before feeding it to the indicator.

The method of measurement and above equipment were developed for testing high frequency dielectrics with small losses (titanates and other ceramic materials, plastics, etc.); the sphere of their application, however, can be extended. In particular it is possible to measure not only solid, but also liquid and gaseous dielectrics placed in a special covering or a hermetically sealed portion of the waveguide. Finally the connection at the output of a recording device provides the possibility of investigating the kinetics of ϵ changes which is very important, for instance, when studying the temperature properties of materials.

LITERATURE CITED

[1] A. I. Tereshchenko, Author's certificate No. 113390.

[2] A. I. Tereshchenko, Annotation of a Paper Read at the Scientific Session Dedicated to Radio Day [in Russian] (A. S. Popov Sci. Tech. Soc. for Radio and Electronic Press, Moscow, 1958).

[3] A. I. Tereshchenko, "Measurement of permittivity at super-high frequencies by means of a wave discriminator" Collection of Works of the A. S. Popov Sci. Tech. Soc. for Radio and Electronics [in Russian] (Svyaz'izdat, Moscow, 1958).

[4] Technique of Measuring in Centimeter Wavelengths [translated from English] ("Sovetskoe Radio" Press, Moscow, v. 1, 1949).

ACOUSTICAL MEASUREMENTS

CALIBRATION OF OBJECTIVE NOISE-METERS BY MEANS OF "STANDARD" NOISES

D. Z. Lopashev

It is known that an objective noise-meter can be used for measuring sound pressure levels by inserting a linear frequency characteristic C; or for measuring a quantity known as the sound level* (in db) by inserting frequency correcting networks which approximate the Fletcher-Munson curves of equal audible loudness.

The calibration of noise meters for the purpose of obtaining frequency corrections for the instrument readings is usually made with pure tones and less often on bands of "white" noise. In practice, however, it is seldom necessary to measure pure tones or narrow bands of noise, but much more often noises with wide-band continuous or line spectra. In these instances the use of frequency characteristics for correcting readings becomes more difficult and even impossible when the noise spectrum is unknown(which is the most common case).

In order to avoid this discrepancy between the conditions of calibration and use of the instrument we investigated and proposed a method of calibration by means of "standard" noises which approach by their characteristic actual man-made noises.

In examining the spectra of transport of industrial noise, which embraces several octaves, let us note a marked tendency for the energy to increase or decrease with a rising frequency in a spectrum reduced to a bandwidth of 1 cps. This spectral tendency can be expressed mathematically by an inclined straight line which approximates the curve of the spectral noise power level according to the well-known method of least squares (with a logarithmic scale both for the frequency and the sound pressure level axes). Let us call this straight line the linear tendency of the spectral power level and write its equation as:

$$y_k = \gamma_0 + \gamma k.$$

Here k is the number of octave or semioctave, etc. intervals along the frequency axis (k = 1,2,3,...,n, where n is the total number of intervals), $y_k = 10 \log w_k/w_0$ is the spectral noise power level in the k-th frequency interval, where: w_0 is the power value corresponding to the threshold pressure of $2 \cdot 10^{-4}$ dyne/cm^2; $w_k = \frac{1}{\Delta f_k} \int_{\Delta f_k} w(f)df$ is the mean power in the spectrum per 1 cps in the k-th frequency interval; f_k is the width of the k-th interval along the frequency axis; w(f) is spectral power.

Let us determine the linear function

$$y(k) = \gamma_0 + \gamma k,$$

which approximates the values of y_k by the method of least squares. At the same time let us set the following conditions: a) the algebraic sum of deviations of y_k from y(k) must be zero, b) the sum of the squares of these deviations must be a minimum.

Let us make up n conditional linear equations of the form:

*Noise-meter readings are sometimes expressed in units of loudness level (phons);this however does not agree with the definition for sound level.

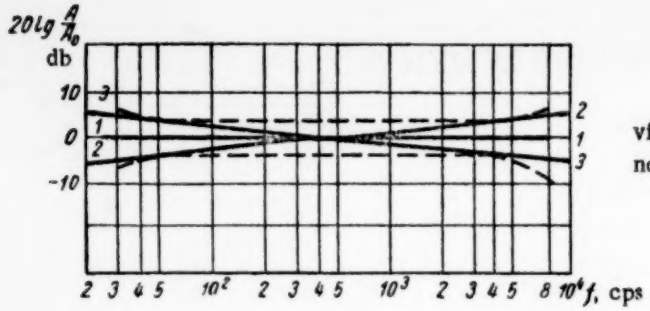

Fig. 1.

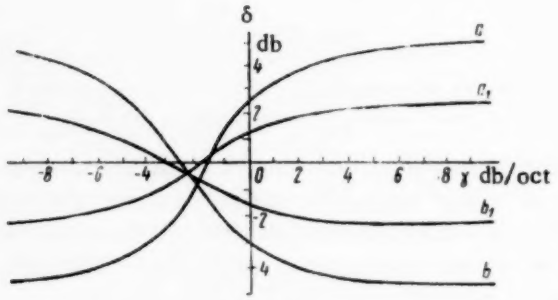

Fig. 2.

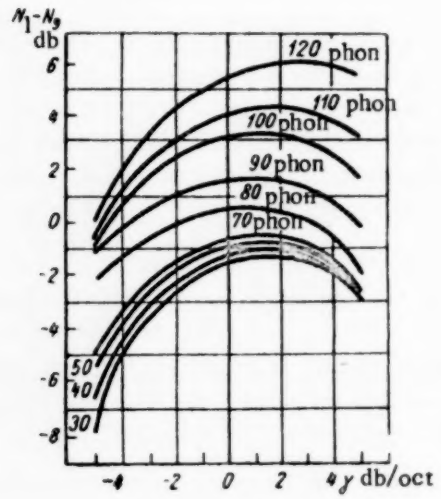

Fig. 3.

$$y_{ki} = \gamma_0 + \gamma k_i.$$

The requirement that the sum of the squared deviations must be at a minimum leads to a system of normal linear equations:

$$n\gamma_0 + \gamma \sum_{k=1}^{n} k = \sum_{k=1}^{n} y_k.$$

$$\gamma_0 \sum_{k=1}^{n} k + \gamma \sum_{k=1}^{n} k^2 = \sum_{k=1}^{n} k y_k.$$

which solved with respect to γ and simplified produce:

$$\gamma = \frac{6}{n(n^2-1)} \sum_{k=1}^{n} (2k - n - 1) y_k.$$

For each noise spectrum it is possible to calculate parameter γ which can assume both negative (decreasing with a rising spectral frequency) and positive value (increasing with a rising frequency). For "white" noise $\gamma = 0$, for spectra with equal levels in the octaves $\gamma = -3$ db/octave.

By means of the spectral parameter γ it is possible to solve certain interesting problems, for instance, to find the relation between the tolerances with respect to the irregularity of frequency characteristics of a noise meter and its readings of noises with different spectra.

The dotted lines in Fig. 1 show the tolerances with respect to the irregularity of the linear frequency characteristic C according to the American standard [1]. Straight lines 2-2 and 3-3 determine the maximum permissible slopes of the linear frequency characteristic of the noise-meter. Following the technique described in [1] let us calculate the systematic errors of a noise-meter, i.e., the difference δ between readings of an instrument with characteristic 1-1 for different values of the spectral parameter γ. The calculation results are shown graphically in Fig. 2. Curve a corresponds to characteristic 2-2 in Fig. 1, curve b to characteristic 3-3. Curves a_1 and b_1 correspond to tolerances twice as large as those given in Fig. 1.

Inspection of curves in Fig. 2 leads to the conclusions that: 1) the calculated systematic errors of a noise-meter due to the irregularities of its frequency characteristic do not exceed the maximum errors for pure tones. With the assumptions made about the spectra and the frequency characteristics, the errors approach their maximum values (± db) asymptotically; 2) for certain noises in this case for $\gamma = -3$db/oct. the calculated errors are at a mimimum; for these noises the irregularity of the frequency characteristic of the noise-meter does not come into effect, i.e., the errors are compensated.

Let us now examine the effect of frequency corrections on the readings of noise-meters for different noise spectra. Let us take the Fletcher-Munson curves of equal audible power [1] as the basis for corrections. The

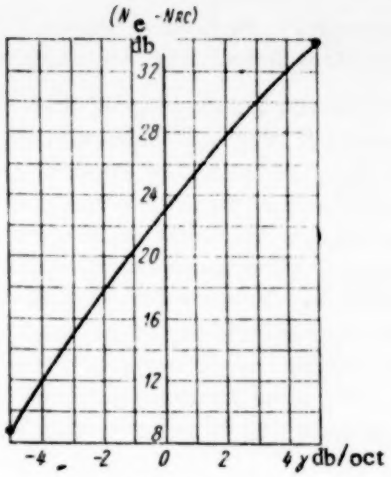

Fig. 4.

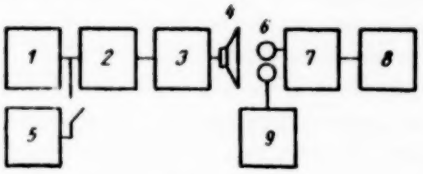

Fig. 5.

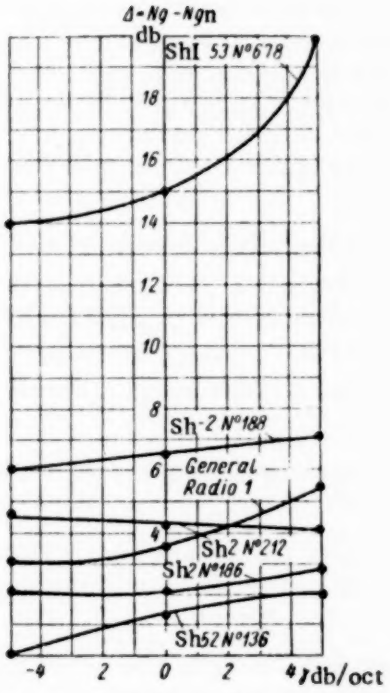

Fig. 6. Experimentally obtained corrections for the readings of various noise meters when measuring a sound pressure level N_g.

calculation results of differences between the sound level N_s and the sound pressure level N_g for values of γ from -5 to $+5$ db /oct.

From the curves in Fig. 3 we can draw the following conclusions: a) in the normally accepted corrections for a noise-meter (40-70 phons) the sound level of noise for values of γ between -5 and $+5$ db/octave is always lower than the level of sound pressure; b) the effect of the normally applied corrections on the readings of a noise meter for the above values of γ amounts to 0.5 to 8 db and increases considerably for more negative values of γ; c) for certain values of parameter γ it is possible to recalculate the noise-meter readings from one correction to another by means of the curves in Fig. 3, or with respect to a correction which does not exist in the given instrument, and this is of practical value.

Above examples which illustrate the relation between systematic errors of noise-meters and between their readings with inserted corrections and the spectral parameter γ of the measured noises led to the idea about the possibility of calibrating noise-meters by means of "standard" noises corresponding to definite values of γ. Readings of a noise-meter in the field of a "standard" noise are calibrated by comparing them with readings of a reference microphone and thus obtaining the measurement errors of the noise-meter.

If it is required to determine the error of a noise-meter with a correcting network it is first necessary to calculate the actual value of the sound level by correcting the "standard" noise spectrum according to the nominal values of the standard noise-meter characteristic. Next the noise-meter readings are compared with the actual values and the errors determined. Tests have shown that calibration results can be applied in industrial measurements over measured noise spectrum of 4 octaves and more. This conditions is satisfied by the majority of noises measured in practice. In order to be able to obtain a correction from a calibration curve of a noise-meter it is necessary to know the value of parameter γ of the measured noise. The noise spectrum, however, is usually unknown and the value of γ cannot be calculated from the formula given above. This difficulty is overcome by measuring parameter γ directly by means of the noise-meter under consideration in the following manner.

With the noise-meter in the field of a "standard" noise the relation of the difference between the noise-meter readings, when a linear frequency characteristic network or one of the correcting networks is inserted, to the "standard" noise parameter γ is plotted. It is even better to use instead of the correcting network a simple RC filter which provides an even drop in the frequency characteristic of 4-5 db per octave. In the latter case the steep curve shown in Fig. 4 is obtained from which it is possible to determine the value of parameter γ for industrial noise by finding the noise-meter readings with a linear characteristic N_e and with an RC filter N_{RC}. The mean square error of a series of measurements of parameter γ for 30 industrial and transport noises was evaluated at 0.5 db/oct.

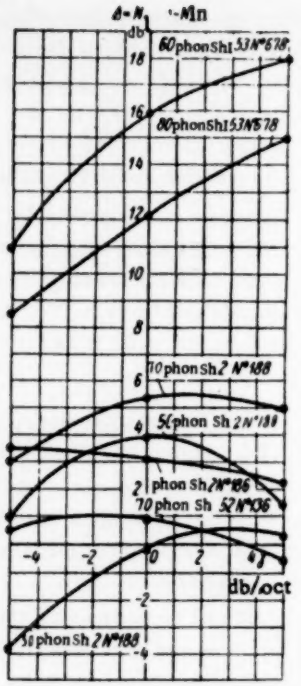

Fig. 7.

For the calibration of noise-meters in the field of "standard" noises the equipment whose block-schematic is shown in Fig. 5 was constructed.

The "white" noise voltage is provided in the range of 50-8000 cps by generator 1. Filters 2 from spectra of "standard" noises with values of $\gamma = -5$ db/oct, $\gamma = 0$, $\gamma = +5$ db/oct, amplified by amplifier 3. The reference microphone and the microphone of the noise-meter 9 are placed into a quasi-spherical sound field which is established at 25-30 cm from loudspeaker 4 along its radiation axis. The microphones are placed in points of equal sound pressures, which are determined in advance. Amplifier 7 and the measuring instrument 8 consititute part of the reference microphone equipment, which is calibrated by the standards methods of producing units of sound pressure. The audio-frequency generator 5 is used for checking the frequency characteristic of the noise reproducing channel.

The equipment is used in normal laboratory premises. The level of the "standard" noises produced must be at least 30 db above any acoustical interference. The field measurements have shown that the maximum deviation from the law of inverse proportionality at distances between 25 and 40 cm from the loudspeaker did not exceed +0.5 db. Measurements of the distribution function of the sound pressure instantaneous values confirmed the existence of a normal (gaussian) distribution law, this circumstance made it possible to correct by calculation for the deviation from the square law of the reference microphone tube voltmeter by by the amount of $+1.05 \simeq +1$ db.

When the equipment passes its final test, corrections are also calculated for all the "standard" noises with respect to the errors in the readings of the reference microphone due to irregularities of its frequency characteristic and the difference between the sound and the sound pressure levels.

The noise-meter is calibrated in the following order. The reference and the noise-meter are placed in the "standard" noise field. The reading of the reference microphone is noted and after applying corrections the actual value of the sound pressure level N_g is obtained (with a mean square error of a series of measurements of $\pm$ 1 db). By adding to N_g the calculated difference $N_l - N_g$, where N_l is the sound level and N_g the sound pressure level, the actual value of the sound level N_l is obtained. Next the noise meter readings N_{gn} with a linear characteristic and those obtained when a correction network is inserted N_{ln} are noted and from their comparison with the actual values the noise meter correction Δ is obtained.

Figures 6 and 7 provide experimentally obtained correction curves for various noise-meters. These corrections attain large values and cannot be ignored despite the usual practice of neglecting them in noise measurements. The noise-meter frequency characteristics even when determined with great accuracy prevent, however, the application of these corrections since the noise spectra are usually unknown.

With known spectra the errors are not applied owing to the large amount of work involved in numerical integration.

Calibration of the noise-meters by means of "standard" noises is an important refinement to their normal calibration by pure tones.

The equipment for calibrating noise-meters by means of "standard" noises was developed in the VNIIFTRI in 1956-57 and is at present being adopted by the testing organizations of the Committee of Standards, Measures and Measuring Instruments. The work was carried out under the guidance of I. G. Rusakov and A. N. Rivin.

Conclusions. 1) The adopted spectral parameter provides the possibility of solving theoretical and practical problems in noise measurements of a complicated spectral composition, 2) Methods of calculating and measuring this parameter by means of an ordinary noise-meter are provided, 3) calibration of noise-meters by means of "standard" noises provides the possibility of correcting noise-meter readings with satisfactory accuracy when the spectral composition of the noise is unknown, which is not the case with conventional methods of calibration.

LITERATURE CITED

[1] L. Beranek, Acoustical Measurements [in Russian translation] (Foreign Literature Press, Moscow, 1952).

AN IONIZATION CHAMBER FOR ABSOLUTE MEASUREMENTS OF THE RADIOACTIVITY OF PREPARATIONS

F. M. Karavaev

Absolute measurements of the activity of γ-radiations can be made by means of ionization chambers whose efficiency can be determined Such chambers include so-called thimble chambers. These chambers, however, are small and are therefore suitable for measuring potent preparations only.

In several papers it was shown [1, 2] that the theory of thimble chambers [3] could be used for calculating the efficiency of larger chambers, the so-called slot ionization chambers [4].

We constructed for absolute measurements of the activity of γ-radiation sources a spherical ionization chamber consisting of two concentric aluminum spheres each of which was made up of two demispheres. The external radii of the external and internal demispheres are 130 and 115 mm respectively. The mean thickness of the demispheres walls is 4.99 mm. The gap between the spheres of an assembled chamber is 10 mm.

Figure 1 shows the cross-section of an ionization chamber. The internal sphere 1 rests on three amber insulators, fixed to the wall of the external sphere 3 by bushes 4 which serve as guard rings. The bushes are insulated from the external sphere by means of ebonite insulators 5. A thin aluminum plate 6, which carriers the preparation 7 in its center, is placed in the diametral plane of the inner sphere.

The inner sphere serves as a collecting electrode and is connected by means of leadout 8, which passes through an amber insulator 9, to an electrometer device. Insulator 9 is supplied with a guard ring 10 fixed by an ebonite bush 11 to the wall of the external sphere.

A voltage of some 700 v is supplied to the external sphere in order to provide saturation in the ionization volume (cavity between the spheres) when preparations with radioactivity of 2 C are measured.

The entire chamber is placed in a grounded metal container 12.

When preparations with radioactivities between 0.1 mC and 2 C are measured, the ionizations currents lie within the limits of 10^{-13} and 10^{-8} amp. In order to measure such currents we used a compensation circuit with a quadrant electrometer which formed a part of a standard VNIIM* equipment for measuring γ-equivalents of radioactive preparations [5]. The accuracy of measurement of the ionization current by means of this circuit amounts approximately to 0.5%.

The radioactivity of preparation A is determined from the measured value of the ionization current I it produces, referred to normal conditions (air pressure of 760 mm Hg, temperature 0°C) and the known efficienty* of the ionization chamber by means of the formula:

$$A=\frac{IK}{i_0}. \qquad (1)$$

* VNIIM = All-Union Scientific Research Institute of Metrology.

where

$$K=\frac{760}{p}\cdot\frac{t+273.1}{273.1}$$

Here i_0 is the efficiency of the chamber, p and t the pressure and temperature of the air during testing.

The efficiency i_0 is calculated by means of the theory of thimble chambers applied to the given chamber. Let the source be placed in the center of the inner sphere and let it radiate on an average per disintegration even n quanta with an energy W. The total number of ion pairs which have formed in the air cavity of the chamber under the action of γ-radiations is equal to:

$$Q=nW\left(\tau+\sigma_\beta+\tau_n\frac{W-2mc^2}{W}\right)e^{-\mu d}\eta\frac{D}{\rho\varepsilon}, \qquad (2)$$

where τ, $\sigma\beta$, τ_n are linear coefficients of γ-ray absorption in the photoeffect, Compton scattering and the formation of ion pairs; μ is the linear γ-ray attenuation coefficient in aluminum; η is the part of the energy of secondary electrons spent in ionization; ρ is ratio of the electron stopping power of aluminum and air; ϵ is the work done in ionization; mc^2 is the rest energy of an electron; d is the thickness of the internal sphere wall; D is the gap between the spheres.

The ionization current produced by a source of 1 mC is:

$$i_0=Qe_0\cdot 3.7\cdot 10^7 \text{ amp/mC} \qquad (3)$$

where e_0 is the elementary charge in coulombs.

If the preparation emits γ-radiations of a complex nature the efficiency should be added up for all the lines of the γ-spectrum.

Of the quantities comprising (2) the coefficients τ, $\sigma\beta$, τ_n, and μ are taken from tables [6]; mc^2 = = 0.511 Mev and the ionization work done is 33.7 ev [7].

The value of ρ changes a little with variations in the energy of the electrons. Figure 2 shows the values of ρ for electron energies of 0.1 to 3 Mev, calculated from well-known theoretical formulas for ionization losses of electrons [8]. In calculations the following composition of air was assumed: the nitrogen, 76.18%, oxygen, 21.9%, and argon, 1.38%. It will be seen from Fig. 2 that it is possible to take ρ as 1870 with an accuracy of 1% for the stated range of energies.

Isotope	Chamber efficiency, $i_0 = 10^{-13}$ amp		Isotope	Chamber efficiency, $i_0 = 10^{-13}$ amp	
	calc.	experiment		calc.	experiment
Na^{24}	216.3		In^{114}	4.820	
K^{42}	14.34		Sb^{124}	152.1	
Cr^{51}	1.64		J^{131}	25.18	
Mn^{54}	52.06		Cs^{134}	99.10	
Fe^{59}	70.58		Cs^{137}	39.10	38.5±1.1
Co^{60}	147.4	145±4	Au^{198}	26.06	26.7±0.8
Zn^{65}	31.09		Hg^{203}	12.78	
Zr^{95}	57.54		Ra (in equilibrium with decay products)	112.3	114.5±0.6
Nb^{95}	46.54				
Ag^{110}	160.0				

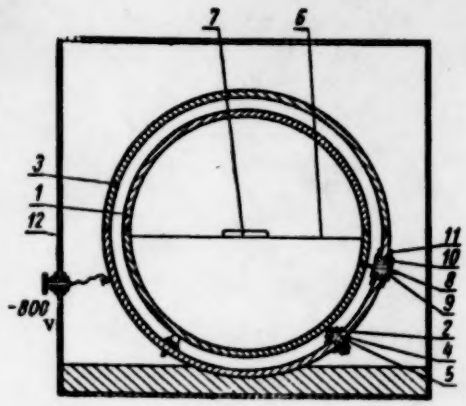

Fig. 1.

Fig. 2.

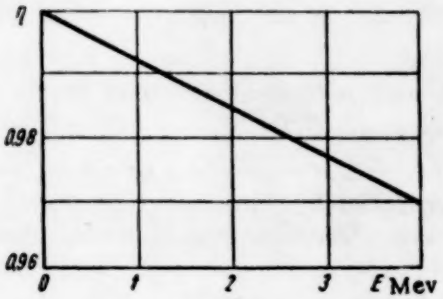

Fig. 3.

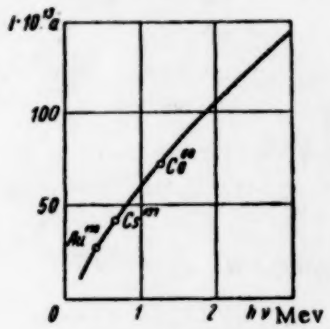

Fig. 4.

Values of η for aluminum [9] are given in Fig. 3.

In (2) the effect of secondary γ-radiation due to Compton scattering and annihilation of positrons which are formed by the absorption of the primary γ-radiation on account of the formation of ion pairs.

Figure 4 shows the relation of the chamber efficiency to energy of γ-rays. The calculated chamber efficiency for various γ-radiations and its experimental values obtained by measuring ionization currents of different isotope preparations of known radioactivity placed in the chamber are given in the table.

In these measurements we used standard radium preparations and those of Co^{60}, Cs^{137}, and Au^{198} whose radioactivity was measured by the calorimetric method. The experimental efficiency referred to the intensity of 1 quantum per disintegration event, is also plotted in Fig. 4. It will be seen both from the table and Fig. 4 that the calculated and experimental values of efficiency agree with a satisfactory degree of accuracy, which indicates the correctness of the calculation method adopted.

Of the quantities used for calculating the efficiency of the chamber those known with the least accuracy are the work done by the ionization of γ-rays in air (error 4.5% [7]), the intensity of the γ-ray spectral lines ($\simeq$ 5%) and the ratio of the stopping powers of aluminum and air ($\simeq$ 1%). The errors of the other quantities comprising (2), i.e., of the γ-ray energy and the absorption coefficient do not exceed, as a rule, 1%.

The ionization current in the range of 10^{-13} to 10^{-8} amp can be easily measured with an accuracy of 0.5%.

The dimensions of the chamber are known with an error not exceeding 0.5%.

A displacement of the sphere centers up to 3 mm decreases the chamber efficiency by only 0.25%.

Self-absorption corrections when radiating over a solid angle of 4π have been calculated only for spherical sources [10]. An accurate evaluation of self-absorption for a cylindrical source and a solid angle of 4π must become the subject of a special study.

Excluding all the systematic errors and taking into account the accuracy of the quantities used in determining radioactivity by this method, the maximum error of measurement amounts to 7-10% according to the accuracy with which compositions of the γ-spectrum are known.

LITERATURE CITED

[1] O. N. Vavilov, Trudy Fiz. Inst. Akad. Nauk, 4, 5, (1949).

[2] I. V. Éstulin, J. Exprtl.-Theoret. Phys. (USSR) 21, 1412, (1951).

[3] L. H. Gray, Proc. Roy. Soc., 156, 578, (1936).

[4] I. V. Éstulin, J. Exptl.-Theort. Phys. (USSR) 22, 414, (1952).

[5] K. K. Ablintsev and F. M. Karavaev, Trudy VNIIM, issue 30 (90) (1957).

[6] C. M. Davisson and R. D. Evans, Rev. Mod. Phys., 24, 79, (1952).

[7] K. K. Aglintsev and G. P. Ostromukhova, Measurement Techniques, No. 2, (1959).

[8] S. Z. Belen'kii, Cascade Processes in Cosmic Rays [in Russian] (GITTL Press, 1948).

[9] B. H. Flowers, J. D. Lawson and E. B. Fossey, Proc. Phys. Soc., 65B, 286, 1952.

[10] M. A. Bak, K. A. Petrzhak and Yu. F. Romanov, J. Tech. Phys. (USSR) 26, No. 2, 579 (1956).

RADIOACTIVE SOURCES IN MEASUREMENT TECHNIQUES

V. S. Merkulov

Radioactive radiations are being used more and more extensively in various branches of measurement techniques and instrument making. At present there are a number of checking and measuring instruments which are based on the measurement of absorption and reflection of radiations by the media under test, or on the ionization of gases, (γ-ray fault location, radiation level meters, thickness gages, density meters, consumption meters, relays, devices for measuring the thickness of coatings, speedometers, pressure gages, devices for measuring the pressure and composition of gases, etc.). In this connection it is useful to list the main applications of radioactive radiations and their characteristics.

Radioactive elements radiate directly α, β, γ-rays, and x-rays (in K-electron capture). As the result of secondary nuclear processes they may serve as sources of neutrons and x-rays.

In developing radioactive instruments and methods of measurement it is of prime importance to choose correctly, sources of radiation according to their radiation energy and radioactivity. When the article which separates the radiator from its receiver is thick, penetrating γ-rays, x-rays or neutrons are used. For checking thin-walled articles β-radiations are used. With a constant radiation flux, maximum accuracy in determining a mass in the radiation path is attained when $\mu_0 = 2/m$ (in the case of a predominance of a statistical error of measurement).* Here $\underline{m}$ is the mass under test (g/cm²) and μ_0 is the mass absorption coefficient (cm²/g). Normally the radiation "hardness" is judged by the value of $\mu_0 m$ in the region of $\mu_0 m = 0.2$ to 4. Let us note that $\underline{m}$ denotes the total mass in the path of the radiation; including the mass of the protecting membranes or walls of the object under test.

β-radiations are widely used when it is required to modulate or cut-off radiations by means of screens as well as for ionization purposes. For intense gas ionization it is advisable to use α-radiations.

When calculating the radioactivity of the source (for any particular purpose) the efficiency of the recevier and the configuration of the object must be taken into account. When working with α and β-preparations their specific radioactivity should be at a maximum.

The duration of the isotope determined by its half-life is also an important factor. For checking and measurement purposes long life isotopes with a half-life not less than several months are of practical interest.

With other properties being satisfactory radioactive isotopes should be inexpensive, easily obtainable and must of course possess the required physical and chemical properties.

This table gives examples of the use of various radioactive radiation sources with an indication of some of their characteristics.

* The conditions are derived from the exponential law of absorption of β, γ-radiations by the substance.

The Most Important Radioactive Sources and the Spheres of Their Application

Radiator type	Radioactive isotope	Half-life	Radiation energy, Mev	Sphere of application (main uses)
α-radiators	Po^{210}	138 days	5.3	Static discharging. Making of luminescent preparations (in a mixture with phosphorus) and neutron sources (in a mixture with beryllium). Measurement of film thicknesses up to 1-2 mg/cm², areas with complex configurations, speed, composition, pressure and consumption of gases, small angular and linear displacements.
	Ra^{226}	1590 years	4.8	
	Pu^{239}	$2.4.10^4$ years	5.15	
β-radiators	$Ru^{106} \rightarrow Rh^{106}$	1 year	3.55	Measurements of the thickness (weight, density) of thin sheet materials of all kinds by the absorption method and thicknesses of coatings, concentrations and compositions of solutions by the reflection method. Static discharging. Making of luminescent compounds, sources of x-rays, and atomic batteries. Measurement of various gas parameters. Production of electron diffraction patterns. Rolled metal marking.
	$Ce^{144} \rightarrow Pr^{144}$	282 days	2.97	
	$Sr^{90} \rightarrow Y^{90}$	19.9 years	2.18	
	Sr^{89}	53 days	1.463	
	Tl^{204}	3.5 years	0.765	
	Pm^{147}	2.6 "	0.223	
	S^{35}	87.1 days	0.167	
Sources of soft γ-rays	Tu^{170}	129 days	0.084	Radiation fault location in thin objects and light materials, measurement of thickness and density. Composition analysis of substances.
	Eu^{155}	1.7 years	0.087	
	Am^{241}	470 days	0.060	
Sources of hard γ-rays	Co^{60}	5.27 years	1.25	Radiation fault location in thick-walled objects and heavy materials, checking internal corrosion in tanks. Measurements of considerable thicknesses, irregularities in tubes and cylinders, densities of liquids and solids (ground, snow, cement, metallurgical pulp, etc.). Measurement of the levels of liquids and loose materials and media boundaries. Measurements of liquid consumption and high gas pressures. Counting sorting of production items, checking of packing. Sampling of oil wells. Pasteurization of commodities, production of polymers.
	Cs^{137}	33 "	0.661	
	Ir^{192}	74.37 days	0.45	
Sources of K-radiations	Fe^{55}	2.94 years	6.2 (kev)	Quantitative analysis of the composition of substances. Determination of the porosity of bodies. Measurements of the thickness and density of light materials. Measurement of the temperature of gases.
	Ni^{59}	8.10^4 years	–	

Radiator type	Radioactive isotope	Half-life	Radiation energy, Mev	Sphere of application (main uses)
Neutron sources	Name of the composition, nuclear reaction			
	Ra–Be; $Be^9(\alpha,n)C^{12}$	1590 years	to 14	Measurements of the humidity of materials, levels of hydrogen-containing substances, density of the ground and checking of temperature.
	Ra–Be; $Be^9(\gamma,n)Be^8$	1590 "	0.12 to 0.51	
	Po–Be; $Be^9(\alpha,n)C^{12}$	138 days	to 8	Quantitative analysis of the composition of substances.
	Pu–Be; $Be^9(\alpha,n)C^{12}$	$2.4 \cdot 10^4$ years	–	Fault location in materials of considerable thickness.
	Sb–Be; $Be^9(\gamma,n)Be^8$			
Sources of x-rays	Radiators of hard γ-rays (Sr^{89}, $Sr^{90} \rightarrow Y^{90}$, P^{32}, Tl^{204}, Pr^{144}) in conjunction with targets made of heavy materials.			Fault location in thin and light materials, measurements of the thickness of thin walled articles and of the density of light materials.

Note: For β-radiations the maximum radiation energy is given, for γ-radiation the mean radiation energy. For $Ru^{106} \rightarrow Rh^{106}$, $Ce^{144} \rightarrow Pr^{144}$, and $Sr^{90} \rightarrow$ $\rightarrow Y^{90}$ the maximum energy of the daughter product β-particles is given.

THE COMMITTEE OF STANDARDS, MEASURES, AND MEASURING INSTRUMENTS

NEW SPECIFICATIONS FOR MEASURES AND MEASURING INSTRUMENTS APPROVED BY THE COMMITTEE ON NEW STANDARDS

(Registered in March-April, 1959)

GOST 3925-59. Notation of basic quantities and conventional representation of instruments in production automation diagrams. Replacing GOST 3925-47.

GOST 9070-59. Viscosimeter for determining the nominal viscosity of lacquer and paint materials. Introduced for the first time.

GOST 9071-59. Tongs for electrical measurements. Technical requirements. Introduced for the first time.

GOST 1594-59. Equipment for determining the quantity of water contained in oil, food and other products. Replacing GOST 1594-42 and OST 10516-40.

GOST 1770-59. Measures of capacity; glass, industrial. Replacing GOST 1770-51 and GOST 6798-53.

GOST 9063-59. Automatic hydraulic jet regulators for general industrial use. Introduced for the first time.

GOST 3029-59. Instrument cases for industrial glass thermometers. Replacing GOST 3029-45.

GOST 6651-59. Resistance thermometers. Replacing GOST 6651-53.

GOST 2923-59. Flat glass plates for interference measurements. Replacing GOST 2923-45.

NEW INSTRUCTIONS FOR CHECKING MEASURES AND MEASURING INSTRUMENTS

(Registered in January-April, 1959)

Instruction 238-59 on checking hardness gages for rubber.

Instruction 281-59 on checking electrical contact transducers. Replacing instruction 5-48 former Kommerpribor. (Commercial Instruments).

Instruction 282-59 on checking pneumatic-electrical transducers.

OPERATING INSTRUCTIONS FOR CHECKING MEASURES AND MEASURING INSTRUMENTS APPROVED BY THE TECHNICAL DEPARTMENT OF THE COMMITTEE

Operating instruction No. 174 on checking objective noise-meters.

ERRATA

In issue No. 4(1959) of the journal on page 22, column B of Table 2, the expression in the first brackets of the denominator of the top fraction should read $(1 - \frac{\omega^2}{\omega_{10}^2})$.